Mechanisms of methanogenic microbial community assembly: anaerobic digester as a model

A Dissertation Presented for the
Doctor of Philosophy
Degree
The University of Tennessee, Knoxville

Liu Cao

August 2019

This dissertation is dedicated to Zhenghao Zhu

ACKNOWLEDGEMENTS

First and foremost, I want to express my great gratitude to my major advisors Dr. Chris Cox and Dr. Qiang He for the support, guidance and dedication throughout my Ph.D. journey. They have both helped me tremendously. Dr. Cox encourages me to think in depth so as to make an impact and leads me into programming and simulations in addition to conducting experiments. I admire Dr. He's endless energy and brilliant ideas and are thankful to him for spending time on discussing with me and providing constructive feedback.

I am also grateful for Dr. Terry Hazen and Dr. Jun Lin who kindly serve as my dissertation committee members. They spent time on reviewing my proposal and dissertation, sharing academic discussion with me and gave precious recommendation on academic research.

It is my fortune that I have received many helps from lab technicians, my colleagues, and other acquaintances. I want to express my thanks to Dan Williams who helps me learn all the genetic techniques from DNA extraction to sequencing. I would also like to thank Sharon Hale, Dominique Joyner, and Katie Manz for their help in the laboratory. I am lucky to have worked with Si Chen, Kristen Wyckoff, Yongfeng Wang, Lu Yang, Yabing Li, Songyi Liu, and Clifford Swanson who spent time on sharing ideas and discussing research projects with me and gave me sincere assistance.

A special thanks to my parents who have been loving and supporting me unconditionally. They have encouraged me and respected my decisions since I was young, which shaped my independency.

Last but not least, I cannot thank my beloved husband enough for his love, encouragement, and support. He is also a great role model for me as he always works hard, thinks critically, and lives passionately.

ABSTRACT

Methanogens are important populations of microbial communities that are responsible for natural recycling of carbon in the biosphere. Methanogenesis has also been engineered into a process termed “anaerobic digestion”, where the degradation of organic matter undergoes a network of complex metabolic pathways by diverse microbial trophic groups under anaerobic conditions. It is of great importance to understand the underlying mechanisms of this process. This research uses anaerobic digestion as a model system to better understand the microbial community assembly mechanism, the microbial interactions, and the impact of source populations on the development of microbial community structures. In Chapter 1, basic concepts of the microbial food web in the anaerobic digestion process and the two known community assembly mechanisms were introduced. In Chapter 2, 13 replicate laboratory-scale semi-continuous anaerobic reactors were inoculated with the same culture and maintained under the identical operational and environmental conditions for a year. The results revealed that despite the change in community composition between time points, overall community structure was remarkably consistent among the 13 replicates, indicating that non-random mechanisms such as selective pressure shapes the changing trajectory of the community structure over long periods of time. Chapter 3 aimed to gain a deeper understanding of the methanogenesis associated with short-chain fatty acids as they are the most common intermediates during anaerobic digestion. Enrichments were set up and kinetics of the anaerobic degradation of the fatty acids was determined by the accumulative methane yields. Based on the results, a food web was proposed for anaerobic degradation of the short chain fatty acids, including both acetoclastic and hydrogenotrophic methanogens, syntrophic bacteria, and other redundant bacteria populations. Chapters 4 developed several groups of propionate enrichment cultures to identify the syntrophic propionate oxidizers and to investigate the effect of diverse sources of inoculum, different sampling points, and altered substrate concentrations on the microbial community structures of propionate enrichment. The results provided various evidences to demonstrate *Syntrophobacter* as the specific obligate syntrophic proton-reducing acetogenic bacteria while its associated

methanogen partners are not definitive. Altogether, this dissertation conducted several bottom-up experiments towards the understanding of anaerobic microbial community assembly.

TABLE OF CONTENTS

LIST OF TABLES

LIST OF FIGURES

LIST OF EQUATIONS

CHAPTER I - INTRODUCTION AND LITERATURE REVIEW

1. Methanogenic environments

Methanogens are important part of microorganisms that are responsible for the natural recycling of carbon in the biosphere. Anaerobes are widely distributed in the environments where dioxygen has been displaced by gaseous products of anaerobic metabolism, such as CH_4, CO_2, and H_2 (Gest, 2003). Those anoxic environments include sediments, rice paddy soil, wetland, deep marine, ruminant digestive system, etc (Henderson et al., 2015; Hori et al., 2006; Nozhevnikova et al., 2001; Schmidt et al., 2017; Stibal et al., 2012).

This natural process has been engineered to anaerobic digestion, a man-made process that involve the degradation of organic matters by a series of complex metabolic pathways among certain microbial groups in absence of oxygen. This technology is widely used to treat various organic wastes, including municipal and industrial wastes, food wastes, agricultural wastes, animal manures, etc., for the following advantages: (1) the majority of the end product is methane gas, which is a renewable fuel and can be used to generate energy; (2) it requires much smaller space and is more cost effective compared with aerobic process; (3) the effluent of digestate is rich in nutrients thus can be utilized as organic fertilizer.

2. Food web of anaerobic digestion process

In anaerobic decomposition, various groups of fermentative anaerobes cooperate in the conversion of complex organic materials to methane and carbon dioxide. A food web describing this process is shown in Figure 1-1.

2.1 Hydrolysis

In hydrolysis, polymeric substrates, including lipids, proteins, and other polysaccharides, are converted primarily to their respective monomers using extracellular enzymes. Hydrolytic bacteria are phylogenetically diverse. The two phyla that are most common in this process is *Firmicutes* and *Bacteroidetes*. Hydrolysis rate mainly depends on the chemical structures of the substrates, particle size, enzyme production, diffusion, etc. hydrolysis can be the rate-limiting step for methane production if the substrates are comparatively recalcitrant; for example,

benzene and phenol related organics, lignin and lignin related compounds (Chen et al., 2008). The environmental factors, such as temperature and pH, on the other side, have less impact on the growth of hydrolytic bacteria.

2.2 Acidogenesis

Acidogenesis involves the breakdown of hydrolysis products to mostly short-chain fatty acids, and minorly alcohols, lactate, CO_2, and H_2. The phyla that contains acidogenic bacteria include *Firmicutes*, *Bacteroidetes*, *Chloroflexi*, *Proteobacteria*, *Actinobacteria, Thermotogae*, etc (Manyi-Loh et al., 2013). The rapidness of the acidogenesis may potentially lead to accumulations of volatile fatty acids and a decrease of pH, which is one of the main inhibitors of methanogenesis.

2.3 Syntrophic interactions

Intermediates such as propionate, butyrate, and methanol are required to be further degraded before being utilized by methanogens to produce methane. Syntrophic acetogenesis is the process in which two or more organisms cooperate in the anaerobic degradation of organic compounds. After acidogenesis process, most monomers (i.e. sugars, etc) are catabolized to short-chain fatty acids (acetate, propionate, and butyrate), alcohols, and hydrogen and carbon dioxide gases. Hydrogen and acetate are consumed by methanogens directly. The bulk of the remaining carbon is in the form of fatty acids and alcohols, which cannot be directly converted to methane by methanogens and require the activities of syntrophic bacteria. Syntrophic bacteria are secondary fermenters as they degrade the primary fermenting products into acetate, hydrogen, and carbon dioxide. For instance, *Syntrophomonas* oxidize C_4 fatty acids, generating acetate, CO_2, and H_2 (Wu et al., 2006); *Syntrophobacter* degrades C_3 (propionate) to acetate, CO_2, and H_2 (Plugge et al., 2012); and *Syntrophus* specializes in aromatic compounds fermenting, yielding acetate, H_2, and CO_2 (McInerney et al., 2007). The reducing equivalents (H_2, acetate) should be efficiently consumed by methanogens, which is essential for the syntrophic partners to grow since this process is endergonic under standard conditions and

thermodynamically feasible when the H_2 partial pressure is kept low (Summers et al., 2010; Zhao et al., 2016).

Although acetate is usually converted to methane and carbon dioxide through acetoclastic methanogenesis pathway, another pathway has been observed for methane production form acetate under certain conditions. The two-step pathway was proposed by Barker (Barker, 1936) that acetate was primarily converted to CO_2 and then CO_2 was concurrently reduced to CH_4. This process has been observed in many cultures especially under thermophilic conditions (Zinder & Koch, 1984) and under high concentrations of ammonia, acetate, salinity, etc (Hao et al., 2011; Hattori, 2008; Müller et al., 2013). Nevertheless, only a few microorganism species have been identified to perform syntrophic acetate oxidization subsequently with hydrogen consuming methanogens (Mosbæk et al., 2016; Westerholm et al., 2012; Westerholm et al., 2018; Westerholm et al., 2016).

2.4 Methanogenesis

Methanogenic archaea catalyze the final step of anaerobic conversion of organics to CH_4 and CO_2. There are three known types of methanogenesis pathways, hydrogenotrophic, acetoclastic, and methylotrophic. Hydrogenotrophic methanogens converts $H_2 + CO_2$ or formate to methane, whereas other methanogens use acetate or methanol.

Acetate is the most important intermediate in anaerobic digestion process. Acetoclastic pathway has been reported to be the major pathway to produce methane as approximately 70% of the total methane generated during sewage anaerobic digestion is via this pathway (Merlino et al., 2013). Only two genera were identified to utilized acetate and produce methane through acetoclastic pathway, *Methanosaeta* and *Methanosarcina*. It is usually believed that *Methanosarcina* tend to dominate over *Methanosaeta* in the digesters where the acetate concentration is high because of its wider range of substrates ad higher growth rate (Conklin et al., 2006; Hori et al., 2006; Venkiteshwaran et al., 2015). The typical anaerobic environment for *Methanosaeta* to be the dominant acetoclastic methanogen populations was found at low acetate concentrations (i.e., <1 mM) (McHugh et al., 2003; Zheng & Raskin, 2000). Some other studies showed the

competitiveness of *Methanosaeta* at elevated acetate (20 mM) (Chen et al., 2017; Leite et al., 2015).

It is critical to maintain a low hydrogen partial pressure so the hydrogenotrophic methanogen are crucial in the anaerobic digestion process. *Methanobacterium*, *Methanospirillum*, *Methanoculleus*, *Methanococcus*, *Methanothermus*, etc. have been reported as commonly observed hydrogenotrophic methanogens (Costa et al., 2013; Demirel & Scherer, 2008).

Methanol is a comparatively rare intermediate in anaerobic digestion, and it can be reduced to methane by methylotrophic methanogens. There are two found methylotrophic pathways and the related reactions are shown in equations (1-1) and (1-2).

$4\ \text{Methanol} \rightarrow 3CH_4 + CO_2 + 2H_2O$

$\Delta G^{o'} = -106$ kJ/reaction

(Equation 1-1)

$H_2 + \text{Methanol} \rightarrow CH_4 + H_2O$

$\Delta G^{o'} = -113$ kJ/reaction

(Equation 1-2)

The recognized methylotrophic archaea include *Paracoccus aminophilus* or *Alphaproteobacteria* (Dziewit et al., 2015), *Methanomassiliicoccales, Candidatus Methanofastidiosa, Verstraetearchaeota* (Vanwonterghem et al., 2016), *Methylobacterium extorquens, Methylobacterium extorquens, Silicibacter pomeroyi, Granulibacter bethesdensis, Burkholderia phymatum, Methylibium petroleiphilum, Methylobacillus flagellates, Methylococcus capsulatus,* and *Verrucomicrobia* (Chistoserdova et al., 2009).

3. Microbial community assembly and succession mechanisms

Many ecological theories have been applied to understand the dynamics of the microbial communities (Ofiteru et al., 2010; Wang et al., 2013). Two major ecological theories exist to explain community assembly and succession mechanisms: neutral theory and niche-based

theory. Niche-based theory states that there is a strong connection between taxonomy attributes and the environmental factors (Pholchan et al., 2013; Vanwonterghem et al., 2014b), whereas neutral theory discards the competition factors in favor or attributing changes in the population to stochastic birth, death, and immigration processes (Woodcock et al., 2007).

3.1 Deterministic mechanism

The traditional niche-based theory stresses that deterministic factors including operational conditions (such as pH, temperature, HRT/SRT, etc), substrate availability (such as inoculum, substrate, perturbation, organic accumulations, etc), and interspecies interactions (such as competition, coexists, etc). It has been demonstrated in many studies that temperature and/or pH regulates deterministic process and the succession of microbial interaction in anaerobic process (De Vrieze et al., 2015; Latif et al., 2017; Lin et al., 2017; Luo et al., 2015; Lv et al., 2013; Wang et al., 2014). There are also many researches illustrating the microbial community structures are shaped by substrates, inhibitors (such as ammonia, high COD, etc), trace nutrients, and/or environmental perturbations (Cai et al., 2017; Chen et al., 2012; De Vrieze et al., 2015; Goux et al., 2015; Park et al., 2018a; Park et al., 2018b; Peces et al., 2018; Razaviarani & Buchanan, 2015).

3.2 Stochastic mechanism

It is assumed in neutral theory that species dynamics are controlled by stochastic process rather than competition and all species or individuals have equivalent functions ecologically (Chave, 2004; Etienne & Olff, 2004; Hubbell, 2001; Zhou & Ning, 2017). There are two contradictories with the fundamental concepts of the niche-based theory, in which stated that (1) all species are ecologically and functionally different and (2) environments are important determinants species distribution. Nevertheless, neutral theory managed to predict some ecological patterns better than niche theory especially in species abundant distribution (Hubbell, 2001; Matthews & Whittaker, 2014).

3.3 Two mechanism jointly determine the community assembly

An agreement has been gradually reached that the community assembly is jointly determined by both deterministic and stochastic processes. However, there is still debate on which mechanism is predominant.

Many researches show that deterministic process predominated the microbial community assembly with little stochastic contribution (Akyol et al., 2016; Lucas et al., 2015; Peces et al., 2018; Tonini et al., 2016; Venkiteshwaran et al., 2015; Wang et al., 2018). Peces et al illustrated that the long-term anaerobic digestion microbiome and its functionality was defined by deterministic factors despite distinct initial microbial community (Peces et al., 2018). Similar conclusion has been drawn by Vanwontergham et al that long-term synchronized population dynamics was guided by deterministic processes in their set-up of replicate anaerobic digesters (Vanwonterghem et al., 2014a). Hu et al concluded that the vertical distribution of bacterial communities in plateau permafrost core was governed by deterministic ecological selection although stochastic processes also contributed by taxonomic and phylogenetic ta diversity analysis (Hu et al., 2015).

On the contrary, there are a number of studies assert that stochastic is likely a major determinant of their system. Caruso et al applied neutral model on 92 dessert locations worldwide and only four cases rejected the neutral model, three cases had a dissimilarity converge while the data from the remaining cases were all consistent with the neutral models, which indicated that the population dynamic can be predicted by stochastic demography (Caruso et al., 2011). Zhou et al set up fourteen single chamber reactors which were inoculated and fed with the same mixture of wastewater and growth medium (50/50 v/v), sampled and sequenced that biomass after two months of operation, and drew a conclusion that stochastic assembly lead to alternative communities with distinct function (Zhou et al., 2013). Graham and Stegen applied a dispersal model to show that stochastic microbial community assembly can decrease the adaptation to local environments and in turn decrease the biogeochemical function (Graham & Stegen, 2017).

A stronger role of stochasticity has also been supported by analyses of phylogenetic temporal turnover (Stegen et al., 2012).

Reference

Akyol, Ç., Turker, G., Ince, O., Ertekin, E., Üstüner, O. and Ince, B. (2016) Performance and microbial community variations in thermophilic anaerobic digesters treating OTC medicated cow manure under different operational conditions. *Bioresource Technology* 205, 191-198.

Barker, H.A. (1936) On the biochemistry of the methane fermentation. *Archives of Microbiology* 7(1), 404-419.

Cai, Y., Hua, B., Gao, L., Hu, Y., Yuan, X., Cui, Z., Zhu, W. and Wang, X. (2017) Effects of adding trace elements on rice straw anaerobic mono-digestion: Focus on changes in microbial communities using high-throughput sequencing. *Bioresource Technology* 239, 454-463.

Caruso, T., Chan, Y., Lacap, D.C., Lau, M.C.Y., McKay, C.P. and Pointing, S.B. (2011) Stochastic and deterministic processes interact in the assembly of desert microbial communities on a global scale. *The Isme Journal* 5, 1406.

Chave, J. (2004) Neutral theory and community ecology. *Ecology Letters* 7(3), 241-253.

Chen, S., Cheng, H., Liu, J., Hazen, T.C., Huang, V. and He, Q. (2017) Unexpected competitiveness of *Methanosaeta* populations at elevated acetate concentrations in methanogenic treatment of animal wastewater. *Applied Microbiology and Biotechnology* 101(4), 1729-1738.

Chen, S., Zamudio Cañas, E.M., Zhang, Y., Zhu, Z. and He, Q. (2012) Impact of substrate overloading on archaeal populations in anaerobic digestion of animal waste. *Journal of Applied Microbiology* 113(6), 1371-1379.

Chen, Y., Cheng, J.J. and Creamer, K.S. (2008) Inhibition of anaerobic digestion process: A review. *Bioresource Technology* 99(10), 4044-4064.

Chistoserdova, L., Kalyuzhnaya, M.G. and Lidstrom, M.E. (2009) The expanding world of methylotrophic metabolism. *Annual Review Microbiology* 63, 477-499.

Conklin, A., Stensel, H.D. and Ferguson, J. (2006) Growth kinetics and competition between *Methanosarcina* and *Methanosaeta* in mesophilic anaerobic digestion. *Water Environmental Resource* 78(5), 486-496.

Costa, K.C., Lie, T.J., Jacobs, M.A. and Leigh, J.A. (2013Independent growth of the hydrogenotrophic methanogen *Methanococcus maripaludis*. *mBio* 4(2).

De Vrieze, J., Saunders, A.M., He, Y., Fang, J., Nielsen, P.H., Verstraete, W. and Boon, N. (2015) Ammonia and temperature determine potential clustering in the anaerobic digestion microbiome. *Water Research* 75, 312-323.

Demirel, B. and Scherer, P. (2008) The roles of acetotrophic and hydrogenotrophic methanogens during anaerobic conversion of biomass to methane: a review. *Reviews in Environmental Science and Bio/Technology* 7(2), 173-190.

Dziewit, L., Czarnecki, J., Prochwicz, E., Wibberg, D., Schlüter, A., Pühler, A. and Bartosik, D. (2015) Genome-guided insight into the methylotrophy of *Paracoccus aminophilus JCM 7686*. *Frontiers in Microbiology* 6, 852.

Etienne, R.S. and Olff, H. (2004) A novel genealogical approach to neutral biodiversity theory. *Ecology Letters* 7(3), 170-175.

Gest, H. (2003) Biochemistry and Physiology of Anaerobic Bacteria. Ljungdahl, L.G., Adams, M.W., Barton, L.L., Ferry, J.G. and Johnson, M.K. (eds), pp. 1-10, Springer New York, New York, NY.

Goux, X., Calusinska, M., Lemaigre, S., Marynowska, M., Klocke, M., Udelhoven, T., Benizri, E. and Delfosse, P. (2015) Microbial community dynamics in replicate anaerobic digesters exposed sequentially to increasing organic loading rate, acidosis, and process recovery. *Biotechnology for Biofuels* 8.

Graham, E.B. and Stegen, J.C. (2017) Stochastic microbial community assembly decreases biogeochemical function. *bioRxiv*.

Hao, L.-P., Lü, F., He, P.-J., Li, L. and Shao, L.-M. (2011) Predominant contribution of syntrophic acetate oxidation to thermophilic methane formation at high acetate concentrations. *Environmental Science & Technology* 45(2), 508-513.

Hattori, S. (2008) Syntrophic acetate-oxidizing microbes in methanogenic environments. *Microbes Environment* 23(2), 118-127.

Henderson, G., Cox, F., Ganesh, S., Jonker, A., Young, W., Global Rumen Census, C., Abecia, L., Angarita, E., Aravena, P., Nora Arenas, G., Ariza, C., Attwood, G.T., Mauricio Avila, J., Avila-Stagno, J., Bannink, A., Barahona, R., Batistotti, M., Bertelsen, M.F., Brown-Kav, A., Carvajal, A.M., Cersosimo, L., Vieira Chaves, A., Church, J., Clipson, N., Cobos-Peralta, M.A., Cookson, A.L., Cravero, S., Cristobal Carballo, O., Crosley, K., Cruz, G., Cerón Cucchi, M., de la Barra, R., De Menezes, A.B., Detmann, E., Dieho, K., Dijkstra, J., dos Reis, W.L.S., Dugan, M.E.R., Hadi Ebrahimi, S., Eythórsdóttir, E., Nde Fon, F., Fraga, M., Franco, F., Friedeman, C., Fukuma, N., Gagić, D., Gangnat, I., Javier

Grilli, D., Guan, L.L., Heidarian Miri, V., Hernandez-Sanabria, E., Gomez, A.X.I., Isah, O.A., Ishaq, S., Jami, E., Jelincic, J., Kantanen, J., Kelly, W.J., Kim, S.-H., Klieve, A., Kobayashi, Y., Koike, S., Kopecny, J., Nygaard Kristensen, T., Julie Krizsan, S., LaChance, H., Lachman, M., Lamberson, W.R., Lambie, S., Lassen, J., Leahy, S.C., Lee, S.-S., Leiber, F., Lewis, E., Lin, B., Lira, R., Lund, P., Macipe, E., Mamuad, L.L., Cuquetto Mantovani, H., Marcoppido, G.A., Márquez, C., Martin, C., Martinez, G., Eugenia Martinez, M., Lucía Mayorga, O., McAllister, T.A., McSweeney, C., Mestre, L., Minnee, E., Mitsumori, M., Mizrahi, I., Molina, I., Muenger, A., Muñoz, C., Murovec, B., Newbold, J., Nsereko, V., O'Donovan, M., Okunade, S., O'Neill, B., Ospina, S., Ouwerkerk, D., Parra, D., Pereira, L.G.R., Pinares-Patiño, C., Pope, P.B., Poulsen, M., Rodehutscord, M., Rodriguez, T., Saito, K., Sales, F., Sauer, C., Shingfield, K., Shoji, N., Simunek, J., Stojanović-Radić, Z., Stres, B., Sun, X., Swartz, J., Liang Tan, Z., Tapio, I., Taxis, T.M., Tomkins, N., Ungerfeld, E., Valizadeh, R., van Adrichem, P., Van Hamme, J., Van Hoven, W., Waghorn, G., John Wallace, R., Wang, M., Waters, S.M., Keogh, K., Witzig, M., Wright, A.-D.G., Yamano, H., Yan, T., Yáñez-Ruiz, D.R., Yeoman, C.J., Zambrano, R., Zeitz, J., Zhou, M., Wei Zhou, H., Xia Zou, C., Zunino, P. and Janssen, P.H. (2015) Rumen microbial community composition varies with diet and host, but a core microbiome is found across a wide geographical range. *Scientific Reports* 5, 14567.

Hori, T., Haruta, S., Ueno, Y., Ishii, M. and Igarashi, Y. (2006) Dynamic transition of a methanogenic population in response to the concentration of volatile fatty acids in a thermophilic anaerobic digester. *Applied Environmental Microbiology* 72(2), 1623-1630.

Hu, W., Zhang, Q., Tian, T., Li, D., Cheng, G., Mu, J., Wu, Q., Niu, F., Stegen, J.C., An, L. and Feng, H. (2015) Relative roles of deterministic and stochastic processes in driving the vertical distribution of bacterial communities in a permafrost core from the Qinghai-Tibet Plateau, China. *PLoS ONE* 10(12), e0145747.

Hubbell, S.P. (2001) The unified neutral theory of biodiversity and biogeography, Princeton, N.J.: Princeton University Press, Princeton, N.J.

Latif, M.A., Mehta, C.M. and Batstone, D.J. (2017) Influence of low pH on continuous anaerobic digestion of waste activated sludge. *Water Research* 113, 42-49.

Leite, A., Janke, L., Lv, Z., Harms, H., Richnow, H.-H. and Nikolausz, M. (2015) Improved monitoring of semi-continuous anaerobic digestion of sugarcane waste: Effects of increasing organic loading rate on methanogenic community dynamics. *International Journal of Molecular Sciences* 16(10), 23210.

Lin, Q., De Vrieze, J., Li, C., Li, J., Li, J., Yao, M., Hedenec, P., Li, H., Li, T., Rui, J., Frouz, J. and Li, X. (2017) Temperature regulates deterministic processes and the succession of microbial interactions in anaerobic digestion process. *Water Research* 123, 134-143.

Lucas, R., Kuchenbuch, A., Fetzer, I., Harms, H. and Kleinsteuber, S. (2015) Long-term monitoring reveals stable and remarkably similar microbial communities in parallel full-scale biogas reactors digesting energy crops. *FEMS Microbiology Ecology* 91(3), fiv004-fiv004.

Luo, G., De Francisci, D., Kougias, P.G., Laura, T., Zhu, X. and Angelidaki, I. (2015) New steady-state microbial community compositions and process performances in biogas reactors induced by temperature disturbances. *Biotechnology for Biofuels* 8.

Lv, W., Zhang, W. and Yu, Z. (2013) Evaluation of system performance and microbial communities of a temperature-phased anaerobic digestion system treating dairy manure: Thermophilic digester operated at acidic pH. *Bioresource Technology* 142, 625-632.

Müller, B., Sun, L. and Schnürer, A. (2013) First insights into the syntrophic acetate-oxidizing bacteria – a genetic study. *Microbiology Open* 2(1), 35-53.

Manyi-Loh, C.E., Mamphweli, S.N., Meyer, E.L., Okoh, A.I., Makaka, G. and Simon, M. (2013) Microbial anaerobic digestion (bio-digesters) as an Approach to the Decontamination of Animal Wastes in Pollution Control and the Generation of Renewable Energy. *International Journal of Environmental Research and Public Health* 10(9), 4390-4417.

Matthews, T.J. and Whittaker, R.J. (2014) Neutral theory and the species abundance distribution: recent developments and prospects for unifying niche and neutral perspectives. Ecological Evolution 4(11), 2263-2277.

McHugh, S., Carton, M., Mahony, T. and O'Flaherty, V. (2003) Methanogenic population structure in a variety of anaerobic bioreactors. *FEMS Microbiology Letter* 219(2), 297-304.

McInerney, M.J., Rohlin, L., Mouttaki, H., Kim, U., Krupp, R.S., Rios-Hernandez, L., Sieber, J., Struchtemeyer, C.G., Bhattacharyya, A., Campbell, J.W. and Gunsalus, R.P. (2007) The genome of *Syntrophus aciditrophicus*: Life at the thermodynamic limit of microbial growth. *Proceedings of the National Academy of Sciences* 104(18), 7600-7605.

Merlino, G., Rizzi, A., Schievano, A., Tenca, A., Scaglia, B., Oberti, R., Adani, F. and Daffonchio, D. (2013) Microbial community structure and dynamics in two-stage vs single-stage thermophilic anaerobic digestion of mixed swine slurry and market bio-waste. *Water Research* 47(6), 1983-1995.

Mosbæk, F., Kjeldal, H., Mulat, D.G., Albertsen, M., Ward, A.J., Feilberg, A. and Nielsen, J.L. (2016) Identification of syntrophic acetate-oxidizing bacteria in anaerobic digesters by

combined protein-based stable isotope probing and metagenomics. *The Isme Journal* 10, 2405.

Nozhevnikova, A.N., Simankova, M.V., Parshina, S.N. and Kotsyurbenko, O.R. (2001) Temperature characteristics of methanogenic archaea and acetogenic bacteria isolated from cold environments. *Water Science and Technology* 44(8), 41-48.

Ofiteru, I.D., Lunn, M., Curtis, T.P., Wells, G.F., Criddle, C.S., Francis, C.A. and Sloan, W.T. (2010) Combined niche and neutral effects in a microbial wastewater treatment community. *Proceedings of National Academy of Sciences U S A* 107(35), 15345-15350.

Park, J.-H., Kumar, G., Yun, Y.-M., Kwon, J.-C. and Kim, S.-H. (2018a) Effect of feeding mode and dilution on the performance and microbial community population in anaerobic digestion of food waste. *Bioresource Technology* 248, 134-140.

Park, J., Lee, B., Shi, P., Kwon, H., Jeong, S.M. and Jun, H. (2018b) Methanol metabolism and archaeal community changes in a bioelectrochemical anaerobic digestion sequencing batch reactor with copper-coated graphite cathode. *Bioresource Technology* 259, 398-406.

Peces, M., Astals, S., Jensen, P.D. and Clarke, W.P. (2018) Deterministic mechanisms define the long-term anaerobic digestion microbiome and its functionality regardless of the initial microbial community. *Water Research* 141, 366-376.

Pholchan, M.K., Baptista, J.d.C., Davenport, R.J., Sloan, W.T. and Curtis, T.P. (2013) Microbial community assembly, theory and rare functions. *Frontiers in Microbiology* 4(68), 1-9.

Plugge, C.M., Henstra, A.M., Worm, P., Swarts, D.C., Paulitsch-Fuchs, A.H., Scholten, J.C.M., Lykidis, A., Lapidus, A.L., Goltsman, E., Kim, E., McDonald, E., Rohlin, L., Crable, B.R., Gunsalus, R.P., Stams, A.J.M. and McInerney, M.J. (2012) Complete genome sequence of *Syntrophobacter fumaroxidans strain* (MPOB(T)). *Standards in Genomic Sciences* 7(1), 91-106.

Razaviarani, V. and Buchanan, I.D. (2015) Anaerobic co-digestion of biodiesel waste glycerin with municipal wastewater sludge: Microbial community structure dynamics and reactor performance. *Bioresource Technology* 182, 8-17.

Schmidt, F., Koch, B.P., Goldhammer, T., Elvert, M., Witt, M., Lin, Y.-S., Wendt, J., Zabel, M., Heuer, V.B. and Hinrichs, K.-U. (2017) Unraveling signatures of biogeochemical processes and the depositional setting in the molecular composition of pore water DOM across different marine environments. *Geochimica et Cosmochimica Acta* 207, 57-80.

Stegen, J.C., Lin, X., Konopka, A.E. and Fredrickson, J.K. (2012) Stochastic and deterministic assembly processes in subsurface microbial communities. *The Isme Journal* 6(9), 1653-1664.

Stibal, M., Wadham, J.L., Lis, G.P., Telling, J., Pancost, R.D., Dubnick, A., Sharp, M.J., Lawson, E.C., Butler, C.E.H., Hasan, F., Tranter, M. and Anesio, A.M. (2012) Methanogenic potential of Arctic and Antarctic subglacial environments with contrasting organic carbon sources. *Global Change Biology* 18(11), 3332-3345.

Summers, Z.M., Fogarty, H.E., Leang, C., Franks, A.E., Malvankar, N.S. and Lovley, D.R. (2010) Direct exchange of electrons within aggregates of an evolved syntrophic coculture of anaerobic bacteria. *Science* 330(6009), 1413-1415.

Tonini, D., Hamelin, L. and Astrup, T.F. (2016) Environmental implications of the use of agro-industrial residues for biorefineries: application of a deterministic model for indirect land-use changes. *GCB Bioenergy* 8(4), 690-706.

Vanwonterghem, I., Evans, P.N., Parks, D.H., Jensen, P.D., Woodcroft, B.J., Hugenholtz, P. and Tyson, G.W. (2016) Methylotrophic methanogenesis discovered in the archaeal phylum *Verstraetearchaeota*. *Nature Microbiology* 1, 16170.

Vanwonterghem, I., Jensen, P.D., Dennis, P.G., Hugenholtz, P., Rabaey, K. and Tyson, G.W. (2014a) Deterministic processes guide long-term synchronised population dynamics in replicate anaerobic digesters. The Isme Journal 8(10), 2015-2028.

Vanwonterghem, I., Jensen, P.D., Ho, D.P. and Tyson, D.J.B.a.G.W. (2014b) Linking microbial community structure, interactions and function in anaerobic digesters using new molecular techniques. *Current Opinion in Biotechnology* 27, 55-64.

Venkiteshwaran, K., Bocher, B., Maki, J. and Zitomer, D. (2015) Relating anaerobic digestion microbial community and process function. *Microbiology Insights 8*(Suppl 2), 37-44.

Wang, J., Shen, J., Wu, Y., Tu, C., Soininen, J., Stegen, J.C., He, J., Liu, X., Zhang, L. and Zhang, E. (2013) Phylogenetic beta diversity in bacterial assemblages across ecosystems: deterministic versus stochastic processes. *Isme journal* 7(7), 1310-1321.

Wang, K., Yin, J., Shen, D. and Li, N. (2014) Anaerobic digestion of food waste for volatile fatty acids (VFAs) production with different types of inoculum: Effect of pH. *Bioresource Technology* 161, 395-401.

Wang, P., Yu, Z., Zhao, J. and Zhang, H. (2018) Do microbial communities in an anaerobic bioreactor change with continuous feeding sludge into a full-scale anaerobic digestion system? *Bioresource Technology* 249, 89-98.

Westerholm, M., Levén, L. and Schnürer, A. (2012) Bioaugmentation of syntrophic acetate-oxidizing culture in biogas reactors exposed to increasing levels of ammonia. *Applied Environmental Microbiology* 78(21), 7619-7625.

Westerholm, M., Müller, B., Singh, A., Karlsson Lindsjö, O. and Schnürer, A. (2018) Detection of novel syntrophic acetate-oxidizing bacteria from biogas processes by continuous acetate enrichment approaches. *Microbial Biotechnology* 11(4), 680-693.

Westerholm, M., Moestedt, J. and Schnürer, A. (2016) Biogas production through syntrophic acetate oxidation and deliberate operating strategies for improved digester performance. *Applied Energy* 179, 124-135.

Woodcock, S., van der Gast, C.J., Bell, T., Lunn, M., Curtis, T.P., Head, I.M. and Sloan, W.T. (2007) Neutral assembly of bacterial communities. *FEMS Microbiology Ecology* 62(2), 171-180.

Wu, C., Liu, X. and Dong, X. (2006) Syntrophomonas cellicola sp. nov., a spore-forming syntrophic bacterium isolated from a distilled-spirit-fermenting cellar, and assignment of *Syntrophospora bryantii* to *Syntrophomonas bryantii comb. nov. International Journal of Systematic and Evolutionary Microbiology* 56(Pt 10), 2331-2335.

Zhao, Z., Zhang, Y., Yu, Q., Dang, Y., Li, Y. and Quan, X. (2016) Communities stimulated with ethanol to perform direct interspecies electron transfer for syntrophic metabolism of propionate and butyrate. *Water Research* 102, 475-484.

Zheng, D. and Raskin, L. (2000) Quantification of *Methanosaeta* species in anaerobic bioreactors using genus- and species-specific hybridization probes. *Microbial Ecology* 39(3), 246-262.

Zhou, J., Liu, W., Deng, Y., Jiang, Y.-H., Xue, K., He, Z., Van Nostrand, J.D., Wu, L., Yang, Y. and Wang, A. (2013) Stochastic assembly leads to alternative communities with distinct functions in a bioreactor microbial community. *mBio* 4(2).

Zhou, J. and Ning, D. (2017) Stochastic community assembly: Does it matter in microbial ecology? *Microbiology and Molecular Biology Reviews* 81(4).

Zinder, S.H. and Koch, M. (1984) Non-aceticlastic methanogenesis from acetate: acetate oxidation by a thermophilic syntrophic coculture. *Archives of Microbiology* 138(3), 263-272.

Appendix: Tables and Figures

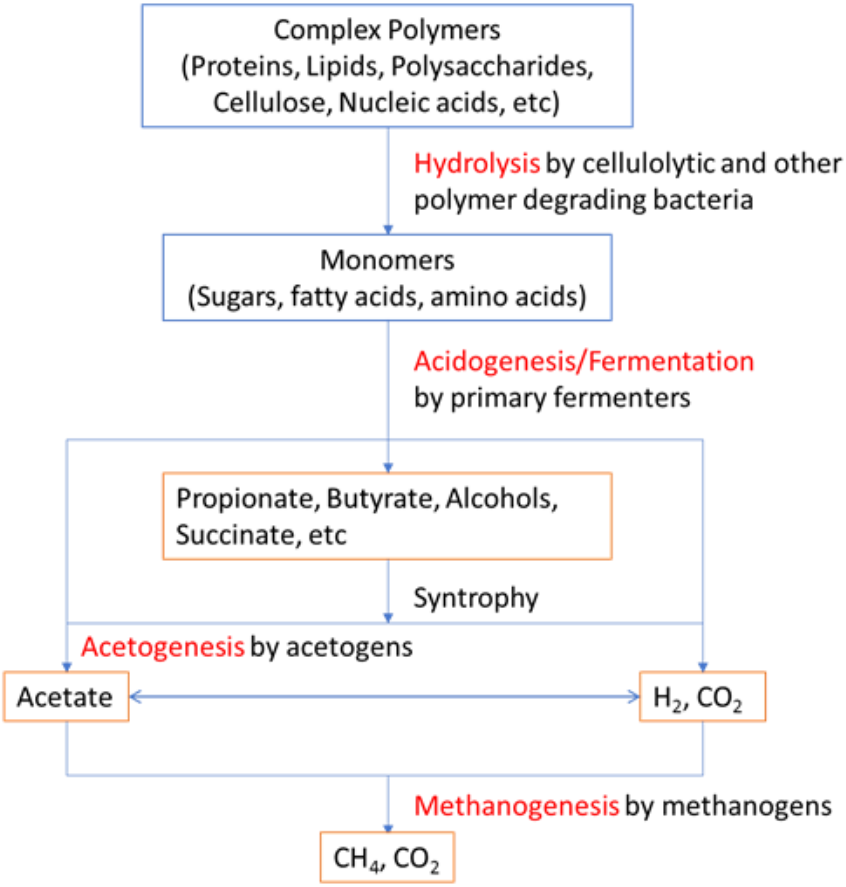

Figure 1-1. Anaerobic decomposition food web.

CHAPTER II - CHARACTERIZATION OF POPULATION SHIFT IN METHANOGENIC COMMUNITIES OF RIGOROUSLY REPLICATED ANAEROBIC DIGESTERS

Abstract

Microbial communities are involved in various engineered waste treatment process as well as diverse natural systems. The mechanisms of assembly in these complex communities are of great importance for the modeling and control of biological treatment processes. Among the four assembly mechanisms, ie. selection, dispersal, speciation, and drift, drift is the most difficult one to study as it is easily masked by other factors. In this study, the contribution of drift is analyzed by setting up thirteen rigorously replicated anaerobic digesters. The performance and microbial community structure of were monitored over a one-year to assess the significance of population changes during the assembly of methanogenic communities. The replicate digesters were inoculated with the same culture and maintained under identical operational and environmental conditions. To prevent potential influences from the immigration of microbial populations in the feed, sterile sucrose was used as the sole substrate for all replicates. The microbial communities in the 13 replicates were profiled with 16S rRNA amplicon library sequencing at two time points 110 days (3.5 SRT) apart after conditions of stable methane production, substrate utilization, and acetate concentration were reached. The community structure across the two time points differed significantly indicating considerable population change long after stable performance conditions were reached. However, despite the change in community composition between time points, overall community structure was remarkably consistent among the 13 replicates, indicating that non-random mechanisms such as selective pressure shapes the changing trajectory of the community structure over long periods of time. Overall community function, as suggested by metagenomics functional analysis, was maintained even as the community structure changes through swapping of OTUs playing similar metabolic and ecological roles, providing evidence of functional redundancy.

Keywords

Anaerobic digestion, microbial community population dynamics, selection, ecological drift, functional redundancy.

1. Introduction

Microbial communities play essential roles in many ecosystems, both natural and engineered. Advancement of next-generation sequencing and computational techniques has fostered interest in understanding microbiome assembly processes (Goldford et al. 2018, Nemergut et al. 2013). Conceptually, it is generally accepted that community assembly is influenced by a combination of selection, dispersal, speciation, and drift (Hanson et al. 2012, Vellend 2010, Zhou and Ning 2017). Due to the complexity of the microbial systems, there are still many limitations to connecting theorical and experimental work towards the understanding of microbial community assembly (Stegen et al. 2015). Several recent bottom-up studies have sought to improve understanding of community assembly mechanisms (Friedman et al. 2017, Goldford et al. 2018, Hekstra and Leibler 2012).

Anaerobic digestion is a sustainable process for the treatment of biodegradable organic wastes and generation of biogas as a renewable source of energy. Both bacterial and archaeal populations mediate the conversion of organic wastes to biogas through four metabolic stages: hydrolysis, acidogenesis, acetogenesis, and methanogenesis (McHugh et al. 2004). Considering the well-defined and relatively simple population structure compared to other organic waste treatment processes, anaerobic digestion provides a good model to study microbial community assembly in engineered processes. From a functional perspective, microbial communities are considered to be driven by substrate, operational conditions, and reactor configurations, etc. Previous studies have found vast diversity in the microbial communities in anaerobic digestion process, as a function of environmental disturbances and changes in operational conditions, such as pH (Wang et al. 2014, Xie et al. 2015), temperature (Chapleur et al. 2016, Scaglia et al. 2014), ammonia concentration (Ortner et al. 2014, Rajagopal et al. 2013), high COD (Ciaciuch et al. 2017, Méndez-Acosta et al. 2016), high acetate concentration (Chen and He 2015, Rodriguez-Chiang et al. 2016), and complexity of the substrates and inhibitors (García-Depraect et al. 2017, Wagner et al. 2013). Despite the wide variety of microbial compositions, a well-balanced

anaerobic digestion process always consists of fermenting bacteria, methanogenic archaea and their syntrophic partners (Ma et al. 2013, Mei et al. 2017).

It is of great importance to better understand the mechanisms of assembly in these complex microbial communities for the modeling and control of biological treatment processes. A survey of full-scale bioenergy systems suggested that syntrophic microbial communities tend to be more stable and resilient while compositions of fermentative bacteria can be characterized by greater redundancy and variability (Werner et al. 2011). A succession of patterns that exhibited increasing modularity but decreasing connectivity among microbial populations was reported during another investigation (Wu et al. 2016), suggesting that community structure changes even when digester performance is stable. However, there are still many interferences that may disturb the microbial assembly, such as the microbial immigration (Ofiţeru et al. 2010), changing substrates (McHugh et al. 2004), and ecological drift (Stegen et al. 2015).

There are four fundamental ecological processes that govern the genetic species diversity, including speciation, selection, dispersal, and ecological drift (Vellend 2010). Many recent studies have suggested that stochastic processes (drift) may play an important role in shaping the microbial community structures (Ofiţeru et al. 2010, Zhou et al. 2014, Zhou and Ning 2017). However, ecological drift is typically masked by many other influences including selection and dispersal and is difficult to identify with small number of replicates.

This study made great effort to minimize many of the factors that contribute to population diversity to better understand the relative roles of selection and ecological drift in community assembly. First, we used sterile feedstock to minimize external population immigration via the feeding process. Second, an unusually large number of anaerobic digesters, i.e. 13 replicates, were used to quantify similarities and differences in community structure across the reactors and over time. Third, a relatively simple substrate, sucrose, was used as sole substrate in this study to potentially reduce the complexity of the anaerobic microbial community. Finally, the use of completely mixed reactors minimizes micro-niches in the reactors to create uniform selective

pressure. Our experimental design minimized the potential influence of many of the mechanisms that may have contributed to microbial community variability in other studies. Nevertheless, the microbial communities in the 13 anaerobic digesters changed significantly and non-randomly over extended time periods (110 days). We observe swapping of OTUs that play similar functional roles in the community, allowing the overall stable process performance despite the lack of stability in community structure. Our results further suggest that selection plays a much larger role than ecological drift in community assembly in our system. The persistence of a dynamic community structure over long period of time suggests that the trajectory of the community structure over time may be influenced by dynamic syntrophic, competitive, and other environmental selective pressures arising from the dynamic community structure itself.

2. Materials and Methods

2.1 Anaerobic digester setup and operation

Thirteen replicate laboratory scale semi-continuous completely mixed anaerobic digestion bioreactors were maintained at 37 (±2) ℃ with a solids and hydraulic retention time of 33 days. Serum glass bottles were used as the reactors with a working volume of 160 mL with a 60 mL of head space and were sealed with butyl rubber stoppers and aluminum caps. A sterile DCB medium with 7 g/L sucrose ($C_{12}H_{22}O_{11}$) was used as the feedstock to provide a simple substrate and to prevent microbial immigration into the system. Every 1 L of the sterile DCB medium was constituted with 1.0 g NaCl, 0.5 g $MgCl_2 \cdot 6H_2O$, 0.2 g KH_2PO_4, 0.3 g NH_4Cl, 0.5 g KCl, 0.0015 g $CaCl_2 \cdot 2H_2O$, 1.5 mg $FeCl_2 \cdot 4H_2O$, 0.19 mg $CoCl_2 \cdot 6H_2O$, 0.1 mg $MnCl_2 \cdot 4H_2O$, 0.07 mg $ZnCl_2$, 0.006 mg H_3BO_3, 0.036 mg $Na_2MoO_4 \cdot 2H_2O$, 0.024 mg $NiCl_2 \cdot 6H_2O$, 0.002 mg $CuCl_2 \cdot 2H_2O$, 0.006 mg $Na_2SeO_3 \cdot 5H_2O$, 0.008 mg $Na_2WO_4 \cdot 2H_2O$, 0.5 mg NaOH, 0.25 mL 0.1% Resazurin, 0.031 g L-cysteine, 0.048g $Na_2S \cdot 9H_2O$, 2.52 g $NaHCO_3$, and 1 mL of the Wolin Vitamins (pH was adjusted to 7.2 by 1 mol/L $NaHCO_3$ and CO_2. The media was boiled, purged with 90% N_2 and 10% CO_2 to remove oxygen and then autoclaved at 120 ℃ for 20 minutes. The bioreactors were inoculated (10% v/v) with a culture obtained from previous laboratory sucrose-fed reactors, which were originally inoculated with digesters fed with cow manure and were maintained with

the same operational conditions described in this paper. BD disposable syringes with luer-lok™ tips and flame-sterilized BD PrecisionGlide™ single-use needles were used to remove 3 mL of the reactor contents and to add 3 mL of feedstock into the systems each day. The feeding process resulted in an organic loading rate of 0.021 g sucrose per reactor per day. The reactors were incubated at 37 ℃ with shaking maintained at 80 x g. At day 80, the feeding process was suspended for 3 days to allow the system to remove accumulated acetate; thereafter, feeding was resumed according to the previous schedule.

2.2 Digestion parameter analysis

2.2.1 Methane production and composition

Biogas production was measured daily using a water replacement method (Demirer and Speece 1998). Gas composition was determined using an HP 5890 gas chromatography with TCD (thermal conductivity detector), a Supelco packing column (60/80 Carbonxen®-1000), and Argon carrier gas with a flow rate of 5 ml/min (Zhu et al. 2011). The temperatures of injection, oven (column), and detection were set to 150 ℃, 125 ℃, and 170 ℃ respectively and the process time was set to 12 minutes for N_2, CH_4, and CO_2 to be fully separated and detected. The peaks of CH_4 and CO_2 appeared at 5.5 minutes and 10.5 minutes respectively. Standard curves of CH_4 and CO_2 were calibrated monthly to maintain accuracy.

2.2.2 Characteristics of digestion sludge

The temperature of the incubator was monitored daily with a thermometer and maintained at 37 (±2) ℃. The pH was measured with pH papers using waste digester slurry. Once per week, waste slurry samples were analyzed and preserved. Slurry was centrifuged at 14000 x g once a week, and the supernatant was analyzed for chemical oxygen demand (since sucrose is soluble, COD = soluble COD was assumed) and volatile fatty acid concentrations. COD was measured with CHEMetrics™ COD Vials Kits according to the standard method (Rice et al. 2012). Exactly 2 mL of the sample was mixed with the chemicals in the vial and placed into the preheated COD reactor block for 2 hours. The heated samples were cooled to room temperature and the

absorbance was determined using Spec 20 Spectrophotometer using glucose/glutamic acid substrate standards. To measure acetate and propionate concentrations, samples were acidified to pH < 2 with 0.5 mL 85% H_3PO_4 and measured by gas chromatography with FID (flame ionization detector) and a Restek Stabilwax®-DA column, using Helium as the carrier gas at a flow rate of 20 mL/min with 1:20 split ratio (Zhang and Jahng 2010). The injection and detection temperatures were set to 250 ℃ and 300 ℃ respectively. There temperature gradient for the oven (column) was: 80 ℃ for 1 minute, an increase of 10 ℃/min to 220 ℃ and maintained at 220 ℃ for 5 minutes. The centrifuged biomass was preserved at -80 ℃ for molecular analysis.

2.3 Microbial community molecular analysis

2.3.1 DNA extraction and purification

Biomass samples from Days 234 and 343 (13 reactors each day, 26 samples total) were used for genomic DNA extraction. The extractions were performed using MP FastDNA™ Spin Kit for Soil according to the manufacturer's instruction (Protocol Revision #116560200-201608). The DNA was then purified with Zymo Genomic DNA Clean & Concentrator™-10 kit according to the instructions provided by the manufacturer. The DNA concentrations were determined using Thermo Scientific NanoDrop ND-3300 Fluorospectrometer.

2.3.2 PCR amplification and 16S rRNA gene amplicon high-throughput sequencing

Polymerase chain reactions were prepared with a cocktail mix containing 12.5 μL Phusion flash Master Mix, 10 μL ultra-pure water, 1 μL forward primer, 1 μL reverse primer, and 2 μL (100 to 150 ng) DNA template. Each universal primer pair was designed to target the V4 region of bacterial and archaeal 16S rRNA genes: forward primer 515F (GTGCCAGCMGCCGCGGTAA) with 5' Illumina adapter (AATGATACGGCGACCACCGAGATCTACAC), forward primer pad (TATGGTAATT), and forward primer link (GT); reverse primer 806R (GGACTACHVGGGTWTCTAAT), with adapter (CAAGCAGAAGACGGCATACGAGAT), link (CC), and a unique 12-base specific barcode for each sequence. The PCR program included one cycle of 94 ℃ for 3 minutes, followed by 35 cycles at 94 ℃ for 45 seconds (denaturation), 55 ℃ for 1 minute (annealing), and 72 ℃ for 1 minute and a half (elongation), a final extension at

72 ℃ for 10 minutes, and then stored at 4 ℃. After the program finished, the samples were run on an Agilent 2100 Bioanalyzer Instruments with Agilent DNA 7500 chips to ensure the amplicon quality and measure the DNA concentrations. Post PCR, amplicons were pooled (a set of 9 or 10) based on the peak height from Agilent DNA 7500 analyses and the concentrations were measured using KAPA Illumina kit for quantifying library (KK4824) from KAPA Biosystems. Samples were pooled again according to the results and number of sequences desired into a final sample and the concentration was measure again with the KAPA quantifying kit. 4 nM pooled libraries were diluted with 10 mM Tris/0.05% tween buffer (pH = 8.5) and denatured with 0.2 N freshly made NaOH solution. The sample was then combined with 20% PhiX control kit to increase the library diversity. The mixture was incubated at 96 ℃ for 2 minutes using a heat block and then put into a water-ice bath for 5 minutes. After the sample was loaded, an Illumina MiSeq System with a MiSeq Reagent Kit v2 (300-cycles) and Metagenomic workflow was selected to execute the 16S protocol using the MiSeq Reporter software (MSR).

2.3.3 Bioinformatics analysis

Amplicon sequences were processed using the CLC Genomic Workbench 9.5.3 with microbial genomic module. First, the sequences were aligned to merge the forward and reverse readings and discard pairs with more than 3 mismatches. Then the merged reads were trimmed at 0.001, discarding sequences less than 250 base pairs (bp). OTUs were determined using a reference-based OTU clustering module with SILVA 16S v 128 97% database (Yilmaz et al. 2014). OTU assignments were based on a similarity threshold of 97%, with a minimum occurrence of 2, chimera crossover cost of 3, and maximum unaligned end mismatches of 5.

The metagenomic content of the samples was inferred based on the 16S rRNA marker genes by PICRUSt (phylogenetic investigation of communities by reconstruction of unobserved states) software package (Morgan et al. 2013). The amplicon sequences were reclassified by QIIME2 (Caporaso et al. 2010) using Greengenes gene database (DeSantis et al. 2006) and an OTU biom table was created and imported into PICRUSt on the Langille Lab PICRUSt Galaxy Instance web platform (Afgan et al. 2016) for functional gene prediction. The biom file was first

normalized by copy number, followed by prediction of the metaphome using KEGG (Kyoto Encyclopedia of Genes and Genomes) orthologs and categorized by function with KEGG pathways at Hierarchy level 3.

2.4 Statistical analysis

Analysis of variance (ANOVA) statistical models were used to analyze differences in methane production, COD, and acetate concentration among the 13 replicates. Chao richness index, Shannon diversity index, and phylogenetic diversity index were calculated to represent the species ecology. A principal coordinate analysis (PCOA) method using weighted UniFrac distance according to the relative abundance of the OTUs was used to determine the similarity and difference of the community structures. A heatmap showing the relative abundance of OTUs was made by the MATLAB heatmap chart function. T-test, Analysis of dissimilarity (ANOSIM), Pearson's Correlation and microbial networks were calculated by Excel and the R packages ggplot2, reshape2, scales, ggcorrplot, and vegan.

3. Results and Discussion

3.1 Digester performance

Thirteen replicate semi-continuous anaerobic bioreactors were inoculated with a common seed and operated for a year at 37 ℃ under complete mix conditions. Sucrose (7 g/L/d; initial COD = 7,860 mg/L) was added to each anaerobic bioreactor as the sole substrate. During the first 100 days of operation, bioreactor performance was unsteady as the population adapted to the process conditions. Around day 75, COD and acetate concentrations increased, and detectable levels of propionate were observed. A few days later, methane production decreased, then rebounded (Figure 2-1), with propionate no longer being detected and digester performance becoming stable after day 130. During the stable period, the average daily methane production ranged between 65 and 80 mL/L with an average level of 74 mL/L. Sucrose utilization was 90% based on a theoretical methane production of 82 mL/L/d and was greater than 90% based on COD removal. More than 80% of the remaining COD could be attributed to acetate. Paired-sample Student *t*-

tests assuming equal variance were run for every pair of the bioreactors (i.e. $^{2}C_{13} = 78$ pairs were tested) for methane production, COD, and acetate concentration, respectively. The results suggested that there were no significant differences among these reactors ($t_{obs} < t_{crit}$ and p-value $> 0.05 = \alpha$ is always true). The two sampling points on days 234 and 243 had stable operation with more than 3 HRT in between.

3.2 Microbial community variations and population shifts

Microbial community analysis was conducted on samples collected on days 234 and 343. Both sampling days occurred while all the replicates were maintained under the same operational and environmental conditions and the performance of the reactors were stable. After trimming and filtering, a total of 435,357 high-quality reads were obtained from amplicon library sequencing, yielding 1331 unique OTUs using the Silva 16SrRNA database and 97% within-sequence-similarity (Yilmaz et al. 2014). A total of 472 non-singlet OTUs were observed, including 420 from the domain Bacteria and 52 from the domain Archaea. The richness and diversity of the microbial communities in the replicate bioreactors did not exhibit significant changes after 109 days of operation, with the average Chao richness index being 109.0 and 112.0 on day 234 and 343, respectively (Table 2-1). Similarly, the average Shannon diversity index and phylogenetic diversity index showed no significant change during the same period of operation (no significant difference of the diversity index between the two time points according to *t*-test).

To visualize changes in the microbial community between the two sampling days, the community structure was compared by principal coordinate analysis (PCoA) using weighted UniFrac distance according to the relative abundance of the OTUs. Bioreactor samples from day 234 and 343 formed two distinct clusters (Figure 2-2), indicating the directional shift in microbial community structure from day 234 to day 343. However, the clustering pattern for replicate bioreactor samples from the same day shows evidence of variations in the community composition of replicate bioreactors.

3.2.1 Variations in microbial community composition among replicates

Although the principal coordinate analysis suggested the similarity of the microbial community across the 13 replicates, there are still variances in the community structure. Analysis of dissimilarity (ANOSIM) was used to test the difference in microbial communities among the reactors between days 234 and 343. A matrix of dissimilarity scores for every pair of reactors was calculated and then converted to ranks. Despite the similarities in performance among the replicate bioreactors, dissimilarity in microbial community structure was not negligible. The result (Figure 2-3) clearly demonstrated the significant difference of microbial communities between the two sampling days while the distributions of dissimilarity scores are similar on the two days. The dissimilarity ranks between and within the two sampling days are listed in Table 2-S1. The scores on day 343 are slightly higher than day 234, suggesting a modest increase in diversity over time.

To further characterize the variability of the microbial populations, RRA (ratio of relative abundance) is defined to describe as the ratio (in log 2 scale) of relative abundance of one OTU of a pair of reactors (relative abundance of reactor 1 it of reactor 2). For each OTU with an average relative abundance greater than 0.5%, the RRA of each pair of replicates was determined, which means there are ${}^{2}C_{13}$ (78) RRA values got for each selected OTU. The closer the RRA value is to 0, the smaller the variation. OTUs with RRA values greater than 1 are considered to be highly variable among the replicates. The result is demonstrated in Figure 2-S1 on each pair of reactors and Figure 2-4 on each OTU. Most OTUs are quite comparable among the replicates with only a few OTUs (OTU 4, *Methanobacterium,* and OTU 8, *Lentimicrobiaceae* belonging to *Bacteroidetes*, in Day 234, and OTU 13, *Spirochaetaceae,* OTUs 16 and 23, *Pelolinea* affiliated to *Chloroflexi*, and OTU 17, *Reikenellaceae* classified *to Bacteroidetes* in Day 343) having median values greater than 1 suggesting those OTUs varied the most. The most variant OTUs seemed to appear randomly since the two sampling days did not share the same variant OTUs. One possible reason for the variation is that the OTUs were experiencing their transition during the sampling time points. For example, the average relative abundance of OTU

8 was only 0.8% on day 234 while it jumped to 6.8% (the 4th most abundant) on day 343. It is indicated in Figure 4 that the RRA for OTU 8 (the most variant OTU on day 234) was extremely high on day 234 but low on day 343. It may be explained that OTU 8 was at the beginning of the rising edge around day 234 and the exact time for the start point was a little different for each reactor despite the same trend and final state. The same phenomenon and justification can be applied to OTUs 4 and 10 (the second and third most variant OTUs on day 234).

To examine the level of overall variability in each reactor, CRRA (cumulative ratio of relative abundance) was defined. $CRRA_i = \Sigma RRA_i/N$, where $CRRA_i$ is the cumulative ratio of relative abundance of bioreactor i; RRA is the ratio of relative abundance of reactor i paired with every other reactor; N is the number of OTUs. The result is illustrated in Figure 2-S2, which suggests slightly higher variability in the microbial community assembly in most reactors on day 343 than day 234, agreeing with the results from ANOSIM.

3.2.2 Changes in microbial community and variability among replicates cannot be explained by ecological drift

Mechanisms responsible for community assembly include selection, dispersal, speciation, and drift (Velland, 2010). In the experimental design, dispersion (movement of microorganisms in space) occurs during daily sampling in which 1/33 of the organisms are removed from the reactor. During the subsequent 24 hours, new cells grow to replace those removed during sampling and cells that die. Together, sampling, cell death and cell growth provide opportunity for the community structure to change over time. Under assumptions of unbiased sampling, no speciation, and neutral regrowth (no selective pressure) the magnitude of ecological drift (random changes in population related to stochasticity during sampling and growth processes) can be estimated via stochastic simulations of the population dynamics under neutral model assumptions (see supplemental materials for details). The analysis shows that for systems characterized by large microbial populations, variations in populations through ecological drift are negligible (Figure 2-S3). Given that our experimental design eliminates many other sources of community structure change, such as dispersion of external cells into the reactor, selection

may be the predominant mechanism driving changes in population that occur over time. The dynamic community structure likely changes the syntrophic, competitive, and environmental conditions in the reactor, creating new selective pressures that continue to drive population changes. The similarity of time-dependent population shifts among replicate reactors, further described in the next section, lends strong evidence that deterministic processes – such as selective pressure – play a large role in community assembly.

3.2.3 Population shifts

Overall 134 genera affiliated with 29 phyla were identified. Figure 2-5 demonstrates the relative abundance of different archaeal and bacterial populations among the biomass samples collected from the 13 reactors on day 234 and day 343 at the phylum and genus levels. Although some variation among all the reactors was observed, the overall population structures in replicate reactors on a given day are very similar. The archaeal population was composed entirely of methanogenic archaea. The average relative abundance of Archaea population across the 13 reactors were 19.58±4.54% and 19.76±2.05% on days 234 and 343 respectively. The distribution of the 420 bacterial OTU into the major phyla on day 234 is as follows: *Thermotogae* 24.54±3.25%, *Firmicutes* 14.26±1.75%, *Spirochaetae* 14.39±1.54%, *Cloacimonetes* 8.07±2.94%, *Bacteroidetes* 6.98±1.34%, *Chloroflexi* 4.85±2.11%, *Synergistetes* 3.26±1.11%, *Proteobacteria* 2.04±0.56, and others 2.03±1.82%. On day 343, an obvious increase (88%) was observed for *Firmicutes* (26.86±2.12%) while dramatic decrease happened with *Thermotogae* (5.62±1.44%). Meanwhile, *Spirochaetae* (18.08±2.35%), *Chloroflexi* (7.34±1.93%), and *Synergistetes* (4.44±2.97%) increased slightly, while *Cloacimontes* (7.29±0.97%), *Bacteroidetes* (7.51±1.92%), *Proteobacteria* (1.96±0.02), and others (2.63±1.35%) remained constant (within 1 %).

To further investigate the function of the microbial communities, the 15 archaeal and bacterial genera exhibiting significant changes in relative abundance between the two sampling days are compared in Figure 2-6. The overall relative abundance of the archaeal population remained constant, consistent with the stable level of methane. Among all the populations, *Mesotogae*, a

rare mesophilic genus of the phylum *Thermotogae* (Ben Hania et al. 2015), was the most abundant member of the bacterial community on day 234. The abundance of *Mosotogae* in our mesophilic sucrose-fed digester was surprising since the genus has been reported to grow on various sugars, peptides and organic acids (Ben Hania et al. 2015). However, the population of *Mosotogae* decreased dramatically from around 25% on day 234 to 5% on day 343 without any environmental or chemical perturbation. At the same time, *Firmicutes* became the most abundant phylum followed by *Spirochaetae*. There were many OTUs of the phylum *Firmicutes*, but among them, only one genus, the *Trichococcus*, accounted for the increase in abundance of this phylum. This group of genera are aerotolerant, fermentative organisms that grow on sugars such as glucose, sucrose, and lactose to produce acids such as lactate, acetate, formate (Liu et al. 2002). The concominant changes in relative abundance of *Trichococcus* and *Mosotogae* across all reactors is illustrated in Figure 2-S3, which lends strong evidence that the change is deterministic.

The phenomenon of one group of bacteria decreasing accompanied by an increase in another group with the same function was observed repeatedly in our results. For example, within the phylum *Bacteroidetes*, *Proteiniphilum* and *Blivii28* were predominant on day 234 but had become less prevalent on day 343 while uncultured *Lentimicrobiaceae* (family) and uncultured *Porphyromonadaceae* (family) had increased from low levels on day 234 to become the predominant *Bacteroidetes* by day 343. The uncultured *Porphyromonadaceae* (family) and *Proteiniphilum* belonged to the same family, which ferment sugars through glucose metabolism to produce lactate, acetate, butyrate and isobutyrate (Jabari et al. 2012). *Blivii28*, a member of family *Rikenellaceae*, grows fermentatively on sugars to produce acetate, H_2, an CO_2 (Su et al. 2014). Family *Lentimicrobiaceae* has also been reported to produce fatty acids and H_2 from glucose and sugars (Sun et al. 2016). Overall, these examples illustrate why the performance of the digester remained steady despite significant shifts in the overall microbial community.

3.3 Prediction of organismal traits suggesting stable microbial function

The significant changes in the microbial community could be considered surprising given that the reactors were operated under conditions of constant temperature, pH, shaking, HRT/SRT and substrate composition and loading. Furthermore, biomass sampling and feeding operations were performed with a flame sterilized needle, minimizing potential for introducing organisms from the external environment. These factors, along with the consistency of the community structure across 13 replicate reactors, lead to the conclusion that the changes in community are likely driven by the community structure itself.

PICRUSt analysis (Morgan et al. 2013) was used to further investigate the functional gene pathways in the reactors. Major functional gene pathways relevant to metabolism, cellular, environmental information processing, human diseases, organismal system, and genetic information processing were investigated. The pathways were classified into 328 functional KEGG pathways at Hierarchy level 3. Analysis of metabolism genes and pathways associated with sugar degradation, fatty acids reduction, and methane production indicated that the abundance of functional genes responsible for the major metabolic pathways remained relatively constant from day 234 to day 343 (Figure 7). In addition, across all pathways, differences from day 234 to day 343 in the number of amplified genes belonging to a particular pathway could be attributed to chance at the 95% confidence level via an assumed-equal-variance two-way student t-test ($t_{obs} = -0.03 < 2.02 = t_{crit}$ and p-value $= 0.976 > 0.05 = \alpha$).

This result is consistent with the conclusion from the previous section that the ecological functions of the archaeal and bacterial populations remained constant despite changes in the microbial community. However, the cause of the population shift remains unknown. Two major ecological theories exist to explain community assembly mechanisms: neutral theory and niche-based theory. Neutral theory discards the competition factors in favor or attributing changes in the population to stochastic birth, death, and immigration processes. However, according to this theory, the community structure should diverge across replicate digesters because of the random population drift, which was not observed in the 13 replicates in this research. On the contrary,

the niche-based theory states that there is a strong connection between taxonomy attributes and the environmental factors (Pholchan et al. 2013, Vanwonterghem et al. 2014). The unchanged exterior environmental condition in this study indicates the shift of microbial community may be caused by interior factors such as changes in intermediates or varied community structure.

3.4 Microbial interaction networks describing the population drift

In several instances, competition between two or more OTUs affiliated with the same genus or family was observed in the microbial network based on correlation between major OTUs (relative abundance greater than 0.5%) on days 234 and 343 (Figure 2-8). For example, OTU 3 and OTU 13 both belong to *Spirochaetaceae* family (genera undetermined), which has been reported to enhance cellulose degradation by *Clostridia* (Pohlschroeder et al. 1994) and to syntrophically produce acetate or hydrogen with methanogens (Lee et al. 2015). Within methanogens, OTUs 4 and 10 (group 2) were negatively correlated with OTU 5 and OTU 11 (group 1), indicating a competitive relationship. Interestingly, the total relative abundance of these four OTUs remained constant across both days even as the relative abundance of individual OTUs within this groups changed. In addition, the abundance of their potential partners the cellulolytic *Clostridia* (phylum *Firmicutes*) also remained constant across both days. A similar trend was observed for OTUs 8, 17, 18, and 19, which are classified to *Bacteroides*, and are known to decompose sugars to organic acids and H_2. Within this group, OTU 8 was negatively correlated to all the other OTUs while the total relative abundance of the 4 OTUs remained constant.

More broadly, two large microbial groups can be observed. Group 1: OTUs 2, 5, 11, 15, 17, 18, 19, 20, 22, 31, and 34; group 2: OTUs 1, 4, 8, 10, 13, 16, 23, 24, 30, 33, and 38. Across the two days, the group 1 increased while group 2 decreased. The populations of OTUs in group 1 were positively correlated with each other and negatively correlated with the OTUs in group 2. Both groups contain sugar fermenting *Bacteroidetes* and *Chloroflexi* (OTUs 15, 17, 18, and 19 in group 1 and OTUs 8, 16, 23, 30, and 33 in group 2), methanogens (OTUs 5 and 11 in group 1 and OTUs 4 and 10 in group 2), and their potential partner(s) *Synergistetes* or *Spirochaetae*

(OTU 20 in group 1 and OTU 13 in group 2). The only phyla that are not in common across both groups are *Thermotogae* (OTU 2 in group 1) and *Firmicutes* (OTU 1 in group 2). But as discussed previously, OTU 2 (*Mesotogae, Thermotogae*) and OTU 1 (*Trichococcus, Firmicutes*) share similar functions of degrading sugars to organic acids. The shift from acetoclastic OTUs 5 and 11 to hydrogenotrophic OTUs 4 and 10 and its potential syntrophic partner OTU 13 suggests the shift from acetoclastic methanogenesis to syntrophic acetate oxidation and hydrogenotrophic methanogenesis. Although different groups predominated on day 234 and day 343, all of the main functions of both bacterial and archaeal populations were present in each group, representing functional redundancy. The stability in bacterial and archaeal populations can by hypothesized to maintain stability in the anaerobic digestion performance.

It is also noticeable that the correlations among populations of OTUs in group 1 are stronger than the correlations within group 2. This suggests that group 1 organisms may behave as a coordinated functional module that as they declined, were replaced by individual OTUs with less interdependence on other taxa within group 2, hinting that the microbial assembly may have shifted from modularity to individuality, which is opposite to the conclusion given by previous studies by Wu et al (Wu et al. 2016). Although both studies demonstrate that stable process performance can be maintained even with changing population dynamics, the mechanisms driving the population change may be very different. Wu et al. used dairy waste as the main feedstock in their experiment, which would facilitate significant microbial migration into the system. In contrast, sterile substrate was used in our study precluding the possibility of significant migration of external populations. Based on the consistent pattern of population change across all 13 reactor replicates in our study, the change in community structure seems to be deterministic. However, the design of the experiments eliminated significant chemical and environmental perturbations and microbial migration as mechanisms driving the change in community structure. This suggests that long-term dynamics of the community structure may create selective pressures within the reactor environment that allow different organisms to be selected at different times in the reactor life-cycle. Mechanisms driving the seemingly non-random community structure change over long periods of time require further study.

4. Conclusion

Noticeable shifts in population were observed in the microbial community structures over extended time periods despite stable digester performance, stable external environmental conditions, and elimination of migration of exogenous microorganisms. Stochastic simulations of population dynamics under neutral model assumptions suggests that population drift is not a significant mechanism for underlying the changes in community structure in our system. Furthermore, changes in community structure were consistent among the 13 replicates, suggesting deterministic mechanisms such as selection may drive population change. Community composition, functional metagenomics, and population networks all suggested that the main microbial functions remained unchanged as the community structure evolved, indicative of functional redundancy. Although the precise mechanisms determining microbial community structure requires additional investigation, we speculate that the dynamic community structure also changes the symbiotic, competitive and other environmental conditions over time, thereby providing new selective pressure for continued development of the community structure.

Reference

CLC Genomics Workbench 9.5.3.

Afgan, E., Baker, D., van Den Beek, M., Blankenberg, D., Bouvier, D., Čech, M., Chilton, J., Clements, D., Coraor, N., Eberhard, C., Grüning, B., Guerler, A., Hillman-Jackson, J., Von Kuster, G., Rasche, E., Soranzo, N., Turaga, N., Taylor, J., Nekrutenko, A. and Goecks, J. (2016) The Galaxy platform for accessible, reproducible and collaborative biomedical analyses: 2016 update. *Nucleic acids research 44*(W1), W3.

Ben Hania, W., Fadhlaoui, K., Brochier-Armanet, C.l., Persillon, C.c., Postec, A., Hamdi, M., Dolla, A., Ollivier, B., Fardeau, M.-L., Le Mer, J. and Erauso, G.l. (2015) Draft genome sequence of *Mesotoga* strain *PhosAC3*, a mesophilic member of the bacterial order *Thermotogales* , isolated from a digestor treating phosphogypsum in Tunisia. *Standards in Genomic Sciences* 10, 12.

Caporaso, J.G., Kuczynski, J., Stombaugh, J., Bittinger, K., Bushman, F.D., Costello, E.K., Fierer, N., Peña, A.G., Goodrich, J.K., Gordon, J.I., Huttley, G.A., Kelley, S.T., Knights, D., Koenig, J.E., Ley, R.E., Lozupone, C.A., McDonald, D., Muegge, B.D., Pirrung, M., Reeder, J., Sevinsky, J.R., Turnbaugh, P.J., Walters, W.A., Widmann, J., Yatsunenko, T., Zaneveld, J. and Knight, R. (2010) QIIME allows analysis of high-throughput community sequencing data. *Nature Methods* 7, 335.

Chapleur, O., Mazeas, L., Godon, J.-J. and Bouchez, T. (2016) Asymmetrical response of anaerobic digestion microbiota to temperature changes. *Applied Microbiology and Biotechnology* 100(3), 1445-1457.

Chen, S. and He, Q. (2015) Persistence of Methanosaeta populations in anaerobic digestion during process instability. *Journal of Industrial Microbiology & Biotechnology* 42(8), 1129-1137.

Ciaciuch, A., Gaca, J. and Lelewer, K. (2017) Effect of the two-stage thermal disintegration and anaerobic digestion of sewage sludge on the COD fractions, p. 130.

DeSantis, T.Z., Hugenholtz, P., Larsen, N., Rojas, M., Brodie, E.L., Keller, K., Huber, T., Dalevi, D., Hu, P. and Andersen, G.L. (2006) Greengenes, a Chimera-checked 16S rRNA gene database and workbenchcompatible with ARB. *Applied and Environmental Microbiology* 72(7).

Friedman, J., Higgins, L.M. and Gore, J. (2017) Community structure follows simple assembly rules in microbial microcosms. *Nature Ecology & Evolution* 1, 0109.

García-Depraect, O., Gómez-Romero, J., León-Becerril, E. and López-López, A. (2017) A novel biohydrogen production process: Co-digestion of vinasse and Nejayote as complex raw substrates using a robust inoculum. *International Journal of Hydrogen Energy* 42(9), 5820-5831.

Goldford, J.E., Lu, N., Bajić, D., Estrela, S., Tikhonov, M., Sanchez-Gorostiaga, A., Segrè, D., Mehta, P. and Sanchez, A. (2018) Emergent simplicity in microbial community assembly. *Science* 361(6401), 469-474.

Hanson, C.A., Fuhrman, J.A., Horner-Devine, M.C. and Martiny, J.B. (2012) Beyond biogeographic patterns: processes shaping the microbial landscape. *Nature Reviews Microbiology* 10(7), 497-506.

Hekstra, Doeke R. and Leibler, S. (2012) Contingency and Statistical Laws in Replicate Microbial Closed Ecosystems. *Cell* 149(5), 1164-1173.

Jabari, L., Gannoun, H., Cayol, J.-L., Hedi, A., Sakamoto, M., Falsen, E., Ohkuma, M., Hamdi, M., Fauque1, G., Ollivier, B. and Fardeau, M.-L. (2012) *Macellibacteroides fermentans gen. nov., sp. nov*., a member of the family *Porphyromonadaceae* isolated from an upflow anaerobic filter treating abattoir wastewaters. *International Journal of Systematic and Evolutionary Microbiology* 62(10), 2522-2527.

Lee, S.-H., Park, J.-H., Kim, S.-H., Yu, B.J., Yoon, J.-J. and Park, H.-D. (2015) Evidence of syntrophic acetate oxidation by *Spirochaetes* during anaerobic methane production. *Bioresource Technology* 190, 543-549.

Liu, J.-R., Tanner, R.S., Schumann, P., Weiss, N., McKenzie, C.A., Janssen, P.H., Seviour, E.M., Lawson, P.A., Allen, T.D. and Seviour, R.J. (2002) Emended description of the genus *Trichococcus*, description of *Trichococcus collinsii sp. nov*., and reclassification of *Lactosphaera pasteurii* as *Trichococcus pasteurii comb. nov*. and of *Ruminococcus palustris* as *Trichococcus palustris comb. nov*. in the low-GMC Gram-positive bacteria. *International Journal of Systematic and Evolutionary Microbiology* 52, 1113-1126.

Méndez-Acosta, H.O., Campos-Rodríguez, A., González-Álvarez, V., García-Sandoval, J.P., Snell-Castro, R. and Latrille, E. (2016) A hybrid cascade control scheme for the VFA and COD regulation in two-stage anaerobic digestion processes. *Bioresource Technology* 218, 1195-1202.

Ma, J., Frear, C., Wang, Z.-w., Yu, L., Zhao, Q., Li, X. and Chen, S. (2013) A simple methodology for rate-limiting step determination for anaerobic digestion of complex substrates and effect of microbial community ratio. *Bioresource Technology* 134, 391-395.

McHugh, S., Carton, M., Collins, G. and O'Flaherty, V. (2004) Reactor performance and microbial community dynamics during anaerobic biological treatment of wastewaters at 16–37 °C. *FEMS Microbiology Ecology* 48(3), 369-378.

Mei, R., Nobu, M.K., Narihiro, T., Kuroda, K., Muñoz Sierra, J., Wu, Z., Ye, L., Lee, P.K.H., Lee, P.-H., van Lier, J.B., McInerney, M.J., Kamagata, Y. and Liu, W.-T. (2017) Operation-driven heterogeneity and overlooked feed-associated populations in global anaerobic digester microbiome. *Water Research* 124, 77-84.

Morgan, G.I.L., Jesse, Z., Caporaso, J.G., Daniel, M., Dan, K., Joshua, A.R., Jose, C.C., Deron, E.B., Rebecca, L.V.T., Rob, K., Robert, G.B. and Curtis, H. (2013) Predictive functional profiling of microbial communities using 16S rRNA marker gene sequences. *Nature Biotechnology* 31(9), 814.

Nemergut, D.R., Schmidt, S.K., Fukami, T., O'Neill, S.P., Bilinski, T.M., Stanish, L.F., Knelman, J.E., Darcy, J.L., Lynch, R.C., Wickey, P. and Ferrenberg, S. (2013) Patterns and processes of microbial community assembly. *Microbiology and molecular biology reviews* 77(3), 342-356.

Ofiţeru, I.D., Lunn, M., Curtis, T.P., Wells, G.F., Criddle, C.S., Francis, C.A. and Sloan, W.T. (2010) Combined niche and neutral effects in a microbial wastewater treatment community. *Proceedings of the National Academy of Sciences of the United States of America* 107(35), 15345-15350.

Ortner, M., Leitzinger, K., Skupien, S., Bochmann, G. and Fuchs, W. (2014) Efficient anaerobic mono-digestion of N-rich slaughterhouse waste: Influence of ammonia, temperature and trace elements. *Bioresource Technology* 174, 222-232.

Pholchan, M.K., Baptista, J.d.C., Davenport, R.J., Sloan, W.T. and Curtis, T.P. (2013) Microbial community assembly, theory and rare functions. *Frontiers in Microbiology* 4(68), 1-9.

Pohlschroeder, M., Leschine, S.B. and Canale-Parola, E. (1994) *Spirochaeta caldaria sp. nov.*, a thermophilic bacterium that enhances cellulose degradation by *Clostridium thermocellum*. *Archives of Microbiology* 161(1), 17-24.

Rajagopal, R., Massé, D.I. and Singh, G. (2013) A critical review on inhibition of anaerobic digestion process by excess ammonia. *Bioresource Technology* 143, 632-641.

Rice, E.W., Baird, R.B., Eaton, A.D. and Clesceri, L.S. (2012) Standard methods for the examination of water and wastewater, 22nd Edition, American Public Health Association, American Water Works Association, Water Environment Federation.

Rodriguez-Chiang, L., Llorca, J. and Dahl, O. (2016) Anaerobic co-digestion of acetate-rich with lignin-rich wastewater and the effect of hydrotalcite addition. *Bioresource Technology* 218, 84-91.

Scaglia, B., D'Imporzano, G., Garuti, G., Negri, M. and Adani, F. (2014) Sanitation ability of anaerobic digestion performed at different temperature on sewage sludge. *Science of The Total Environment* 466-467, 888-897.

Stegen, J.C., Lin, X., Fredrickson, J.K. and Konopka, A.E. (2015) Estimating and mapping ecological processes influencing microbial community assembly. *Frontiers in Microbiology* 6(370).

Su, X.L., Tian, Q., Zhang, J., Yuan, X.Z., Shi, X.S., Guo, R.B. and Qiu, Y.L. (2014) *Acetobacteroides hydrogenigenes gen. nov., sp. nov.*, an anaerobic hydrogen-producing bacterium in the family *Rikenellaceae* isolated from a reed swamp. *International Journal of Systematic and Evolutionary Microbiology* 64(Pt 9), 2986-2991.

Sun, L., Toyonaga, M., Ohashi, A., Tourlousse, D.M., Matsuura, N., Meng, X.-Y., Tamaki, H., Hanada, S., Cruz, R., Yamaguchi, T. and Sekiguchi, Y. (2016) *Lentimicrobium saccharophilum gen. nov., sp. nov.*, a strictly anaerobic bacterium representing a new family in the phylum *Bacteroidetes*, and proposal of *Lentimicrobiaceae fam. nov*. *International Journal of Systematic and Evolutionary Microbiology* 66(7), 2635-2642.

Vanwonterghem, I., Jensen, P.D., Ho, D.P. and Tyson, D.J.B.a.G.W. (2014) Linking microbial community structure, interactions and function in anaerobic digesters using new molecular techniques. *Current Opinion in Biotechnology* 27, 55-64.

Vellend, M. (2010) Conceptual synthesis in community ecology. *The Quarterly Review of Biology* 85(2), 183-206.

Wagner, A.O., Lins, P., Malin, C., Reitschuler, C. and Illmer, P. (2013) Impact of protein-, lipid- and cellulose-containing complex substrates on biogas production and microbial communities in batch experiments. *Science of The Total Environment* 458-460, 256-266.

Wang, K., Yin, J., Shen, D. and Li, N. (2014) Anaerobic digestion of food waste for volatile fatty acids (VFAs) production with different types of inoculum: Effect of pH. *Bioresource Technology* 161, 395-401.

Werner, J.J., Knights, D., Garcia, M.L., Scalfone, N.B., Smith, S., Yarasheski, K., Cummings, T.A., Beers, A.R., Knight, R. and Angenent, L.T. (2011) Bacterial community structures are unique and resilient in full-scale bioenergy systems. *Proceedings of the National Academy of Sciences* 108(10), 4158.

Wu, L., Yang, Y., Chen, S., Zhao, M., Zhu, Z., Yang, S., Qu, Y., Ma, Q., He, Z., Zhou, J. and He, Q. (2016) Long-term successional dynamics of microbial association networks in anaerobic digestion processes. *Water Research* 104, 1-10.

Xie, S., Ma, Y., Strong, P.J. and Clarke, W.P. (2015) Fluctuation of dissolved heavy metal concentrations in the leachate from anaerobic digestion of municipal solid waste in commercial scale landfill bioreactors: The effect of pH and associated mechanisms. *Journal of Hazardous Materials* 299, 577-583.

Yilmaz, P., Parfrey, L.W., Yarza, P., Gerken, J., Pruesse, E., Quast, C., Schweer, T., Peplies, J., Ludwig, W. and Glöckner, F.O. (2014) The SILVA and "All-species Living Tree Project (LTP)" taxonomic frameworks. *Nucleic acids research* 42(D1), D643-D648.

Zhang, L. and Jahng, D. (2010) Enhanced anaerobic digestion of piggery wastewater by ammonia stripping: Effects of alkali types. *Journal of Hazardous Materials* 182, 536-543.

Zhou, J., Deng, Y., Zhang, P., Xue, K., Liang, Y., Van Nostrand, J.D., Yang, Y., He, Z., Wu, L., Stahl, D.A., Hazen, T.C., Tiedje, J.M. and Arkin, A.P. (2014) Stochasticity, succession, and environmental perturbations in a fluidic ecosystem. *Proceedings of the National Academy of Sciences* 111(9), E836-E845.

Zhou, J. and Ning, D. (2017) Stochastic community assembly: Does it matter in microbial ecology? *Microbiology and Molecular Biology Reviews* 81(4), e00002-00017.

Zhu, Z., Hsueh, M.K. and He, Q. (2011) Enhancing biomethanation of municipal waste sludge with grease trap waste as a co-substrate. *Renewable Energy* 36(6), 1802-1807.

Appendix: Tables and Figures

Table 2-1. Diversity Index

	Chao richness	Shannon diversity	Phylogenetic diversity
Day 234	109.0	4.05	6.11
Day 343	112.0	4.20	6.05

Table 2-S1. ANOSIM dissimilarity ranks between and within the two sampling days. N is the number of pairs scored

	0%	25%	50%	75%	100%	N (pairs)
Between	154	199	241	283	325	169
Day 234	4	34.75	72.5	111.75	152	78
Day 343	1	47.25	82.5	121.5	167	78

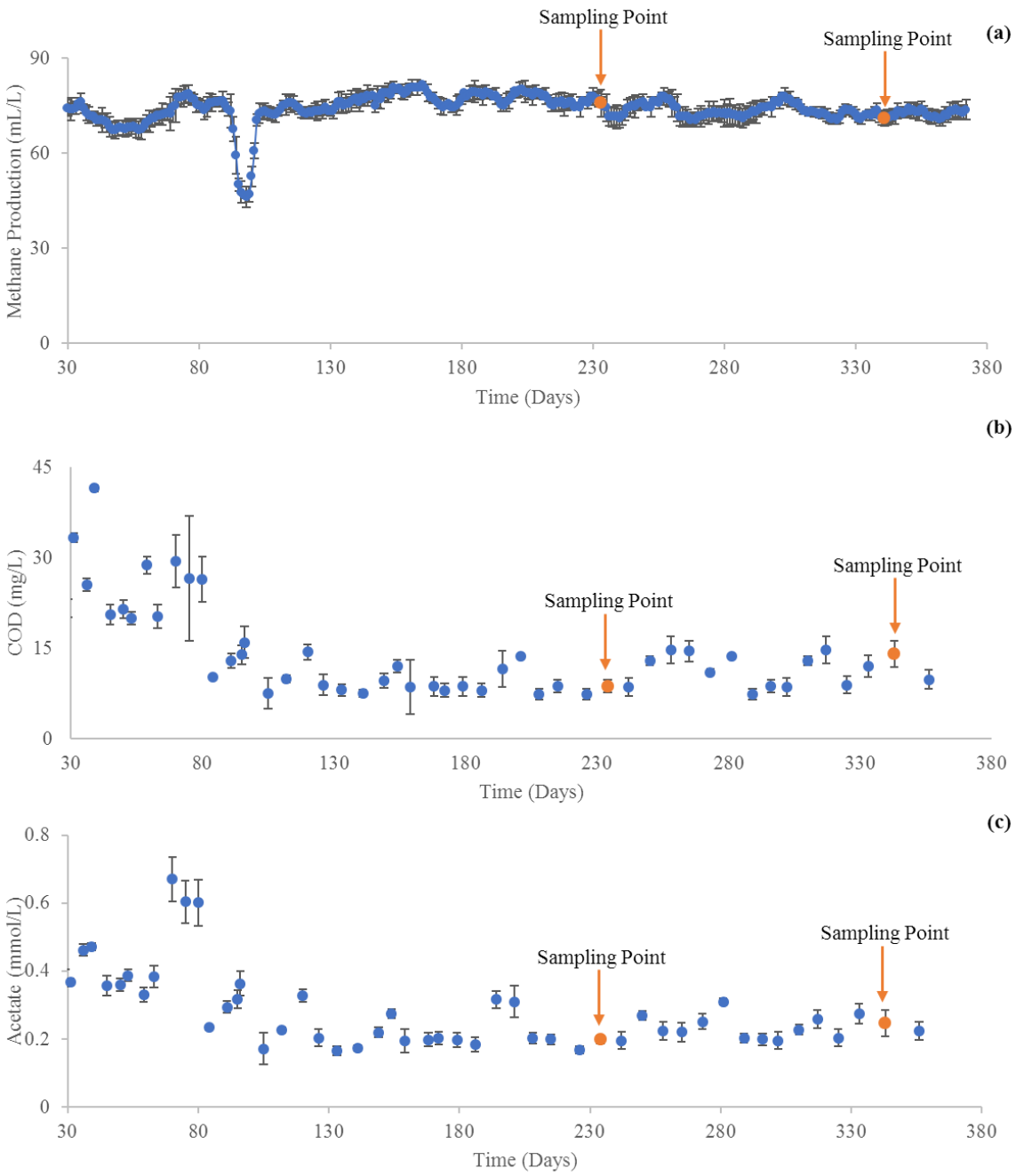

Figure 2-1. Performance of the 13 replicate sucrose-fed bioreactors. (a) 7-day running average methane production; (b) organic level as measured by COD concentration; (c) acetate concentration in mM. The two data point in orange designated the time of biomass sampling.

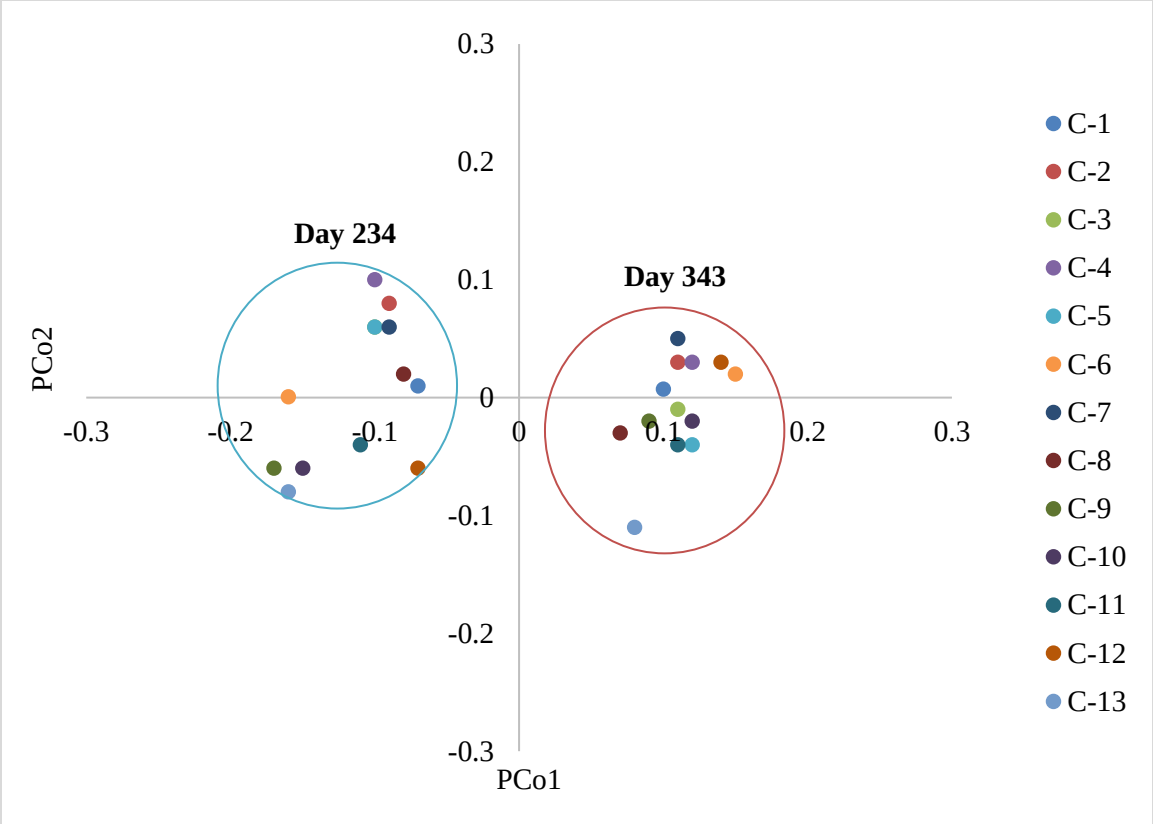

Figure 2-2. The clustering pattern of microbial community structures among the 13 replicate bioreactors and between two sampling days according to Principal coordinate analysis (PCoA) based on weighted Uni-Frac distance. Relative abundance and phylogenetic data of each OTU were inputted for this analysis. Each bioreactor is represented by a unique color is the ratio of relative abundance of reactor i paired with every other reactors; N is the number of OTUs.

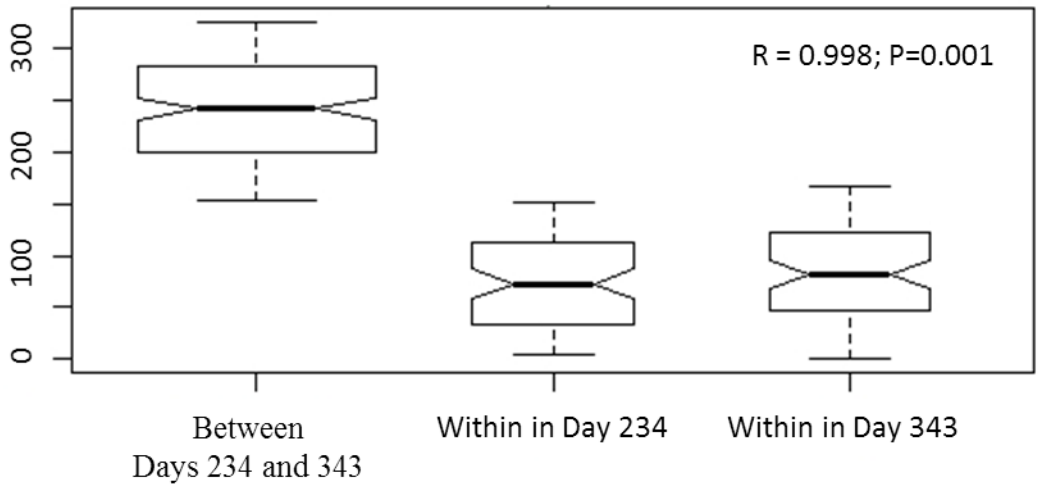

Figure 2-3. Structure difference in microbial community composition between and within the two sampling time points demonstrated by rank distribution of analysis of dissimilarity (ANOSIM). R statistic is the ratio between dissimilarities between sites with a day and the dissimilarities between sites that are in different days. %. Box edges represent 75% and 25% tails, inside bar median, error bars maximum and minimum, and dots outliers. P is the significance value of R, determined by permuting the membership of sites in the 2 sampling days.

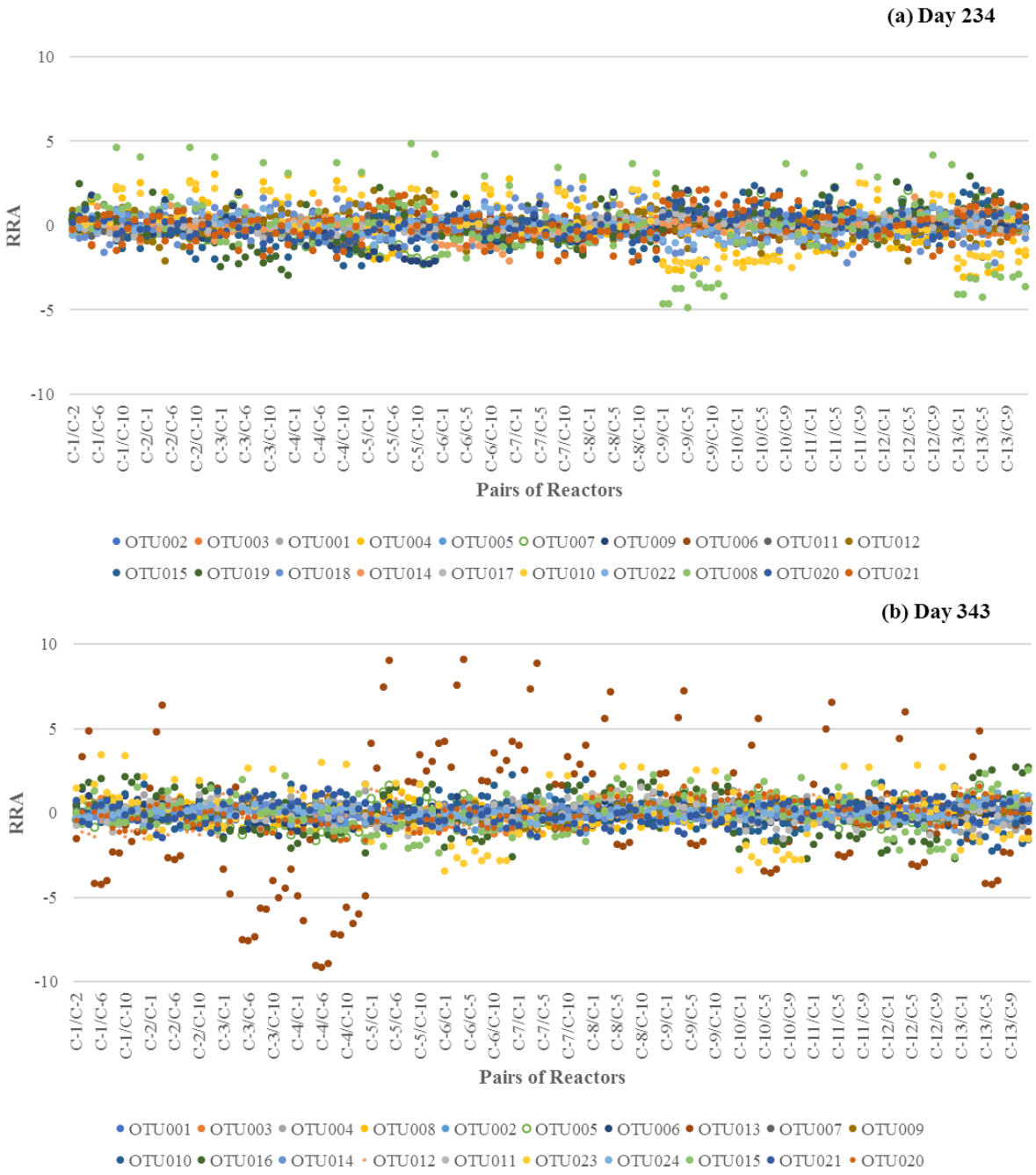

Figure 2-S1. Ratios of a particular OTU's relative abundance of any two replicate bioreactors (log_2 scale). For each pair of reactors, RRA = log_2 (relative abundance of reactor 1 / relative abundance of reactor 2). Each tick on x-axis represents a pair of reactors.

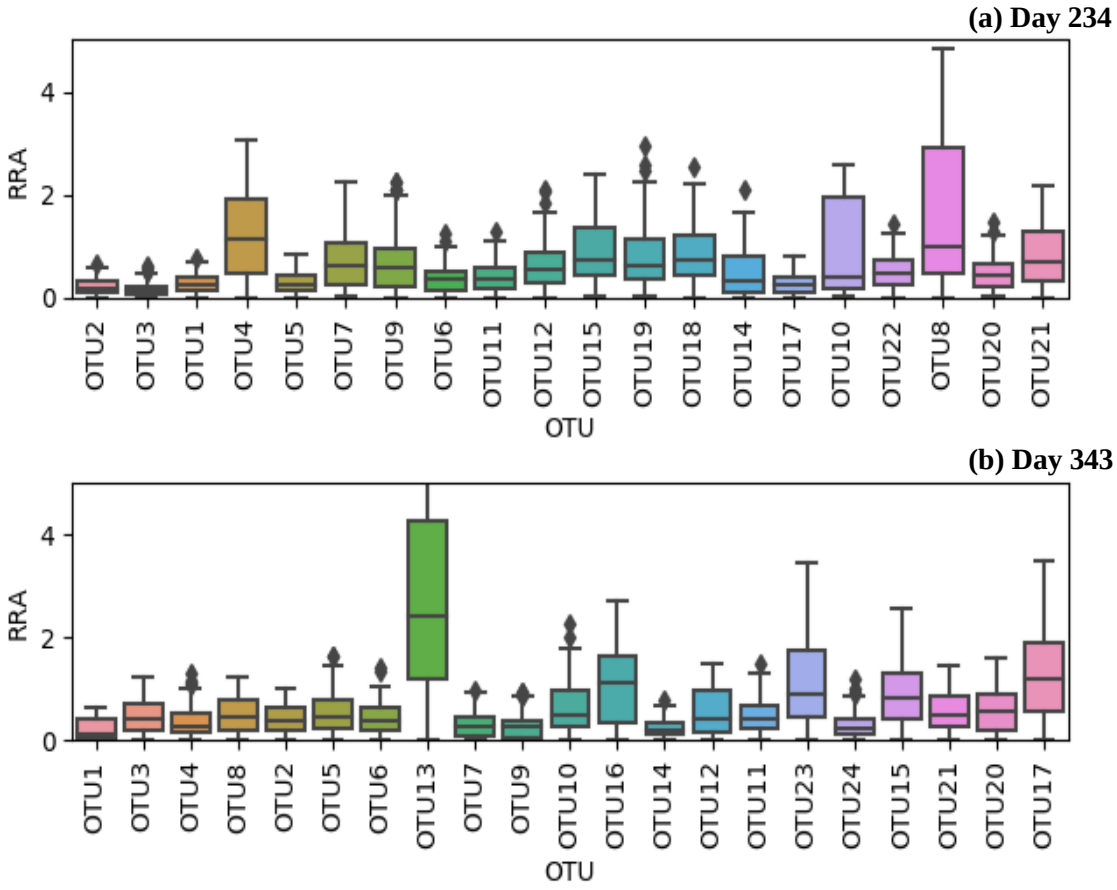

Figure 2-4. Ratio of an OTU's relative abundance of any pair of two bioreactors (log2 scale). For each pair of bioreactors, RRA = absolute (log2 (relative abundance of reactor 1 / relative abundance of reactor 2)). Each box represents 78 ($^{2}C_{13}$) ratios of a certain OTU. OTU selected for analysis represent those taxonomy with a relative abundance greater than 0.5%. The left-to right order of OTUs is descending relative abundant, with box edges of 75% and 25% tails, inside bar of median, error bars of maximum and minimum, and dots of outliers.

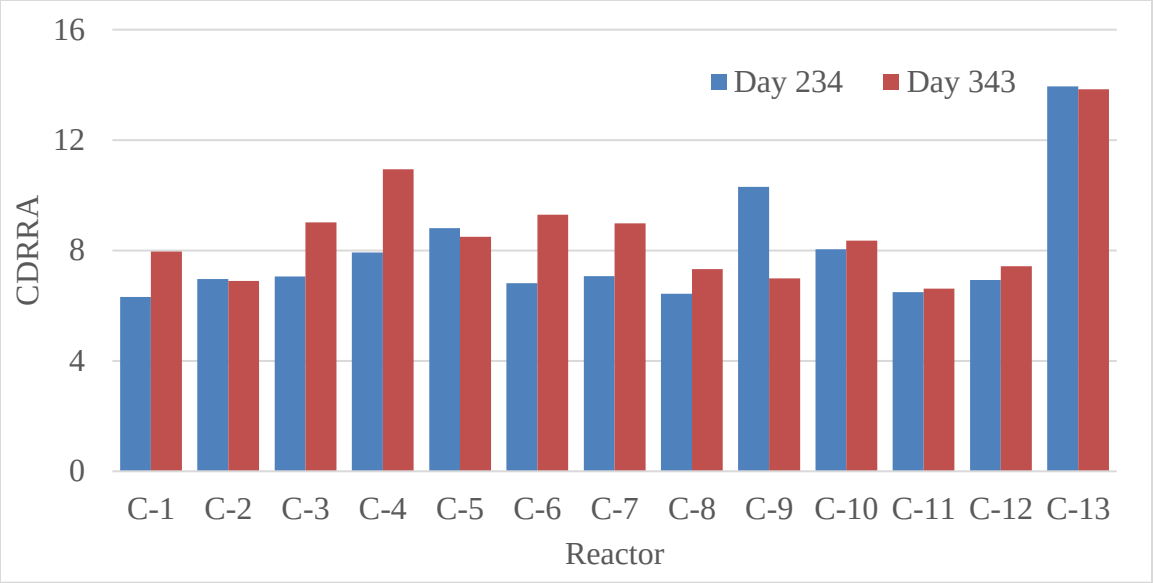

Figure 2-S2. Cumulative RRA of one reactor (sum of ratio of RRA of a certain reactor). For each reactor, CRRAi = ΣRRAi/N. CRRAi is the cumulative ratio of relative abundance of reactor I; RRA is the ratio of relative abundance of reactor i paired with every other reactors; N is the number of OTUs.

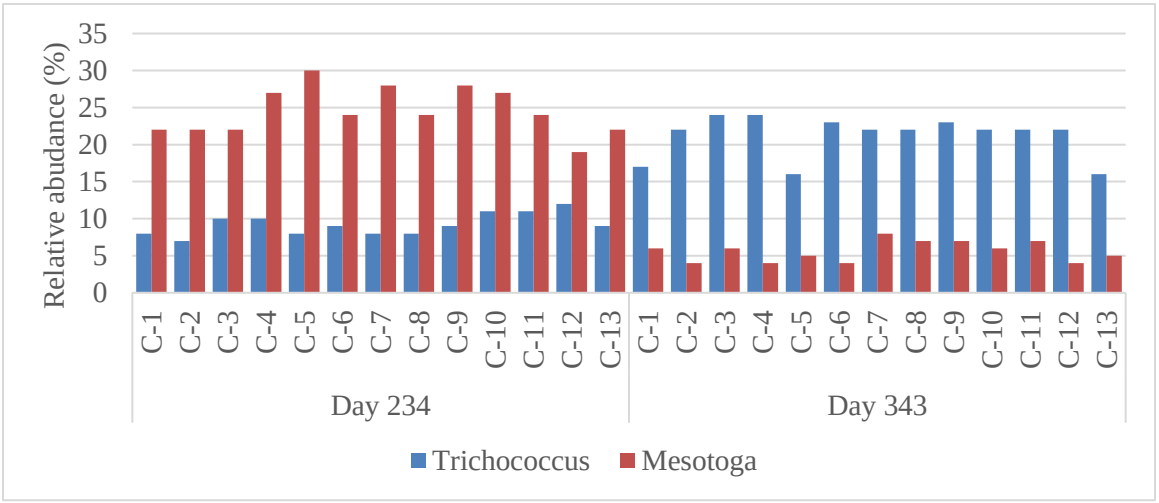

Figure 2-S3. Cumulative RRA of one reactor (sum of ratio of RRA of a certain reactor). For each reactor, CRRAi = ΣRRAi/N. CRRAi is the cumulative ratio of relative abundance of reactor I; RRA

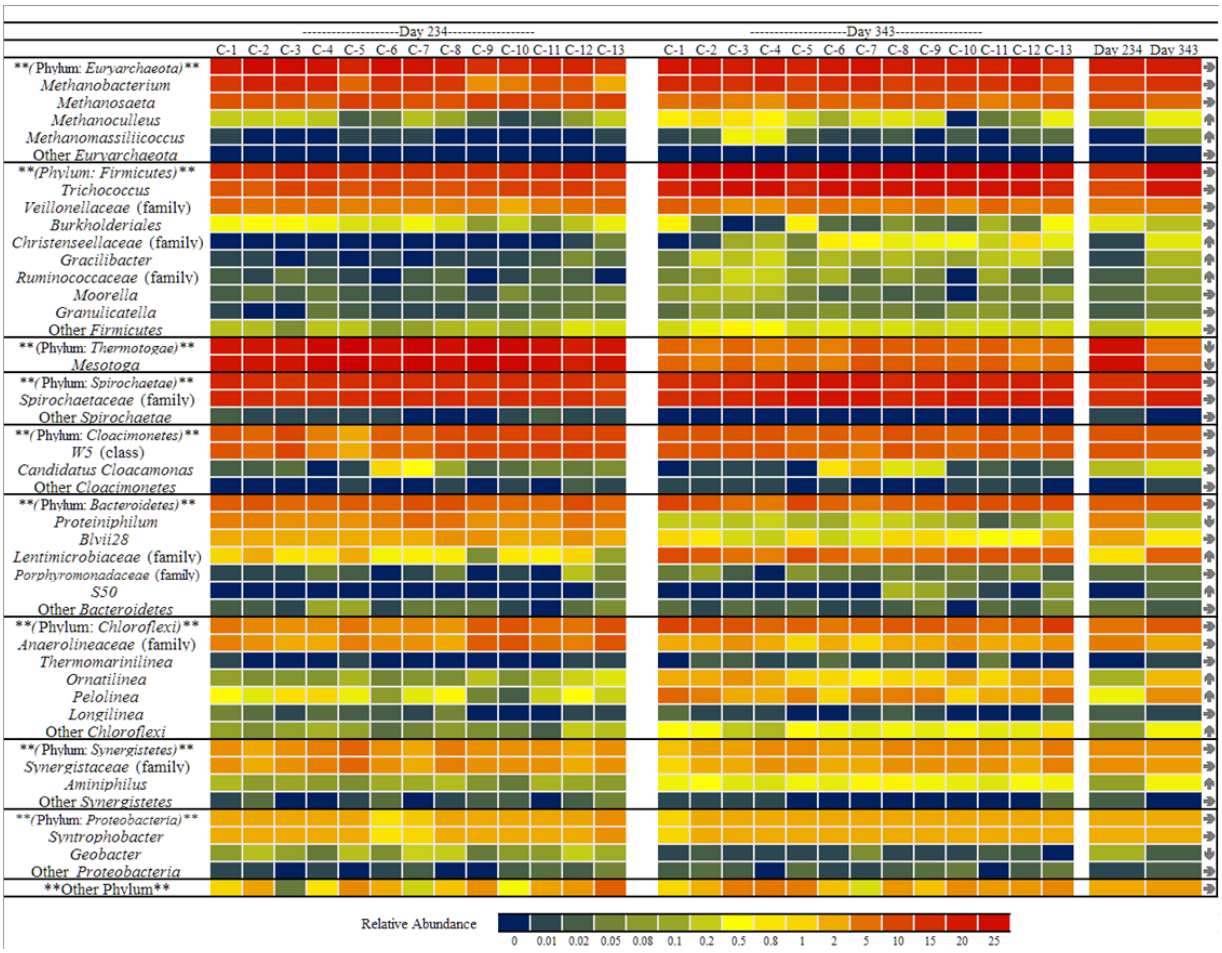

Figure 2-5. Heatmap of taxonomic assignment of sequencing reads from the 13 semi CSRT digesters on Day 234 and Day 343 at (phylum) and genus levels. The last two column showed the average values on each day. Each phylum was shown in "(phylum name)**" and its affiliated genera or the most confident classification achievable with the level shown in "()" were represented right below. Relative abundance was defined as: the number of sequencing reads affiliated with a given taxon / total sequencing reads (Unit: %). Phylum groups with a relative abundance less than 1% and genus groups with a relative abundance lower than 0.03% were listed as "other".**

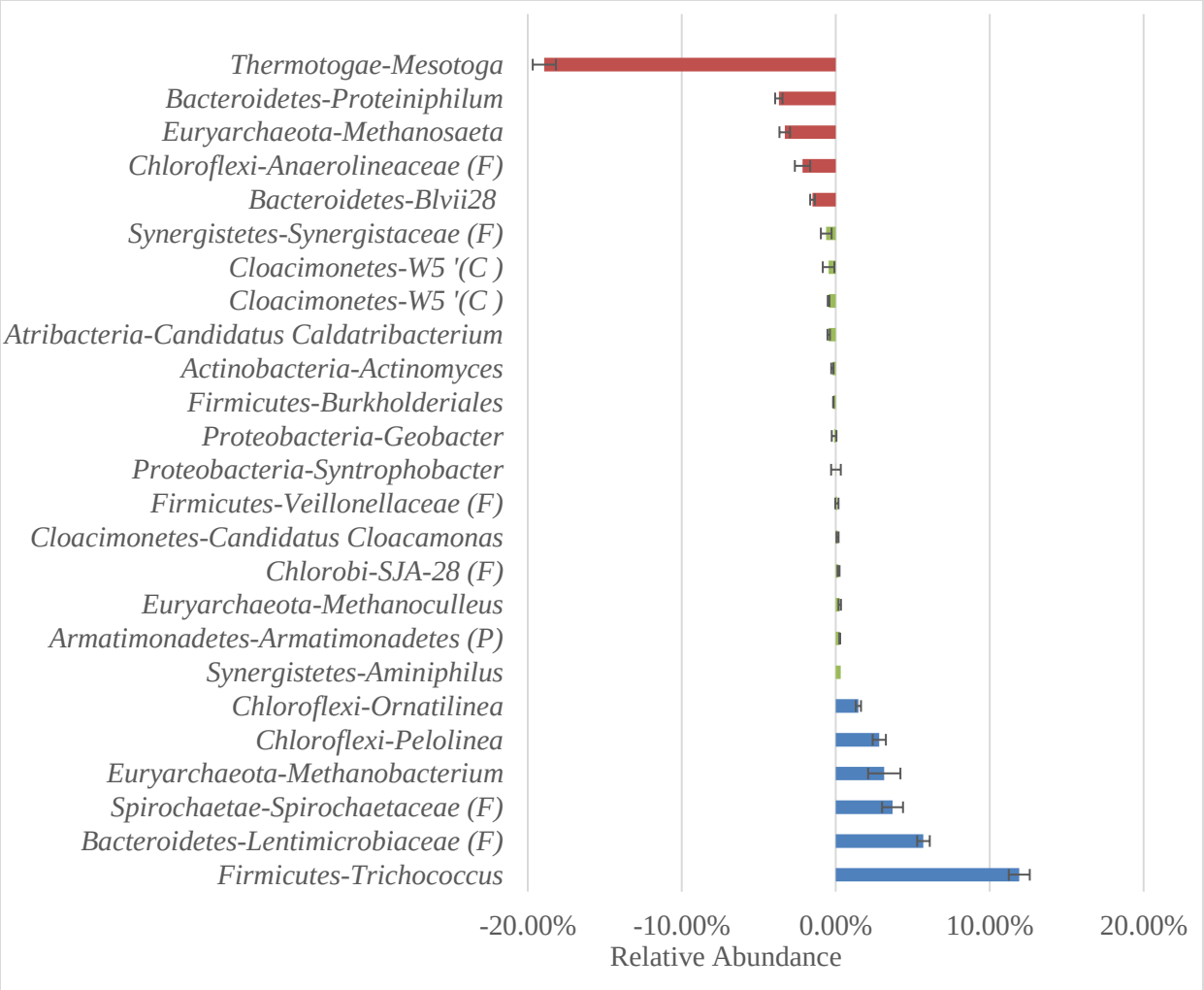

Figure 2-6. Difference in relative abundance of major archaeal and bacterial genus populations (average relative abundance > 0.5%) from day 234 to day 343. Red: major decrease; gray: comparatively stable; blue: major increase

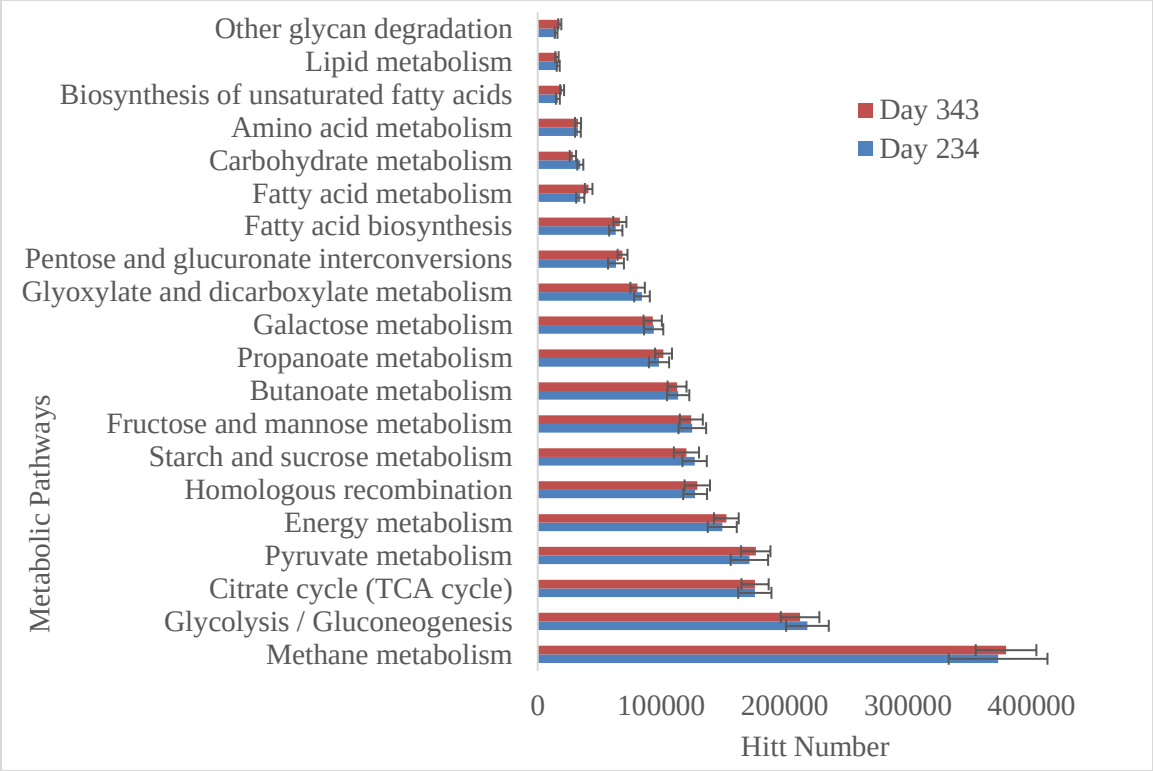

Figure 2-7. Potential gene functions predicted by PICRUSt using 16S rRNA marker gene with KEEG database on day 234 and day 343. The y-axis showed the relevant metabolism pathways and the x-axis showed the average number of hit of the amplified genes to the pathways. The error bar represented the standard deviation.

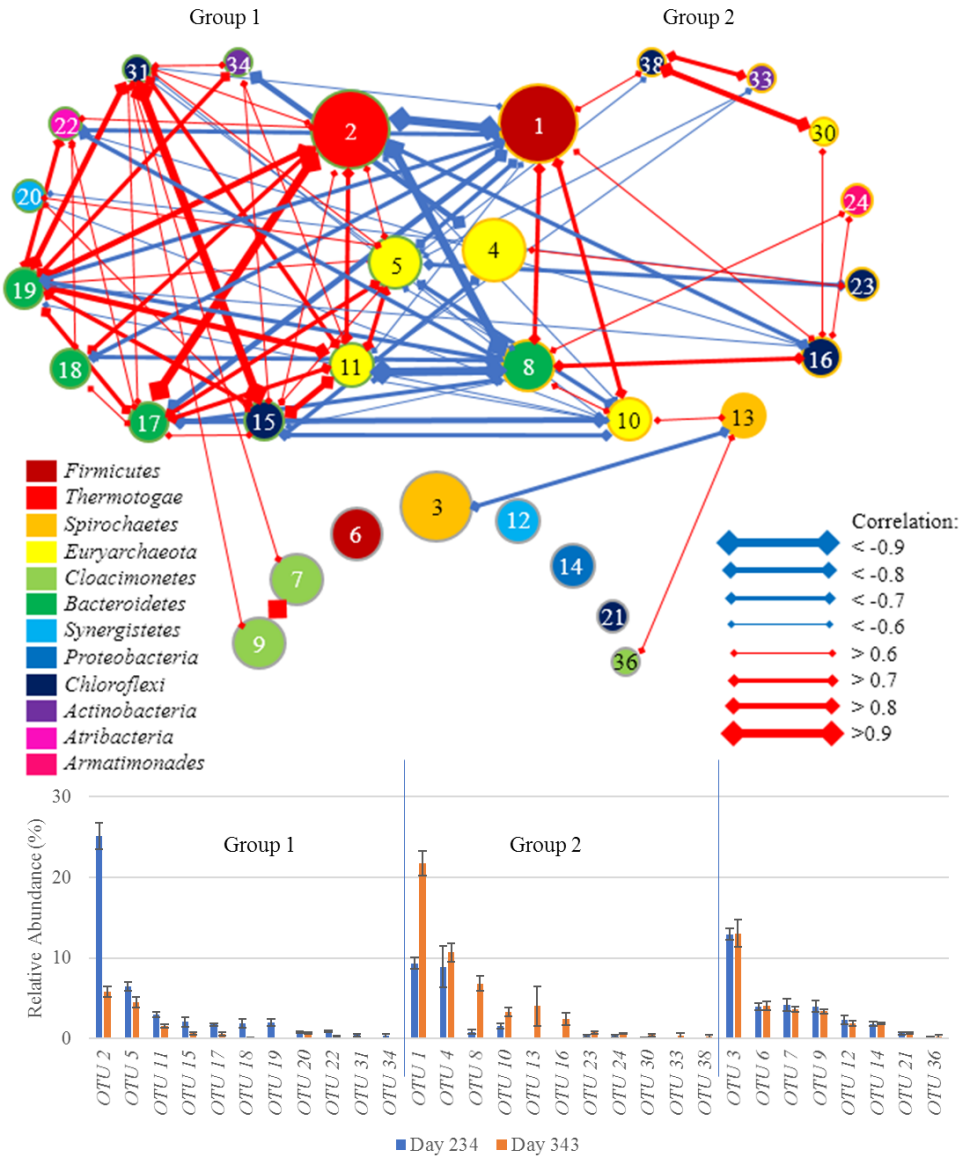

Figure 2-8. Microbial network analysis based on correlation between two major OTUs (relative abundance > 0.5%) according to Pearson's correlation coefficient formula on a combination of both days respectively. Each node represented one OTU and the size of the node reflected the relative abundance (the larger the node, the more abundant). The colors of the nodes represented different phyla. The red line represented positive correlation while blue, negative. The thicker the line is, the stronger the correlation is. Only correlation coefficient greater than 60% (or less than -60%) were considered in the network.

CHAPTER III - KINETICS ANALYSIS AND COMMUNITY CHARACTERIZATION OF SYNTROPHIC METHANOGENIC ENRICHMENTS

Abstract

Short-chain fatty acids including acetate, propionate, and butyrate are the most common intermediates after acidogenesis and acetogenesis processes and act as precursors of methanogenesis. This study is among the first to seek a deeper understanding of the methanogenesis through a systematic investigation of both community structure and kinetics as impacted by VFA substrates investigating the impact of substrates both on community structure and kinetics. The kinetics of anaerobic degradation of fatty acids was determined by the accumulative methane yields. Acetate demonstrated the highest specific growth rate among the selected fatty acids with similar carbon concentration based on mg/L COD. Microbial community structures were analyzed by 16S rRNA sequencing and PICRUSt gene prediction to understand the role of methanogens and other bacterial populations in the methanogenesis phase. A novel food web was proposed for anaerobic degradation of the short chain fatty acids, including both acetoclastic and hydrogenotrophic methanogens, syntrophic bacteria, and other redundant bacteria populations. The microbial structures also indicated that the competition between the two acetoclastic methanogens *Methanosarcina* and *Methanosaeta* does not solely depend on the concentration of the acetate. *Methanosarcina* are more likely to be predominant under stress and stimulate the methanogenesis process.

Keywords

Anaerobic enrichment, Fatty acid, competition between *Methanosarcina* and *Methanosaeta*, food web

1. Introduction

Anaerobic digestion, a series of biological processes in which microorganisms break down biodegradable material in the absence of oxygen and produce biogas, plays an important role in many wastewater treatment processes. It is comprised of four steps: hydrolysis, acidogenesis,

acetogenesis, and methanogenesis (Ali Shah et al., 2014). During hydrolysis, complex substrates are broken down into monomeric sugars, long-chain fatty acids, and nucleic acids (Li et al. 2011). These byproducts are then converted by acidogenic bacteria into volatile fatty acids (VFAs). The bacteria associated with hydrolysis and acidogenesis are quite diverse reflecting the complex nature of raw substrates, such as sewage and municipal sludge, animal wastes, food wastes, and agriculture residues (Carlsson et al., 2012; Romero-Güiza et al., 2016). VFAs are converted to acetate during acetogenesis. Alternatively, homoacetogenic organisms may generate acetate from H_2 and CO_2 via a reaction mediated by Acetyl-CoA. Acetogenic and methanogenic microbial communities are less diverse since the substrates for these processes are much less complex (Goswami et al., 2016). Methanogenesis is the key step of removal of the majority of COD (chemical oxygen demand) as it converts acetate and H_2/CO_2 to methane (Li et al., 2016).

Earlier studies investigated methanogenesis from the perspective of methane production kinetics from formate, acetate, and H_2/CO_2 (Pan et al., 2016) and C1 to C5 organic acids (Yang et al., 2015). However, little was revealed about the corresponding microbial community structures. Others explored the competition of acetoclastic methanogens (Chen et al., 2017; Ma et al., 2013b) or the association between hydrogenotrophic methanogens and syntrophic bacteria (Hattori, 2008; Mathai et al., 2015; Westerholm et al., 2016). Those studies addressed how the concentration of various substrates affect community structure, but discussion did not include kinetics.

This study is among the first to seek a deeper understanding of the methanogenesis through a systematic investigation of both community structure and kinetics as impacted by VFA substrates investigating the impact of substrates both on community structure and kinetics. Kinetics of methanogenesis during anaerobic degradation were investigated in reactors enriched with acetate, propionate, and butyrate. Microbial community structures were analyzed by 16S rRNA sequencing and PICRUSt metagenomic analysis to understand the role of methanogens and other bacterial populations in the methanogenesis phase of anerobic digestion.

2. Materials and Methods

2.1 Experimental setup of fatty acid anaerobic enrichment

Enrichment cultures grown with different fatty acid substrates were used to investigate different substrate-specific microbial communities. Four enrichment cultures were established in duplicate as described in Table 3-1: A-200, A-20, P-15, and B-10. A-200 reactors were fed with 200 mM sodium acetate and the biomass were transferred to the next generation after the end of methane production. A-20, P-15, and B-10 were fed with 20 mM sodium acetate, 15 mM sodium propionate, and 10 mM sodium butyrate, respectively. Fatty acid concentrations in A-20, P-15, and B-10 were selected to give similar COD concentrations. Each of these reactors was fed with identical amounts of substrate in 10 feeding cycles before transferring the culture to the next generation. The purpose of the enrichment and transfer is to develop a stable community specifically for the fatty acid degradation and to eliminate the other non-essential microbial species. All eight digesters were maintained at 37 (±1) ^{o}C and a shaking speed of 80 rpm to ensure complete-mix conditions. Aluminum-capped glass serum bottles with a working volume of 100 mL and a head space of 60 mL were used as the enrichment digesters. The bottles were sealed by butyl rubber stoppers to ensure anaerobic conditions.

Each liter of the selective sterile medium contains the following: 1.0 g NaCl, 0.5 g KCl, 0.5 g $MgCl_2 \cdot 6H_2O$, 0.3 g NH_4Cl, 1.7 g KH_2PO_4, 3.0 g K_2HPO_4, 0.0015 g $CaCl_2 \cdot 2H_2O$, 1.5 mg $FeCl_2 \cdot 4H_2O$, 0.19 mg $CoCl_2 \cdot 6H_2O$, 0.1 mg $MnCl_2 \cdot 4H_2O$, 0.07 mg $ZnCl_2$, 0.036 mg $Na_2MoO_4 \cdot 2H_2O$, 0.024 mg $NiCl_2 \cdot 6H_2O$, 0.008 mg $Na_2WO_4 \cdot 2H_2O$, 0.006 mg H_3BO_3, 0.006 mg $Na_2SeO_3 \cdot 5H_2O$, 0.002 mg $CuCl_2 \cdot 2H_2O$, 0.5 mg NaOH, 0.25 mL 0.1% Resazurin, 0.048g $Na_2S \cdot 9H_2O$, 0.031 g L-cysteine, and 1 mL of the Wolin Vitamins (which contained 0.02 mg/L biotin, 0.02 mg/L folic acid, 0.1 mg/L pyridoxine hydrochloride, 0.05 mg/L riboflavin, 0.05 mg/L thiamine, 0.05 mg/L nicotinic acid, 0.05 mg/L pantothenic acid, 0.001 mg/L vitamin B12, 0.05 mg/L p-aminobenzoic acid, and 0.05 mg/L thioctic acid). The pH of the medium was adjusted to 7.2 by 1 mol/L K_2HPO_4 if too low and 1 mol/L KH_2PO_4 if too high. The medium was heated to the boiling point and purged with N_2 to eliminate oxygen before Resazurin and

Na_2S $9H_2O$ were added. The sealed bottles were then autoclaved for 20 minutes at 120 ℃. The medium was formulated to exclude carbonate and bicarbonate, to simplify carbon mass balance calculations since carbon dioxide could only originate in the substrate or inoculum. The anaerobic digesters were inoculated with the well-mixed sludge from previous laboratory sucrose fed reactors as the inoculum (10/90 volume/volume).

2.2 Methane production and composition measurement

Biogas (a mixture of CH_4 and CO_2) production was measured daily using a water replacement method. Gas composition was monitored by HP 5890 gas chromatography with TCD (thermal conductivity detector) and a Supelco packing column (60/80 Carbonxen®-1000). Argon was used as the carrier gas with a flow rate of 5 ml/min (Zhu et al., 2011). The temperatures of injection, oven (column), and detection were set to 150 ℃, 125 ℃, and 170 ℃ respectively and the process time was set to 12 minutes for N_2, CH_4, and CO_2 to be fully separated and detected. The peaks of CH_4 and CO_2 appeared at 5.5 minutes and 10.5 minutes respectively. Standard curves of CH_4 and CO_2 were calibrated monthly to ensure accuracy.

2.3 Carbon mass balance and estimation of kinetic parameters

Daily and cumulative methane production were calculated by equations (3-1) and (3-2) respectively.

$$V_{CH4,i} = V_{gas} \times \frac{C_{CH4}}{C_{CH4}+C_{CO2}}$$

(Equation 3-1)

$$V_{CH4} = \sum_{i=1}^{i} V_{CH4,i}$$

(Equation 3-2)

where C_{CH4} and C_{CO2} are the measured methane and carbon dioxide concentration each day; $V_{CH4,i}$ is the methane production each day; and V_{CH4} is the cumulative methane production.

To eliminate uncertainty caused by CO_2, mass balance of the anaerobic microbial growth was calculated on the basis of COD assuming a complete consumption of substrate as equations (3-3) and (3-4) (Yang et al., 2015).

$$C_xH_yO_z \rightarrow f_e\ CH_4 + f_s\ biomass$$

(Equation 3-3)

$$f_e + f_s = 1$$

(Equation 3-4)

where f_e and f_s are the portions of the electron-donor substrate diverted to energy production (in this case, CH_4) and biomass production. The f_e value corresponds to the methane yield rate and can be calculated by equation (3-5).

$$f_e = \frac{X_{CH4}}{X_{substrate}}$$

(Equation 3-5)

where X_{CH4} and $X_{substrate}$ are the cumulative methane and substrate mass concentrations expressed as mg COD/L. Considered to be inherent, f_e and f_s can be used to calculate the specific microbial growth rate with the concentration of substrate as equation (3-6).

$$\mu = \frac{f_s}{f_e}\frac{V_{CH4}}{T}\frac{1}{X_{substrate}-X_{CH4}}$$

(Equation 3-6)

where V_{CH4} is the cumulative methane production for one feed and T is the total time consumed for methane production; ($X_{substrate} - X_{CH4}$) represents the biomass concentration.

The maximum specific microbial growth rate and half saturation constant K_S (mg/L) were estimated by nonlinear regression of the experimental data using Monod equation (3-7), which is commonly used to describe microbial growth.

$$\mu = \mu_{max}\frac{S}{K_S+S}$$

(Equation 3-7)

where S is the substrate concentration (mg/L); and μ_{max} is the maximum specific growth rate (day^{-1}).

2.4 Microbial community characterization

2.4.1 DNA extraction ad PCR amplification

Slurry samples were taken at the end of the 3rd generation of each enrichment reactor by syringe and were centrifuged at 15,000 x for 20 minutes. DNA was extracted from the biomass pellet using MP Biomedical FastDNA™ Spin Kit for soil according to manufacturer's instruction with minor modification. The extracted DNA was purified by ZYMO Genomic DNA Clean & ConcentrationTM-10 kit according to instructions manual provided by the manufacturer. The qualities and concentrations of DNA were determined by NanoDrop 1000 spectrophotometer. The purified DNA was stored at -20 ℃ for future analysis.

For high-throughput sequencing, the DNA was amplified with primers cap515F (GTGCCAGCMGCCGCGGTAA) and 806R (GGACTACHVGGGTWTCTAAT) targeting the V4 region of bacterial and archaeal 16S rRNA genes. Barcodes that allow the multiplexing of the samples during the sequencing were incorporated between the reverse primer and the adapter. The 25 μL PCR mixtures contained 12 μL Phusion flash Master Mix, 2 μL (100 to 150 ng) DNA template, 1 μL forward primer, 1 μL reverse primer, and 10 μL ultra-pure water. The thermocycling conditions were: one cycle of 94 ℃ for 3 minutes, followed by 35 cycles of 94 ℃ for 45 seconds, 55 ℃ for 1 minute, 72 ℃ for 1 minute and 30 seconds, and then 72 ℃ for 10 minutes.

2.4.2 16S rRNA sequencing and bioinformatics analysis

Concentrations of PCR products were determined by a capillary electrophoresis bioanalyzer (Agilent 2100 Electrophoresis Bioanalyzer) using the Agilent DNA 7500 kit. Based on the peak height from Agilent DNA 7500 analyses, amplicons were pooled, and quantified using KAPA Illumina kit (KK4824 from KAPA Biosystems). Final libraries were denatured with 0.2 N fresh-made NaOH solution and diluted with 10 mM Tris/0.05% tween buffer (pH = 8.5). The library was then combined with 20% of a PhiX control kit to increase the library diversity. Subsequently, the sample was loaded to Illumina MiSeq System with a MiSeq Reagent Kit v2

(300-cycles) by Illumina, Metagenomic workflow was selected to demonstrate 16S protocol using the MiSeq Reporter software (MSR).

Amplicon sequences were processed using the CLC Genomic Workbench 10 with microbial genomic module. First, sequences were aligned to merge the forward and reverse readings and discard pairs with more than 3 mismatches. Then, the merged reads were trimmed at 0.001, discarding sequences below 250 bp. Sequences were analyzed using a reference-based OTU clustering module with SILVA 16S v 128 97% database. Analysis parameters were set as follows: taxonomy similarity 97%; minimum occurrence of 2; chimera crossover cost at 3; and maximum unaligned end mismatches at 5.

The metagenomic content of the samples was inferred based on the 16S rRNA marker genes by PICRUSt (phylogenetic investigation of communities by reconstruction of unobserved states) software package (Morgan et al., 2013). The amplicon sequences were reclassified by QIIME 2 (Caporaso et al., 2010) using Greengenes gene database (DeSantis et al., 2006) and an OTU biom table was created and imported into PICRUSt on the Langille Lab PICRUSt Galaxy Instance web platform (Afgan et al., 2016) for functional gene prediction. The biom file was first normalized by copy number, followed by prediction of the metagenome using KEGG (Kyoto Encyclopedia of Genes and Genomes) orthologs and categorized by function with KEGG pathways at Hierarchy level 3.

3. Results and Discussion

3.1 Methane production and kinetic parameters

Four duplicate enrichment digesters (A-200, A-20, P-15, and B-10) were operated in this study. The A-200 digester was fed with 200 mM acetate, and 3% of the biomass was transferred to the next generation at the end of methane production. The first generation experienced a lag time of 5 days before any methane was generated. Each subsequent generation had a shorter lag time and a higher growth rate, which indicates a better adapted and more stable microbial community. The A-20, P-15, and B-10 digesters were fed 20 mM of acetate, 15 mM of propionate, and 10 mM of

butyrate, respectively. At the completion of the methane production, the quantity of substrate was added again, and the process repeated 10 times. After 10 feeding cycles, 3% of the biomass was transferred to the next generation and the feeding scenario repeated. The purpose of the enrichment and transfer is to develop a stable community specific to the fatty acid of interest and to eliminate non-relevant organisms. The accumulative methane production profile of each feed cycle and over three generations are shown in Figure 3-1. Overall, acetate and butyrate cultures had similar growth rates, while the growth rate of propionate was slower. Propionate also had a much longer lag time than the acetate and butyrate cultures., The biomass growth rate during the first feeding of each generation was much lower than during subsequent feeding periods. Occasionally, the gas production of the enrichments was observed to slow during the last few feedings, probably due to the limitation of nutrition.

Table 3-2 summarizes stoichiometric and kinetic parameters of the fatty acid anaerobic degradation. The methane yields of enrichment A-200, A-20, P-15, and B-10 were 0.5946 ± 0.0096, 0.5591 ± 0.0185, 0.6000 ± 0.0322, 0.6090 ± 0.0142 mg CH_4 COD/mg substrate COD respectively. With an average methane yield of 0.61 mg COD/ mg COD, the butyrate enrichment produced the most methane gas among the four kinds of enrichment. At similar concentration, acetate had a greater specific growth rate than propionate or butyrate, as it was directly utilized by acetoclastic methanogens, while both propionate and butyrate required conversion to acetate and hydrogen before methanogenesis could occur. The A-20 enrichment produced methane directly after feeding, while the A-2, P-15 and B10 enrichments experienced lag times of 5, 11, and 2 days, respectively. There are two explanations for the longer adaption time. Longer adaption times for propionate and butyrate substrates is partly due to the energy barriers they needed to overcome (equations (3-8)-(3-13)) (Müller et al., 2010).

Propionate:

$$CH_3CH_2COO^- + 3\ H_2O \rightarrow CH_3COO^- + HCO_3^- + H^+ + 3\ H_2$$

$$\Delta G^{o\prime} = +76.1 \text{ kJ/mol propionate}$$

(Equation 3-8)

$3\ H_2 + 0.75\ HCO_3^- + 0.75\ H^+ \rightarrow 0.75\ CH_4 + 2.15\ H_2O$

$\Delta G^{o\prime} = -101.7$ kJ/3mol hydrogen

(Equation 3-9)

Overall: $CH_3CH_2COO^- + 0.75\ H_2O \rightarrow 0.75\ CH_4 + CH_3COO^- + 0.25\ HCO_3^- + 0.25\ H^+$

$\Delta G^{o\prime} = -25.6$ kJ/mol propionate

(Equation 3-10)

Butyrate:

$CH_3CH_2CH_2COO^- + 2\ H_2O \rightarrow 2CH_3COO^- + H^+ + 2\ H_2$

$\Delta G^{o\prime} = +48.3$ kJ/mol butyrate

(Equation 3-11)

$CH_3COO^- + H^+ \rightarrow CH_4 + CO_2$

$\Delta G^{o\prime} = -36$ kJ/mol hydrogen

(Equation 3-12)

Overall: $CH_3CH_2CH_2COO^- + 2\ H_2O + H^+ \rightarrow 2CH_4 + 2CO_2 + 2\ H_2$

$\Delta G^{o\prime} = -23.7$ kJ/mol butyrate

(Equation 3-13)

The other explanation for the delay in methanogenesis is the self-inhibition characteristics. The longer the lag time was, the more self-inhibition was considered for the substrates. The possible cause for the self-inhibition for P-200 is the high acetate concentration while toxicity characteristics of propionate are likely responsible for the self-inhibition in P-15. The self-inhibition is also apparent in comparing the specific growth rates of A-200 to A-20 and comparing P-15 to B-10.

3.2 Microbial community dynamics

Biomass from both inoculum and enrichment reactors were sequenced. After the trimming and filtering processes, an average of 25,386 high-quality sequencing reads and were detected from the PCR amplicons for each sample, within which 978 unique OTUs were identified using the Silva 16S rRNA database with 97% similarity identified in the anaerobic digester sludge. Ignoring singlets, 354 OTUs including 22 OTUs for the domain Archaea and 332 OTUs for Bacteria, were identified. The 354 OTUs were assigned to 29 phyla (2 archaeal and 27 bacterial) with only 0.46(±0.35) % of sequences characterized as unclassifiable at the phylum level.

To visualize the microbial community difference among enrichment cultures with different substrates, the similarity of community structure was clustered by principal coordinate analysis (PCOA). The Bray-Curtis distance was selected for this analysis because it avoids the assumption of linear relationships among variables. The cluster result is presented in Figure 3-2 and it clearly demonstrates the distinct phylogenetic difference in microbial structure caused by different substrates and the different concentrations of the same substrate.

3.2.1 Microbial community of the inoculum

Taxonomic classification of the inoculum at the genus level was examined to verify the dynamics of the microbial community. Overall, 252 genera were identified, of which 20 that each had a relative abundance greater than 0.1% were found to account for 95% of the population abundance (Figure 3-3). Of the microbial population, 18% was archaea, with 10% of acetoclastic *Methanosaeta* and 8% of the hydrogenotrophic *Methanobacterium*. Among the bacterial populations, *Mesotoga* (25%) was the most abundant genus, followed by *Spirochaetaceae* (13%), *Trichococcus* (12%), 2 uncultured *W5* genera (7% and 6%, respectively) belonging to phylum *Cloacimonetes*, and uncultured genus (5%) belong to family *Anaerolineaceae* and phylum *Chloflexi*. The inoculum was taken from a sucrose fed continuous bench scale anaerobic reactor and the composition seemed to be reasonable considering its simpler substrate compared to other anaerobic digesters. From the microbial community

structure of the inoculum, the proportion of the two methanogenetic pathways (acetoclastic and hydrogenotrophic) is similar.

3.2.2 Archaeal community of the enrichment cultures

Overall, there were 14 genera belonged to 2 phyla observed in all 8 enrichment cultures. P-15 had the most archaeal population (59.06±5.07%) followed by B-10 (46.94±8.40%), A-20 (43.33±1.79%) and A-200 (40.7±0.52%). A possible reason for the high archaeal population in P-20 is that it has the lowest reaction rate, thus the redundant bacterial population had a longer time to die out. Among the populations, more than 99.5% belonged to *Euryarchaeota* and the distributions were shown in Figure 3-4.

3.2.2.1 Acetate enrichment

As expected, acetate enrichments were dominated by acetoclastic methanogens. The low concentration acetate (A-20) enrichment cultures were dominated by *Methanosaeta* (89.44%) followed by *Methanosarcina* (2.96%) and other methanogens (altogether 7.6%). The similar trend was observed in high concentration acetate (A-200) enrichment culture, with dominant *Methanosaeta* (68.88%), followed by *Methanosarcina* (12.19%), *Methanobacterium* (10.42%), *Mathanoculleus* (6.10%), and others (altogether <3%). It is usually believed that *Methanosarcina* tend to dominate over *Methanosaeta* in the digesters where the acetate concentration is high because of its wider range of substrates and higher growth rate (Conklin et al., 2006; Hori et al., 2006; Venkiteshwaran et al., 2015). The typical anaerobic environment for *Methanosaeta* to be the dominant acetoclastic methanogen population was found at low acetate concentrations (i.e., <1 mM) (McHugh et al., 2003; Zheng & Raskin, 2000). Some other studies showed the competitiveness of *Methanosaeta* at elevated acetate (20 mM) (Chen et al., 2017; Leite et al., 2015). The dominant *Methanosaeta* in our 20 mM acetate enrichments supports the latter observations. Even more surprisingly, although the 200 mM acetate enrichments had a higher *Methanosarcina* ratio than A-20 enrichments, they are still dominated by *Methanosaeta*. The higher hydrogenotrophic methanogens observed in A-200 indicate the possibility of syntrophic acetate oxidation, which is often observed in microbial ecosystems with more extreme conditions

such as high ammonia concentration (Jiang et al., 2018), high temperature (Mayumi et al., 2011), high acetate concentration (Hao et al., 2011).

3.2.2.2 Propionate and butyrate enrichment

Both propionate (P-15) and butyrate (B-10) enrichment cultures were dominated by *Methanospirillum* (47.19% and 40.26% respectively). The next most abundant methanogen in P-15 is *Methanobacterium* (26.31%) following by *Methanosaeta* (15.19%), *Methanosarcina* (5.93%), and *Methanoculleus* (4.45%) while *Methanosaeta* (31.13%) was observed to be the next most abundant archaea in B10 followed by *Methanobacterium* (20.59%). A small number (<1%) of *Methanomassiliicoccus*, which produces methane by reducing methanol and oxidizing hydrogen (Dridi et al., 2012), were observed in all reactors as well. It is reasonable to see more hydrogenotrophic methanogens in propionate than butyrate and more acetoclastic *Methanosaeta* in butyrate than propionate as propionate produces more H_2/CO_2 and butyrate produces more acetate with syntrophic bacteria according to equation (8) and (11). In this study, more *Methanosarcina* were observed in propionate cultures than in both acetate and butyrate enrichments with similar substrate concentration (based on mg/L COD). The acetate concentration in the propionate enrichment should be low because the conversion of propionate to acetate is thermodynamically unfavorable ($\Delta G^{o'} = +76.1$ kJ/mol propionate, as shown in equation (8)). The appearance of *Methanosarcina* suggests that the competition between the two methanogens does not solely depend on the concentration of acetate and *Methanosarcina* are more likely to be present under stress.

3.2.3 Bacterial community of the enrichment cultures

More than seven hundred bacterial OTUs were identified in the enrichment culture based on 97% similarity and those OTUs were affiliated with 149 genera and 26 phyla. The 46 bacterial genera with a relative abundance over 0.5% represent more than 95% of the total bacterial sequences and are shown in Figures 3-5 and 3-6.

3.2.3.1 Acetate enrichment

Although the archaeal communities of both A-20 and A-200 were dominated by *Methanosaeta*, the structures of the bacterial communities in these digesters were distinct. The three most abundant bacterial taxa in the high concentration acetate enrichment (A-200) were most similar to *Mesotoga* within *Thermotogae* (17.04% of total bacterial population), an unclassified genus within class *Clostridia*, phylum Firmicutes (15.42% of total bacterial population), and an unclassified genus within *Bacteroidetes* (8.86%) while the three most abundant genera in low concentration acetate enrichment (A-20) were *Mesotoga* within *Thermotogae* (19.55% of total bacterial population), an unclassified genus within *Bacteroidetes* (15.41%, different genus from the one dominant in A-200), and a genus belongs to family *Thermovirgaceae* within *Synergistetes* (12.29%).

The vast majority of the bacteria in A-20 and A-200, including quite a few genera within *Clostridia*, *ML635J-40*, *Caldicoprobacter*, *Thermovirgaceae*, *Porphyromonadaceae*, *Tenericutes*, *Treponema*, etc, are known for hydrolysis and fermentation of sugars (Bouanane-Darenfed et al., 2011; Guo et al., 2015; Hu et al., 2016; Itävaara et al., 2016; Sakamoto, 2014). Among them, the most abundant *Mesotogae* was comprised of only one unusual mesophilic OTU from the usually thermophilic or hyperthermophic phylum *Thermotogae* (Ben Hania et al., 2015). Species affiliated to this genus have been reported to grow on various sugars, peptides and organic acids (Ben Hania et al., 2013), so it seems to be unusual for it to be so predominant in an enrichment culture with a fatty acid as the sole substrate. However, it should be noted that is relative abundance in the enrichment (10%) has been reduced by half from the sucrose-fed inoculum (25%). This phenomenon can be explained by redundancy which enables a flexible community structure and an increased stability (De Vrieze et al., 2017; Werner et al., 2011a). Although most bacteria in the acetate enrichments are fermentative and scavengers, the population structures in A-200 and A-20 are distinct. This can be explained by the adaptation to different acetate concentrations as the bacteria appear in A-200 are likely more acetate tolerant. One genus in A-200, *Thermacetogenium*, has a unique function compared to the other bacteria. *Thermacetogenium* has been discovered as syntrophic acetate-oxidizing bacterium (Hattori et al.,

2000), which explained the occurrence of hydrogenotrophic methanogens and syntrophic acetate oxidation in A-200.

3.2.3.2 Propionate enrichment and butyrate enrichment

Given that the enrichment cultures were fed a single fatty acid, either sodium propionate or sodium butyrate, it was expected that the bacteria associated with syntrophic fatty propionate or butyrate degradation would be abundant. As expected, *Syntrophobacter* within *Proteobacteria*, whose species were known to be capable of degrading propionate (Harmsen et al., 1998; Liu et al., 1999), was the most predominant genus (relative abundance 35%) of the bacterial community in propionate enrichment. Meanwhile, *Syntrophomonas* within *Firmicutes*, was the most predominant genus in the butyrate enrichment. was dominated by more than 20% *Syntrophomonas* is involved in syntrophic butyrate degradation and hydrogen formation (Crable et al., 2016). The syntrophic bacteria in both the B-10 and P-15 are associated with hydrogenotrophic *Methanospirillum* and *Methanobacterium*. Interestingly, the butyrate enrichment had a lower relative abundance of syntrophic bacteria (20% compared to 35%) and a greater predominance of acetoclastic methanogens compared to the propionate enrichment. Therefore, the bacterial and archaeal community compositions indicate that acetoclastic pathways may be more predominant in the butyrate enrichment.

In the propionate enrichment, unclassified sequences affiliated to family *Thermovirgaceae* (phylum *Synergistetes*), whose known relatives are capable of synergistic hydrocarbon degradation (Duncan et al., 2009), were ranked as the 3rd most abundant OTU in the bacterial community (relative abundance of 8.08%), just after *Mesotogae* (17.77%) mentioned previously. The 4th to 7th ranked genera in propionate enrichment were an unknown genus classified to *Bacteroidetes* (5.22%), *W22* within family *Cloacamonaceae* (3.42%), *Treponema* within *Spirochaetes* (3.18%), and *Desulfovibrio* within *Proteobacteria* (3.17%). Both *W22* and *Treponema* were found to play important roles in acetogenesis (Guo et al., 2015; Tong et al., 2017). These two genera were most likely associate with *Methanosarcina*, most of whose species can utilize hydrogen and carbon dioxide in addition to acetate (Conklin et al., 2006; Liu &

Whitman, 2008). Within the butyrate enrichment, other abundant populations include: *W5* within *Cloacamonales* (12.47%), *Mesotogae* within *Thermotogae* (9.45%), 2 unknown genera within *Bacteroidetes* (9.14% and 5.57% respectively), and *W22* within *Cloacamonales* (8.85%), *Treponema* within *Spirochaetes* (5.59%), three genera belonging to order *Synergistales* within *Synergistetes* (4.53%, 2.97%, and 1.97% respectively), and *C1_B004* belonging to family *Anaerolinaceae* within *Chloroflexi* (3.12%). Populations such as *Cloacamonales*, *Spirochaetes*, and *Synergistetes* have been reported to be members of core communities in biogas digesters (Rui et al., 2015) and to participate in hydrogenotrophic methanogenesis by converting fatty acids into acetate and H_2/CO_2 (Chojnacka et al., 2015b; Pelletier et al., 2008b; Pham et al., 2009). It is noteworthy that *Spirochaetes* is claimed to take part in syntrophic oxidation of acetate (Lee et al., 2015b), thereby explaining the predominance of hydrogenotrophic methanogens, although theoretically butyrate can be converted to acetate and then be utilized by acetoclastic methanogens.

3.3 PICRUSt results

PICRUSt (phylogenetic investigation of communities by reconstruction of unobserved states) analysis suggests major functional gene pathways relevant to metabolism, cellular, environmental information processing, human diseases, organismal systems, and genetic information processing based on 16S rRNA sequencing results (Morgan et al., 2013). The pathways were classified into 328 functional KEGG pathways at Hierarchy level 3. The metabolism genes and pathways associated with sugar degradation, fatty acids reduction, and methane production were selected and investigated. To emphasize changes in microbial community structure in the enrichment cultures compared to the inoculum, we define the increase percentage as:(hit number in reactor – hit number in inoculum)/hit number in inoculum * 100%). as shown in Figure 3-7. An increase rate greater than zero indicates an increase in the metabolism pathway from inoculum to enrichment, while a value lower than zero indicates a decrease. Major changes of gene functions from inoculum to the enrichment cultures are observed. The most dramatic increase is in methane metabolism (an increase of 39.96% - 55.81% from inoculum to enrichments), which is understandable as the substrate for the

enrichment cultures is simpler and the abundance of methanogens increased. Methane metabolism is more active in the A-200 enrichment compared to the A-20 enrichment, despite slightly lower methanogen abundance in A-200. Methane metabolism genes were more abundant in propionate enrichment cultures than in butyrate enrichments despite higher $\Delta G^{o'}$ values (see equation (3-8) to (3-13) in previous section) to overcome during the syntrophic methanogenesis. A-200 and P-15 were considered to be self-inhibited due to the high concentration or the chemical characteristics (i.e. toxicity) so they experienced a much longer lag time. However, they showed a more robust methane metabolism. Both A-200 and P-15 have higher amount of *Methanosarcina* in their cultures compared to A-20 and B-10, which suggests *Methanosarcina* may play an important role in stimulating the methane production activity.

Differences were also noted in butanoate metabolism and propanoate metabolism. It is not surprising that the propionate enrichment had the most propanoate metabolism gene pathways hits among all the enrichment cultures and butyrate enrichment had the most butanoate ones. Meanwhile, propionate cultures had the second most butanoate metabolism pathways and butyrate cultures had the second most propanoate metabolism pathways, suggesting some interconversion between propionate and butyrate. The relative absence of these genes in the acetate enrichment further suggests that inter-conversions between acetate and the two fatty acids did not occur. Additional evidence supporting this conclusion includes by the greater abundance of fatty acid biosynthesis and fatty acid metabolism pathways in the propionate and butyrate enrichments. Major decreases of the functional gene pathways were observed for metabolism of fructose and mannose metabolism, homologous recombination, starch and sucrose metabolism, pentose and glucuronate interconversions, fatty acid biosynthesis, carbohydrate metabolism, and lipid metabolism. These pathways were important in the sucrose-fed anaerobic digesters, but less so in the fatty acid enrichment cultures. It is reasonable to see the drop since the fatty-acid enrichment cultures did not have any carbon source from sugars. However, the functional gene pathways did not disappear completely, despite the fact that the cultures had been transferred for several generations. This is because the functional redundancy, which has been reported repeatedly as one of the keys of stable reactor performance for it maintains a population reservoir

capable of performing the same ecological function (Allison & Martiny, 2008; Valent ń-Vargas et al., 2012).

Based on the microbial community structures and PICRUSt results of the fatty acid enrichments, a novel food web of butyrate, propionate, and acetate degradation was proposed and demonstrated in figure 3-8. However, the proportions of each pathway will shift depending on different substrate, concentration of substrate, stress level, and other factors.

4. Conclusion

Stochiometric parameters of the short chain fatty acids were estimated on the basis on methane production of the enrichment cultures. Acetate represented the highest specific growth rate among the selected fatty acids with similar carbon concentration based on mg/L COD while propionate represented the lowest. Propionate and higher concentration of acetate enrichment demonstrated self-inhibition, suggested by the long adaption period. As expected, the acetate enrichments were dominated by *Methanosaeta* and acetoclastic methanogenesis pathways while propionate and butyrate enrichments were dominated by hydrogenotrophic methanogens and their syntrophic partners. For 200 mM acetate enrichment, the observation of *Thermovirgaceae* suggests a small proportion of syntrophic acetate oxidation pathway under high acetate concentration. By investigating the microbial community structures, we proposed a food web for anaerobic degradation of the short chain fatty acids, including both acetoclastic and hydrogenotrophic methanogens, syntrophic bacteria, and other redundant bacteria populations. Furthermore, the microbial structures indicate that the competition between the two acetoclastic methanogens *Methanosarcina* and *Methanosaeta* does not solely depend on the concentration of the acetate. *Methanosarcina* are more likely to appear under stress and stimulate the methanogenesis process.

References

Ali Shah, F., Mahmood, Q., Maroof Shah, M., Pervez, A., Ahmad Asad, S. 2014. Microbial Ecology of Anaerobic Digesters: The Key Players of Anaerobiosis. *The Scientific World Journal*, **2014**, 183752.

Allison, S.D., Martiny, J.B.H. 2008. Resistance, resilience, and redundancy in microbial communities. *Proceedings of the National Academy of Sciences of the United States of America*, **105**(Suppl 1), 11512-11519.

Ben Hania, W., Postec, A., Aullo, T., Ranchou-Peyruse, A., Erauso, G., Brochier-Armanet, C., Hamdi, M., Ollivier, B., Saint-Laurent, S., Magot, M., Fardeau, M.L. 2013. Mesotoga infera sp. nov., a mesophilic member of the order Thermotogales, isolated from an underground gas storage aquifer. *International Journal of Systematic and Evolutionary Microbiology*, **63**(Pt 8), 3003-8.

Bouanane-Darenfed, A., Fardeau, M.L., Gregoire, P., Joseph, M., Kebbouche-Gana, S., Benayad, T., Hacene, H., Cayol, J.L., Ollivier, B. 2011. Caldicoprobacter algeriensis sp. nov. a new thermophilic anaerobic, xylanolytic bacterium isolated from an Algerian hot spring. *Current Microbiology*, **62**(3), 826-32.

Carlsson, M., Lagerkvist, A., Morgan-Sagastume, F. 2012. The effects of substrate pre-treatment on anaerobic digestion systems: A review. *Waste Management*, **32**(9), 1634-1650.

Chen, S., Cheng, H., Liu, J., Hazen, T.C., Huang, V., He, Q. 2017. Unexpected competitiveness of Methanosaeta populations at elevated acetate concentrations in methanogenic treatment of animal wastewater. *Applied Microbiology and Biotechnology*, **101**(4), 1729-1738.

Chojnacka, A., Szczęsny, P., Błaszczyk, M.K., Zielenkiewicz, U., Detman, A., Salamon, A., Sikora, A. 2015. Noteworthy Facts about a Methane-Producing Microbial Community Processing Acidic Effluent from Sugar Beet Molasses Fermentation. *PLOS ONE*, **10**(5), e0128008.

Conklin, A., Stensel, H.D., Ferguson, J. 2006. Growth kinetics and competition between Methanosarcina and Methanosaeta in mesophilic anaerobic digestion. *Water Environment Resources*, **78**(5), 486-96.

Crable, B.R., Sieber, J.R., Mao, X., Alvarez-Cohen, L., Gunsalus, R., Ogorzalek Loo, R.R., Nguyen, H., McInerney, M.J. 2016. Membrane Complexes of Syntrophomonas wolfei Involved in Syntrophic Butyrate Degradation and Hydrogen Formation. *Frontiers in Microbiology*, **7**(1795).

De Vrieze, J., Christiaens, M.E.R., Walraedt, D., Devooght, A., Ijaz, U.Z., Boon, N. 2017. Microbial community redundancy in anaerobic digestion drives process recovery after salinity exposure. *Water Research*, **111**, 109-117.

Dridi, B., Fardeau, M.L., Ollivier, B., Raoult, D., Drancourt, M. 2012. Methanomassiliicoccus luminyensis gen. nov., sp. nov., a methanogenic archaeon isolated from human faeces. *International Journal of Systematic and Evolutionary Microbiology*, **62**(Pt 8), 1902-7.

Duncan, K.E., Gieg, L.M., Parisi, V.A., Tanner, R.S., Tringe, S.G., Bristow, J., Suflita, J.M. 2009. Biocorrosive thermophilic microbial communities in Alaskan North Slope oil facilities. *Environmental Science & Technology*, **43**(20), 7977-84.

Goswami, R., Chattopadhyay, P., Shome, A., Banerjee, S.N., Chakraborty, A.K., Mathew, A.K., Chaudhury, S. 2016. An overview of physico-chemical mechanisms of biogas production by microbial communities: a step towards sustainable waste management. *3 Biotech*, **6**(1), 72.

Guo, J., Peng, Y., Ni, B.-J., Han, X., Fan, L., Yuan, Z. 2015. Dissecting microbial community structure and methane-producing pathways of a full-scale anaerobic reactor digesting activated sludge from wastewater treatment by metagenomic sequencing. *Microbial Cell Factories*, **14**, 33.

Hao, L.-P., Lü, F., He, P.-J., Li, L., Shao, L.-M. 2011. Predominant Contribution of Syntrophic Acetate Oxidation to Thermophilic Methane Formation at High Acetate Concentrations. *Environmental Science & Technology*, **45**(2), 508-513.

Harmsen, H.J., Van Kuijk, B.L., Plugge, C.M., Akkermans, A.D., De Vos, W.M., Stams, A.J. 1998. Syntrophobacter fumaroxidans sp. nov., a syntrophic propionate-degrading sulfate-reducing bacterium. *International Journal of Systematic and Evolutionary Microbiology*, **48 Pt 4**, 1383-7.

Hattori, S. 2008. Syntrophic acetate-oxidizing microbes in methanogenic environments. *Microbes Environment*, **23**(2), 118-27.

Hattori, S., Kamagata, Y., Hanada, S., Shoun, H. 2000. Thermacetogenium phaeum gen. nov., sp. nov., a strictly anaerobic, thermophilic, syntrophic acetate-oxidizing bacterium. *International Journal of Systematic and Evolutionary Microbiology* **50 Pt 4**, 1601-9.

Hori, T., Haruta, S., Ueno, Y., Ishii, M., Igarashi, Y. 2006. Dynamic transition of a methanogenic population in response to the concentration of volatile fatty acids in a thermophilic anaerobic digester. *Applied and Environmental Microbiology*, **72**(2), 1623-30.

Hu, P., Tom, L., Singh, A., Thomas, B.C., Baker, B.J., Piceno, Y.M., Andersen, G.L., Banfield, J.F. 2016. Genome-Resolved Metagenomic Analysis Reveals Roles for Candidate Phyla and Other Microbial Community Members in Biogeochemical Transformations in Oil Reservoirs. *mBio*, **7**(1).

Itävaara, M., Salavirta, H., Marjamaa, K., Ruskeeniemi, T. 2016. Chapter One - Geomicrobiology and Metagenomics of Terrestrial Deep Subsurface Microbiomes. in: *Advances in Applied Microbiology*, (Eds.) S. Sariaslani, G.M. Gadd, Vol. 94, Academic Press, pp. 1-77.

Jiang, Y., Banks, C., Zhang, Y., Heaven, S., Longhurst, P. 2018. Quantifying the percentage of methane formation via acetoclastic and syntrophic acetate oxidation pathways in anaerobic digesters. *Waste Management*, **71**, 749-756.

Lee, S.H., Park, J.H., Kim, S.H., Yu, B.J., Yoon, J.J., Park, H.D. 2015. Evidence of syntrophic acetate oxidation by Spirochaetes during anaerobic methane production. *Bioresource Technology*, **190**, 543-9.

Leite, A., Janke, L., Lv, Z., Harms, H., Richnow, H.-H., Nikolausz, M. 2015. Improved Monitoring of Semi-Continuous Anaerobic Digestion of Sugarcane Waste: Effects of Increasing Organic Loading Rate on Methanogenic Community Dynamics. *International Journal of Molecular Sciences*, **16**(10), 23210.

Li, Y., Park, S.Y. and Zhu, J. (2011) Solid-state anaerobic digestion for methane production from organic waste. *Renewable and Sustainable Energy Reviews* 15(1), 821-826.

Li, Y., Zhang, Y., Liu, Y., Zhao, Z., Zhao, Z., Liu, S., Zhao, H., Quan, X. 2016. Enhancement of anaerobic methanogenesis at a short hydraulic retention time via bioelectrochemical enrichment of hydrogenotrophic methanogens. *Bioresource Technology*, **218**, 505-11.

Liu, Y., Balkwill, D.L., Aldrich, H.C., Drake, G.R., Boone, D.R. 1999. Characterization of the anaerobic propionate-degrading syntrophs Smithella propionica gen. nov., sp. nov. and Syntrophobacter wolinii. *International Journal of Systematic and Evolutionary Microbiology*, **49**(2), 545-556.

Liu, Y., Whitman, W.B. 2008. Metabolic, phylogenetic, and ecological diversity of the methanogenic archaea. *Annals of the New York Academy of Sciences*, **1125**, 171-89.

Müller, N., Worm, P., Schink, B., Stams, A.J.M., Plugge, C.M. 2010. Syntrophic butyrate and propionate oxidation processes: from genomes to reaction mechanisms. *Environmental Microbiology Reports*, **2**(4), 489-499.

Ma, J., Zhao, B., Frear, C., Zhao, Q., Yu, L., Li, X., Chen, S. 2013. Methanosarcina domination in anaerobic sequencing batch reactor at short hydraulic retention time. *Bioresource Technology*, **137**, 41-50.

Mathai, P.P., Zitomer, D.H., Maki, J.S. 2015. Quantitative detection of syntrophic fatty acid-degrading bacterial communities in methanogenic environments. *Microbiology*, **161**(6), 1189-97.

Mayumi, D., Mochimaru, H., Yoshioka, H., Sakata, S., Maeda, H., Miyagawa, Y., Ikarashi, M., Takeuchi, M., Kamagata, Y. 2011. Evidence for syntrophic acetate oxidation coupled to hydrogenotrophic methanogenesis in the high-temperature petroleum reservoir of Yabase oil field (Japan). *Environmental Microbiology*, **13**(8), 1995-2006.

McHugh, S., Carton, M., Mahony, T., O'Flaherty, V. 2003. Methanogenic population structure in a variety of anaerobic bioreactors. *FEMS Microbiology Letter*, **219**(2), 297-304.

Pan, X., Angelidaki, I., Alvarado-Morales, M., Liu, H., Liu, Y., Huang, X., Zhu, G. 2016. Methane production from formate, acetate and H2/CO2; focusing on kinetics and microbial characterization. *Bioresource Technology*, **218**, 796-806.

Pelletier, E., Kreimeyer, A., Bocs, S., Rouy, Z., Gyapay, G., Chouari, R., Rivière, D., Ganesan, A., Daegelen, P., Sghir, A., Cohen, G.N., Médigue, C., Weissenbach, J., Le Paslier, D. 2008. "Candidatus Cloacamonas acidaminovorans": Genome sequence reconstruction provides a first glimpse of a new bacterial division. *Journal of Bacteriology*, **190**(7), 2572-2579.

Pham, V.D., Hnatow, L.L., Zhang, S., Fallon, R.D., Jackson, S.C., Tomb, J.F., DeLong, E.F., Keeler, S.J. 2009. Characterizing microbial diversity in production water from an Alaskan mesothermic petroleum reservoir with two independent molecular methods. *Environmental Microbiology*, **11**(1), 176-187.

Romero-Güiza, M.S., Vila, J., Mata-Alvarez, J., Chimenos, J.M., Astals, S. 2016. The role of additives on anaerobic digestion: A review. *Renewable and Sustainable Energy Reviews*, **58**, 1486-1499.

Rui, J., Li, J., Zhang, S., Yan, X., Wang, Y., Li, X. 2015. The core populations and co-occurrence patterns of prokaryotic communities in household biogas digesters. *Biotechnology for Biofuels*, **8**.

Sakamoto, M. 2014. The Family Porphyromonadaceae. in: *The Prokaryotes: Other Major Lineages of Bacteria and The Archaea*, (Eds.) E. Rosenberg, E.F. DeLong, S. Lory, E. Stackebrandt, F. Thompson, Springer Berlin Heidelberg. Berlin, Heidelberg, pp. 811-824.

Tong, H., Chen, M., Li, F., Liu, C., Liao, C. 2017. Changes in the microbial community during repeated anaerobic microbial dechlorination of pentachlorophenol. *Biodegradation*, **28**(2-3), 219-230.

Valent ín-Vargas, A., Toro-Labrador, G., Massol-Dey á, A.A. 2012. Bacterial Community Dynamics in Full-Scale Activated Sludge Bioreactors: Operational and Ecological Factors Driving Community Assembly and Performance. *PLoS ONE,* **7**(8), e42524.

Venkiteshwaran, K., Bocher, B., Maki, J., Zitomer, D. 2015. Relating Anaerobic Digestion Microbial Community and Process Function. *Microbiology Insights,* **8**(Suppl 2), 37-44.

Werner, J.J., Knights, D., Garcia, M.L., Scalfone, N.B., Smith, S., Yarasheski, K., Cummings, T.A., Beers, A.R., Knight, R., Angenent, L.T. 2011. Bacterial community structures are unique and resilient in full-scale bioenergy systems. *Proceedings of the National Academy of Sciences*, **108**(10), 4158.

Westerholm, M., Moestedt, J., Schn ürer, A. 2016. Biogas production through syntrophic acetate oxidation and deliberate operating strategies for improved digester performance. *Applied Energy*, **179**, 124-135.

Yang, Y., Chen, Q., Guo, J., Hu, Z. 2015. Kinetics and methane gas yields of selected C1 to C5 organic acids in anaerobic digestion. *Water Research*, **87**, 112-8.

Zheng, D., Raskin, L. 2000. Quantification of Methanosaeta Species in Anaerobic Bioreactors Using Genus- and Species-Specific Hybridization Probes. *Microbial Ecology*, **39**(3), 246-262.

Appendix: Tables and Figures

Table 3-1. Detailed enrichment conditions

	Substrate	Concentration	Generation	Feed times per generation	Duration (days)
A-200-1	Sodium Acetate	200 mM	3	1	185
A-200-2	Sodium Acetate	200 mM	3	1	185
A-20-1	Sodium Acetate	20 mM	3	10	216
A-20-2	Sodium Acetate	20 mM	3	10	216
P-15-1	Sodium Propionate	15 mM	3	10	266
P-15-2	Sodium Propionate	15 mM	3	10	266
B-10-1	Sodium Butyrate	10 mM	3	10	211
B-10-2	Sodium Butyrate	10 mM	3	10	211

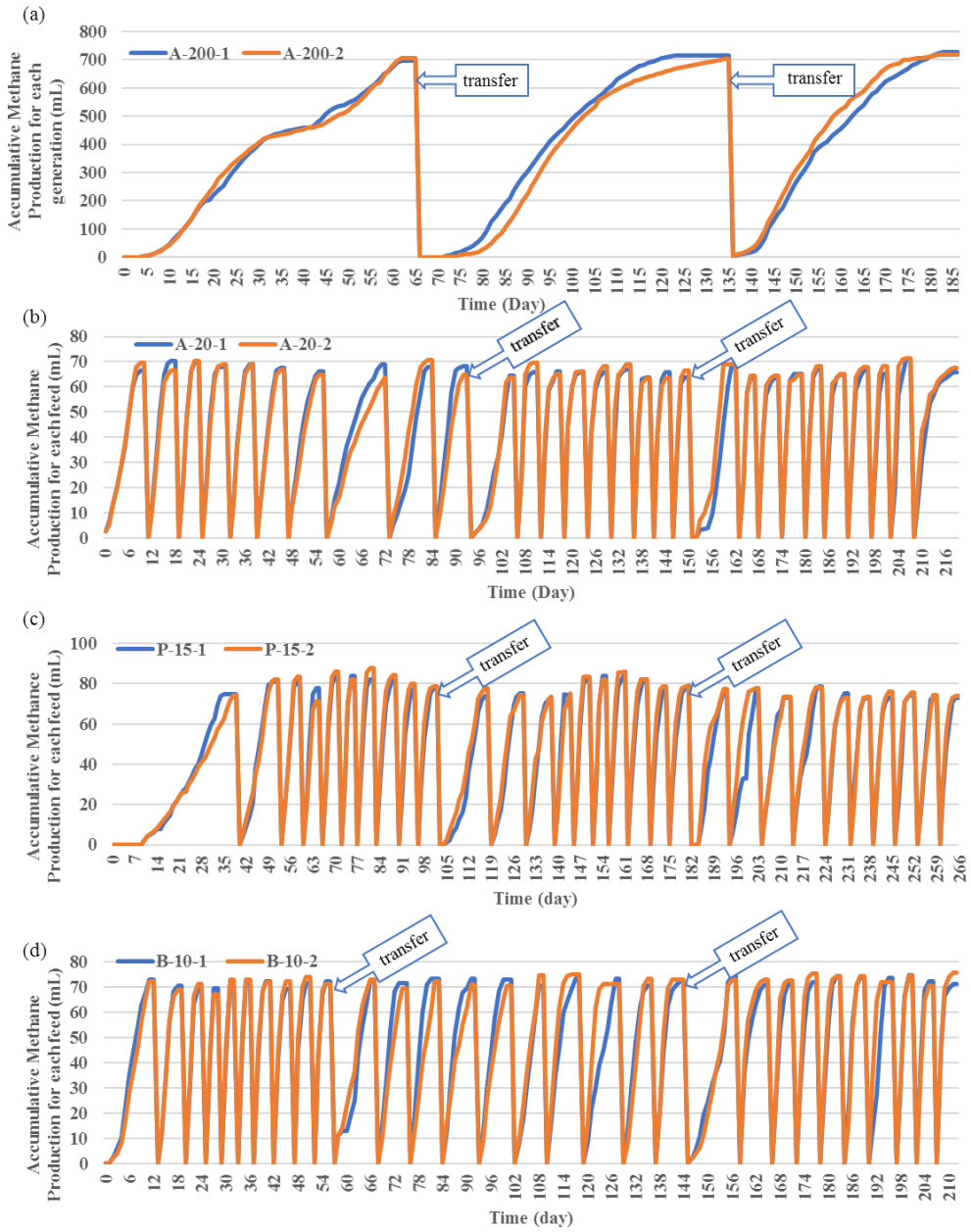

Figure 3-1. Accumulative methane production (a) 200 mM acetate enrichment (b) 20 mM acetate enrichment (c) 15 mM propionate enrichment (d) 10 mM butyrate enrichment

Table 3-2. Kinetic parameters of fatty acid degradation under anaerobic digestion

	200 mM Acetate	20 mM Acetate	15 mM Propionate	10 mM Butyrate
lag time for the 1st generation (day)	5	0	11	2
substrate COD (mg/L)	8640	864.0	941.4	859.1
cumulative methane production (mg/L as COD)	5137.5 ±83.1	483.1 ±16.0	564.8 ±30.3	523.2 ±12.21
f_e (methane yields)	0.5946 ±0.0096	0.5591 ±0.0185	0.6000 ±0.0322	0.6090 ±0.0142
$/f_s$	0.4053 ±0.0096	0.4408 ±0.0185	0.4000 ±0.0322	0.3909 ±0.0142
average μ (/day)	0.0024 ±0.0005	0.0300 ±0.0112	0.0226 ±0.0094	0.0261 ±0.0098
maximum μ (/day)	0.0031	0.0487	0.0416	0.0473
minimum μ (/day)	0.0019	0.009	0.0031	0.0118
μ_{max} (/day)	0.0806 ±0.0815	0.0773 ±0.0026	0.0830 ±0.0044	0.0842 ±0.0020

Figure 3-2. Principal coordinate analysis (PCOA) clustering using the Bray-Curtis distance

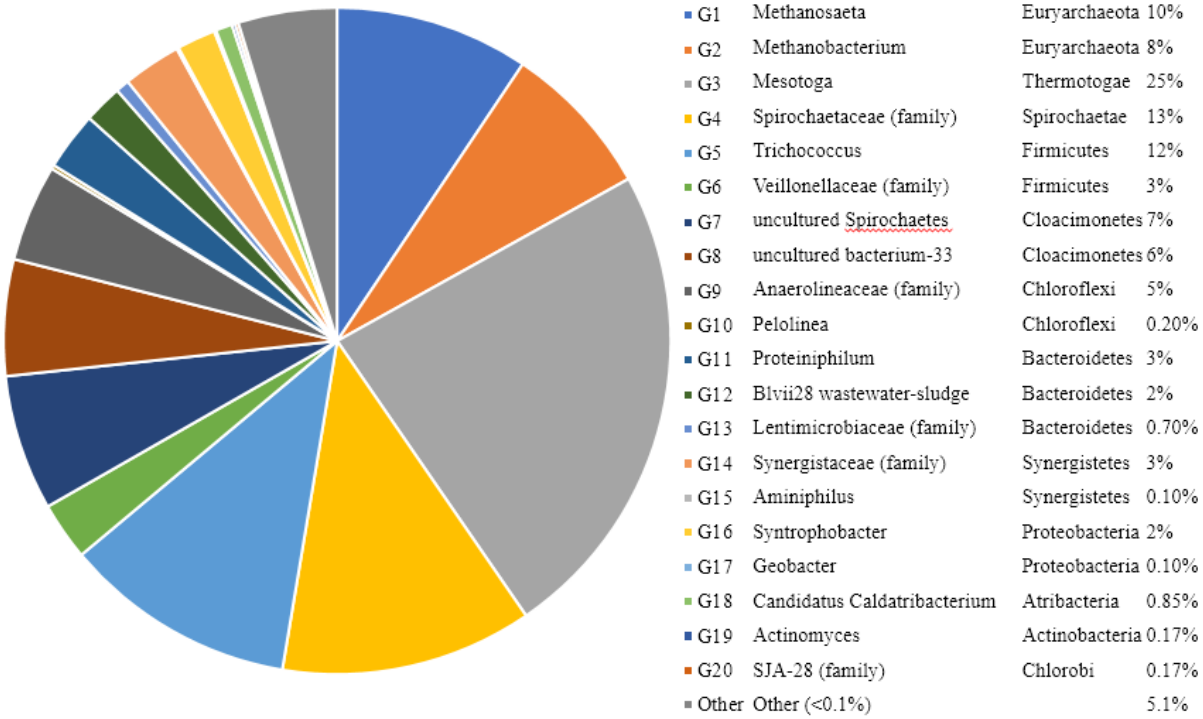

Figure 3-3. Microbial community structure of inoculum

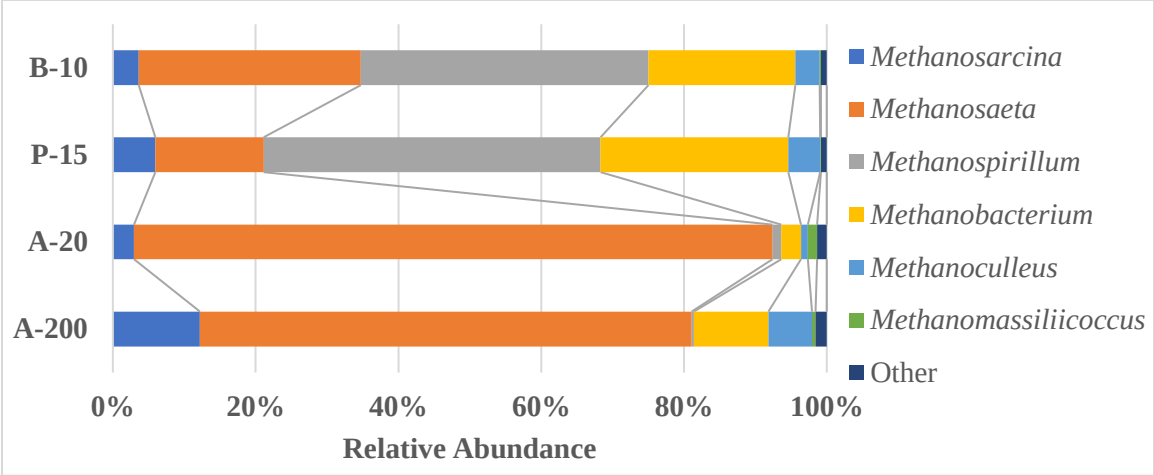

Figure 3-4. Relative abundance of archaeal community in the enrichment cultures on genus level. A-200: 200 mM acetate; A-20: 20 mM acetate; P-15: 15 mM propionante; B-10: 10 mM butyrate

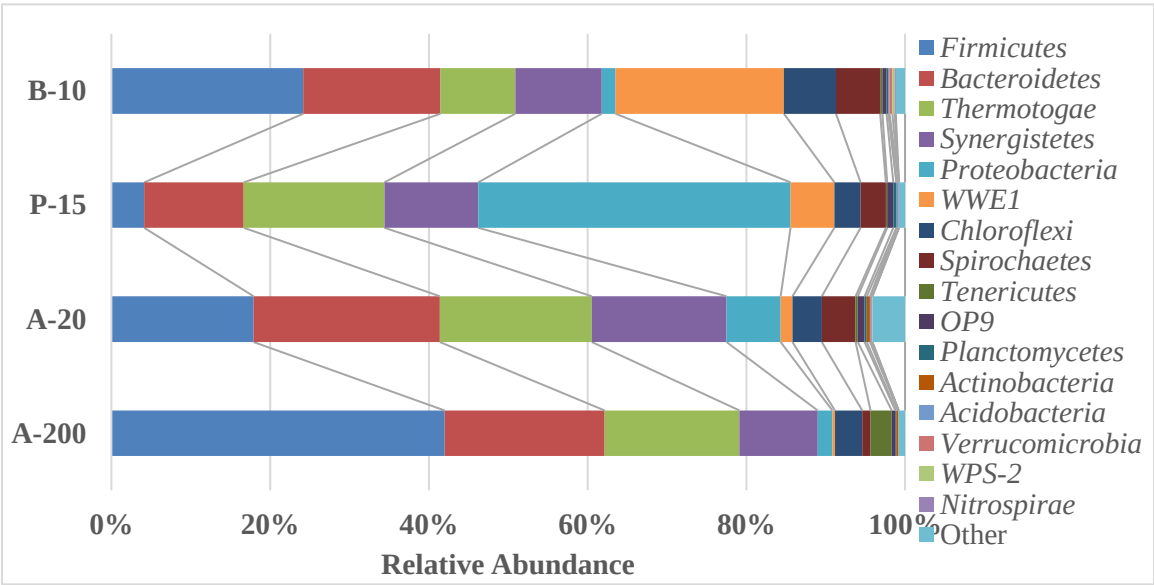

Figure 3-5. Relative abundance of bacterial community in the enrichment cultures on phylum level. A-200: 200 mM acetate; A-20: 20 mM acetate; P-15: 15 mM propionate; B-10: 10 mM butyrate

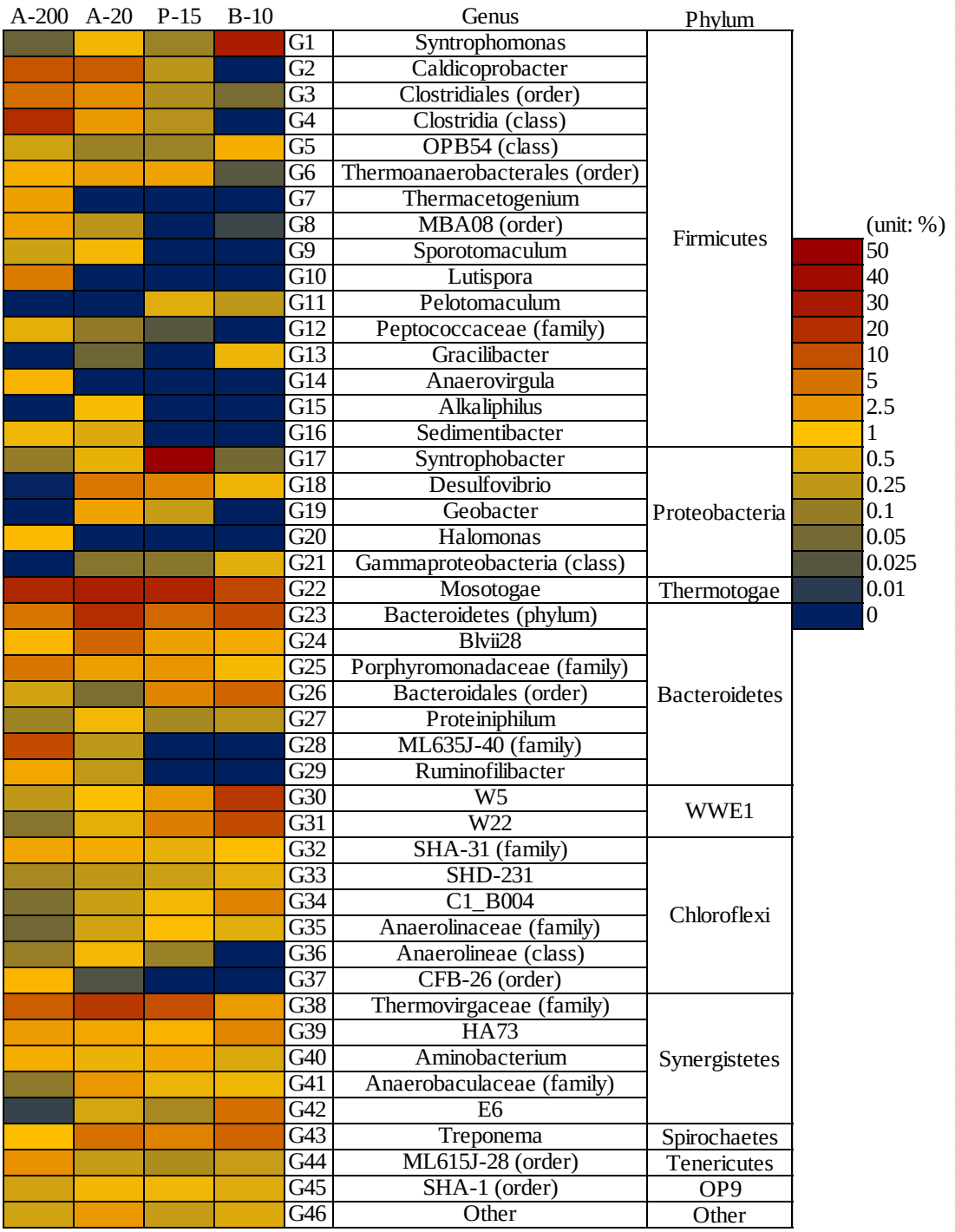

Figure 3-6. Heatmap showing relative abundance of bacterial community in the enrichment cultures on genus and phylum level. A-200: 200 mM acetate; A-20: 20 mM acetate; P-15: 15 mM propionante; B-10: 10 mM butyrate

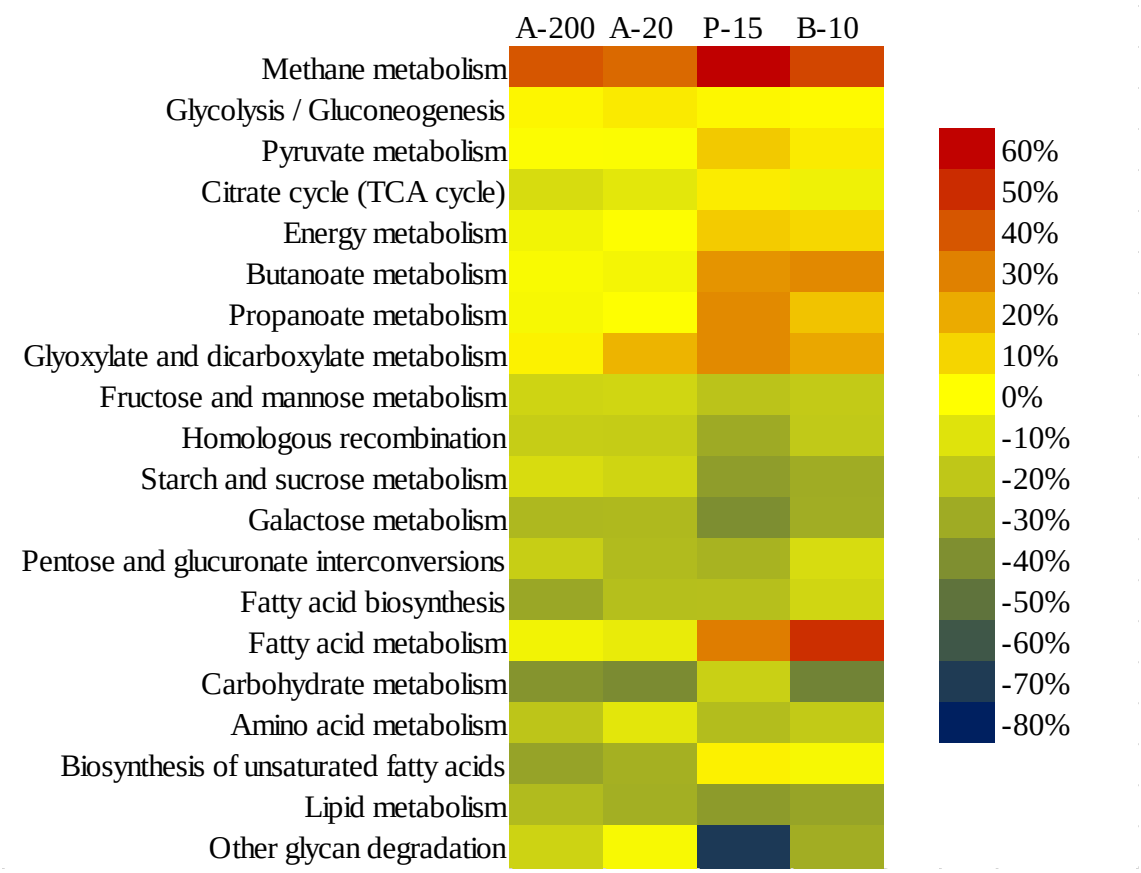

Figure 3-7. Heatmap showing the increase percentage (increase percentage = (hit number in reactor – hit number in inoculum)/hit number in inoculum * 100%) of selected potential gene functions predicted by PICRUSt using 16S rRNA marker gene with KEEG database on fatty acid enrichment. Increase rate greater than zero means there is an increase in the metabolism pathway from inoculum to biomass from reactor whole lower than zero means there is a decrease. All the data is from the average of the duplicate reactors. A-200: 200 mM acetate; A-20: 20 mM acetate; P-15: 15 mM propionate; B-10: 10 mM butyrate.

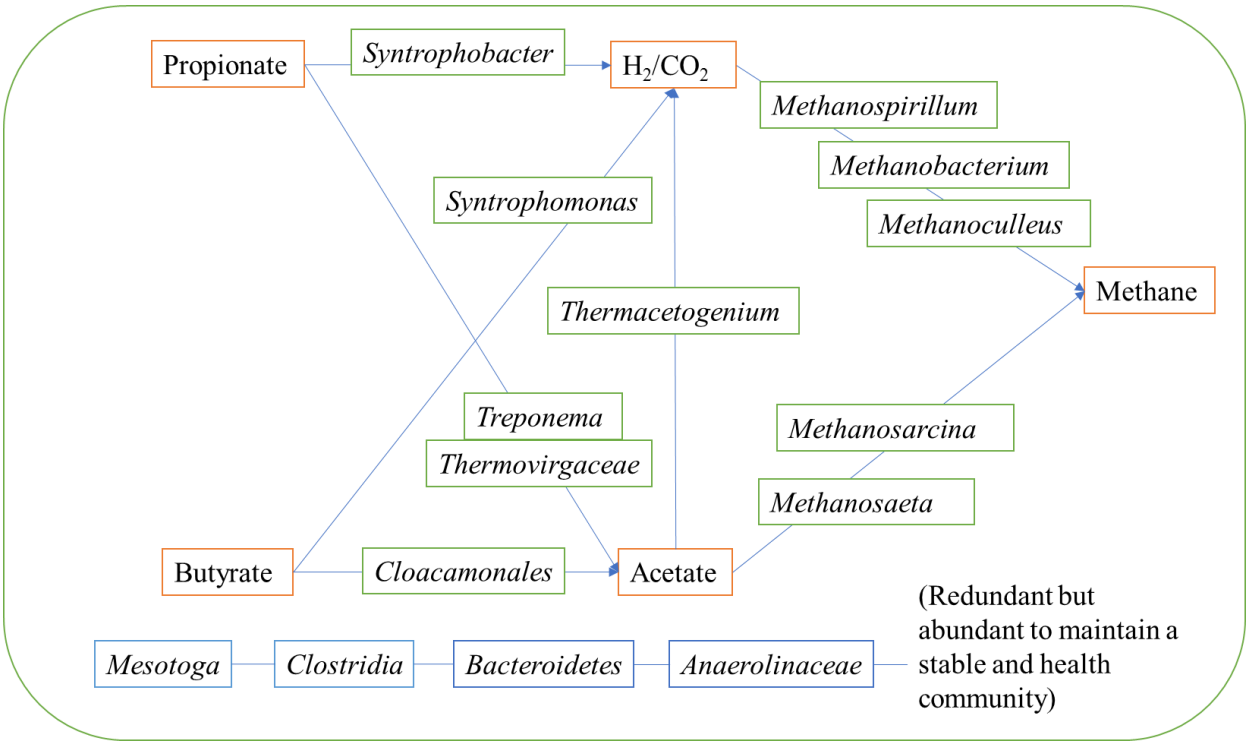

Figure 3-8. Proposed food web of butyrate, propionate, and acetate anaerobic degradation based on community structures and PICRUSt results

CHAPTER IV - SPECIFIC SYNTROPHIC PARTNER WITH UNSPECIFIC HYDROGENOTROPHIC METHANOGENS IN THE ANAEROBIC DEGRADATION OF PROPIONATE

Abstract

Propionate is one of the essential intermediates production during anaerobic digestion process and the degradation of propionate is critical for stable performance owing to its unfavorable thermodynamic nature. It is crucial to better understand the syntrophic propionate degradation to enhance the stability and efficiency of anaerobic digestion. This study developed several groups of propionate enrichment cultures to identify the syntrophic propionate oxidizers and to investigate the effect of diverse sources of inoculum, different sampling points, and altered substrate concentrations on the microbial community structures of propionate enrichment. The results provided various evidences to demonstrate *Syntrophobacter* as the specific obligate syntrophic proton-reducing acetogenic bacteria while its associated methanogen partners are not definitive although *Methanoculleus* tend to be dominant under more extreme conditions, which indicates that the introduction of enriched *Syntrophobacter* and *Methanoculleus* may be more effective bioaugmentation facing accumulation of propionate to obtain a desired process function.

Keywords

Methanogenesis, Syntrophy, Anaerobic propionate degradation

1. Introduction

Anaerobic degradation of complex organics has attracted much attention as it minimizes the carbon footprint while recovering methane as a renewable energy source, which is realized through four sequential steps, hydrolysis, acidogenesis, acetogenesis, and methanogenesis (Qiao et al. 2015). Propionate is an essential organic intermediate in this process as it accounts for approximately one third of the biogenic methane production in nature (McCarty and Smith 1986). Under standard conditions, the conversion of propionate to acetate, formate, carbon dioxide, and hydrogen is endergonic (ΔG^o = +76.1 kJ/mol at 25^{o}C). The spontaneous conversion is dependent on a sufficiently low hydrogen pressure maintained by methanogenesis, which consumes hydrogen (Muller et al. 2010). Due to its unfavorable thermodynamics, the

degradation of propionate can be interrupted when the propionate concentration reaches a homeostatic equilibrium; thus, acetogenesis is critical for the whole digestion process (Gallert and Winter 2008). Accumulation of propionate is often followed by spikes in hydrogen partial pressure, thus inhibiting the syntrophic propionate degradation (Li et al. 2018a). Therefore, a better understanding of syntrophic propionate oxidation is key to improving the efficiency of anaerobic degradation of organics.

This study investigates the microbial population associated with anaerobic propionate oxidation under the impact of diverse source populations (inocula), different sampling times, and distinct concentrations of propionate. The results demonstrated that *Syntrophobacter* is the most abundant bacteria in the enrichment cultures while the archaeal populations varied substantially; thus, we came to the conclusion that the *Syntrophobacter* is the specific syntrophic propionate oxidizer associated with a number of unspecific methanogens in our enrichments.

Two bacterial genera are reported to be involved in syntrophic degradation of propionate through two distinct pathways: *Syntrophobacter* involved in syntrophic degradation associated with hydrogenotrophic methanogens (Chen et al. 2005a, Plugge et al. 2012), and *Smithella* involved in dismutation of propionate to acetate and butyrate via a six-carbon intermediate (Dolfing 2013, Liu et al. 1999). Although only *Syntrophobacter* was identified in our enrichment cultures, we were still curious about whether the other syntrophic propionate oxidation pathway was present even though it was not detected by the 16S rRNA amplicon sequencing. Therefore, we further conducted some cross-feeding experiments to show that the *Smithella* pathway did not occur in our enrichment as butyrate was not detected as an intermediate in the cultures.

2. Materials and Methods

2.1 High-level experimental design

This study was designed to investigate community composition of acetogenic and methanogenic organisms with propionate substrates. The experiments to investigate particular questions are described below.

2.1.1 General culture methods

Various inocula were fed with various substrates in groups of 10 feeding cycles of approximately equivalent carbon content. The end of each feeding period was indicated by cessation of biogas formation, at which time the next increment of substrate was added to the reactor. After 10 feeding cycles, biomass was transferred to a new bottle at 3% biomass concentration and the 10x feeding cycle repeated. The purpose of the enrichment and transfer procedures is to develop a stable community specifically for the fatty acid degradation and to eliminate other redundant biomass. All enrichment cultures were kept at 37 (±1) ^{o}C with shaking at 80 rpm to ensure complete mixed conditions. Serum glass bottles with a working volume of 160 mL and a head space of 60 mL with aluminum caps were used as the enrichment digesters. The bottles were sealed by butyl rubber stoppers to ensure anaerobic conditions.

Each liter of the selective sterile medium contains the following: 1.0 g NaCl, 0.5 g KCl, 0.5 g $MgCl_2 \cdot 6H_2O$, 0.3 g NH_4Cl, 1.7 g KH_2PO_4, 3.0 g K_2HPO_4, 0.0015 g $CaCl_2 \cdot 2H_2O$, 1.5 mg $FeCl_2 \cdot 4H_2O$, 0.19 mg $CoCl_2 \cdot 6H_2O$, 0.1 mg $MnCl_2 \cdot 4H_2O$, 0.07 mg $ZnCl_2$, 0.036 mg $Na_2MoO_4 \cdot 2H_2O$, 0.024 mg $NiCl_2 \cdot 6H_2O$, 0.008 mg $Na_2WO_4 \cdot 2H_2O$, 0.006 mg H_3BO_3, 0.006 mg $Na_2SeO_3 \cdot 5H_2O$, 0.002 mg $CuCl_2 \cdot 2H_2O$, 0.5 mg NaOH, 0.25 mL 0.1% Resazurin, 0.048g $Na_2S \cdot 9H_2O$, 0.031 g L-cysteine, and 1 mL of the Wolin Vitamins (which contained 0.02 mg/L biotin, 0.02 mg/L folic acid, 0.1 mg/L pyridoxine hydrochloride, 0.05 mg/L riboflavin, 0.05 mg/L thiamine, 0.05 mg/L nicotinic acid, 0.05 mg/L pantothenic acid, 0.001 mg/L vitamin B12, 0.05 mg/L p-aminobenzoic acid, and 0.05 mg/L thioctic acid). pH of the medium was adjusted to 7.2 by 1 mol/L K_2HPO_4 if too low and 1 mol/L KH_2PO_4 if too high. The medium was heated to the boiling point and purged with N_2 to get rid of the oxygen before Resazurin and $Na_2S \cdot 9H_2O$ were added. The sealed bottles were then autoclaved for 20 minutes under 120 ℃. The medium was selected specifically to avoid the presence of carbonate and bicarbonate to facilitate carbon balance calculations. The only carbon sources contributing to carbon dioxide are the organic feeding stock (main) and inoculum.

2.1.2 Investigation of the effect of inocula on community composition

In this group of experiments, various inocula were fed 15 mM of propionate in each feeding cycle. Inocula investigated include: dairy manure, cattle manure, full-scale anaerobic digestion sludge, pilot-scale anaerobic digestion sludge, and lab-scale anaerobic bioreactor sludge. A total of five biomass transfers were conducted with biomass sequencing conducted after the third and fifth transfer.

2.1.3 Investigation of the effect of propionate concentration on community composition

In this group of experiments, the anaerobic digesters were seeded with the well-mixed sludge from previous laboratory sucrose fed reactors as the inoculum (10/90 volume/volume). Propionate concentrations of 15 mM and 150 mM were used. Only two biomass transfers were conducted at the higher propionate concentration because of slow biomass growth.

2.1.4 Identification of propionate degradation pathways present in propionate enriched digesters

In this group of experiments, the anaerobic digesters were seeded with the well-mixed sludge from previous laboratory sucrose fed reactors as the inoculum (10/90 volume/volume).

Different digesters were fed with propionate (P), Acetate (A) or Butyrate (B) at concentrations equivalent to 15mM propionate on a carbon basis. After five transfer cycles, substrates were switched to other substrates for five feeding cycles. These cross-feeding experiments were designated P-A, P-B, A-P, A-B, B-A, and B-P.

2.2 Chemical analysis

Biogas (CH_4 and CO_2) production was measured daily using a water displacement method (Demirer and Speece 1998). Gas composition was determined using an HP 5890 gas chromatography with thermal conductivity detector, Supelco packing column (60/80 Carbonxen®-1000), and Argon carrier gas with a flow rate of 5 ml/min (Zhu et al. 2011). The temperatures of injection, oven (column), and detection were set to 150 ℃, 125 ℃, and 170 ℃ respectively and the process time was set to 12 minutes for N_2, CH_4, and CO_2 to be fully

separated and detected (Zhu et al. 2011). The peaks of CH_4 and CO_2 appeared at 5.5 minutes and 10.5 minutes respectively. Standard curves of CH_4 and CO_2 were calibrated monthly to maintain accuracy.

The temperature of the incubator was monitored daily with a thermometer and maintained at 37 (±2) ℃. After the utilization of propionate, waste slurry samples were analyzed and preserved. Slurry was centrifuged at 14000 x g; the biomass was preserved at -80 ℃ for molecular analysis and the supernatant was analyzed for chemical oxygen demand (COD) and volatile fatty acid concentrations (VFA). COD was measured with CHEMetrics™ COD Vials Kits and Spec 20 Spectrophotometer according to the standard method (Rice et al. 2012). VFA (acetate and propionate) was measured by gas chromatography with FID (flame ionization detector) and a Restek Stabilwax®-DA column, using Helium as the carrier gas at a flow rate of 20 mL/min with 1:20 split ratio (Zhang and Jahng 2010). The injection and detection temperatures were set to 250 ℃ and 300 ℃ respectively. There temperature gradient for the oven (column) was: 80 ℃ for 1 minute, an increase of 10 ℃/min to 220 ℃ and maintained at 220 ℃ for 5 minutes. Samples were acidified to pH < 2 with 0.5 mL 85% H_3PO_4.

2.3 Community analysis

DNA was extracted using MP FastDNA™ Spin Kit for Soil according to the manufacturer's instruction (Protocol Revision #116560200-201608) with minor modification (i.e., adding extra washing step) and purified with Zymo Genomic DNA Clean & Concentrator™-10 kit according to the instruction manual. The qualities (260/230, 260/280) and concentrations of the DNA were determined using Thermo Scientific NanoDrop ND-3300 Fluorospectrometer.

Polymerase chain reactions targeting V4 region of 16S rRNA genes were prepared with a cocktail mix (25 μL) containing 12 μL Phusion flash Master Mix, 1 μL forward primer (515F: GTGCCAGCMGCCGCGGTAA), 1 μL reverse primer (806R: GGACTACHVGGGTWTCTAAT with a unique 12-base specific barcode for each sequence), 2 μL (100 to 150 ng) DNA template, and 9 μL ultra-pure water. The PCR program is set as follows: one cycle of 94 ℃ for 3 minutes, 35 cycles at 94 ℃ for 45 seconds (denaturation), 55 ℃

for 1 minute (annealing), and 72 ℃ for 1 minute and a half (elongation), a final extension at 72 ℃ for 10 minutes, and then stored at 4 ℃. Post PCR, the quality and concentrations of amplicons were measured on an Agilent 2100 Bioanalyzer Instruments with Agilent DNA 7500 chips. Concentration of pooled library were determined using KAPA Illumina kit for quantifying library (KK4824) from KAPA Biosystems and were diluted with 10 mM Tris/0.05% tween buffer (pH = 8.5) targeting 4 nM and denatured with 0.2 N freshly made NaOH solution. The sample was then combined with 20% PhiX control kit to increase the library diversity. The library was finally loaded at 10 pM to an Illumina MiSeq System with a MiSeq Reagent Kit v2 (300-cycles) and Metagenomic workflow was selected to execute the 16S protocol using the MiSeq Reporter software (MSR).

Amplicon sequences were processed using the CLC Genomic Workbench 9.5.3 with microbial genomic module. First, the overlapped sequences were aligned so that the forward and reverse readings were merged and pairs with more than 3 mismatches were discarded. Then the merged reads were trimmed at 0.001, filtering out sequences less than 250 base pairs (bp). OTUs were determined using a reference-based OTU clustering module with SILVA 16S v 128 97% database (Yilmaz et al. 2014). OTU assignments were based on a similarity threshold of 97%, with a minimum occurrence of 2, chimera crossover cost of 3, and maximum unaligned end mismatches of 5.

3. Results and Discussion

3.1 Impact of different inocula on the microbial composition of the propionate enrichments

We sought to investigate how the inocula influences the composition of the microbial population. Four stages (hydrolysis, acidogenesis, acetogenesis, and methanogenesis) comprise the anaerobic digestion process. Each step is catalyzed by specialized, yet diverse, microorganisms. A common challenge in conducting fundamental studies of anaerobic digestion is that the substrate often contains organisms that influence the microbial community through migration. Several studies have been conducted using substrates that also serve as the community inoculum, including rice

straw (Gu et al. 2014), food waste (Dhamodharan et al. 2015), cattle manure (Saidu et al. 2013), waste vegetable oil (Hidalgo and Mart ń-Marroqu ń 2014), etc. Overall these studies have shown that no matter how different the community structure is, the main phyla of the fermenting bacteria remain the same*: Firmicutes, Proteobacteria, Bacteroidetes, Chloroflexi, Actinobacteria, Spirochetes*, etc. (Chojnacka et al. 2015, Chouari et al. 2005). Nevertheless, the substrate(s) of those anaerobic digesters were all complex so the main differences in microbial community are reflected by the hydrolysis and acidogenesis microbial populations. With the hydrolytic and acidogenic bacteria being most prominent, the impact of source populations on acetogenesis and methanogenesis microorganisms is difficult to determine.

To address this issue, we designed a bottom-up experiment that used sodium propionate as the sole carbon source to eliminate both the need and source populations for hydrolysis and acidogenesis populations to the largest extent, thereby allowing us to determine how the inocula affects the acetogenic and methanogenic populations.

Propionate-fed enrichment cultures were grown from inocula sampled from a lab-scale anaerobic digestion fed with dairy manure (L), dairy manure (D), sludge from secondary treatment from Knoxville Utility Board (S), cattle manure (C), and sludge from lab scale anaerobic bioreactor fed with sucrose (W).

The utilization of propionate was accompanied with the production of methane gas in the enrichment cultures at approximately 565 mg/L cumulative CH_4 as COD per transfer, which corresponds to a propionate/methane molar ratio of 4/7 consistent with the stoichiometry of syntrophic propionate oxidation (Equations 4-1 ~ 4-4). The methane production result confirmed that the microbial populations enriched by propionate correspond to the syntrophic degradation of propionate under anaerobic environment for methanogenesis.

Syntrophic propionate oxidation: $C_2H_5COO^- + 2H_2O \rightarrow CH_3COO^- + CO_2 + 3H_2$

(Equation 4-1)

Acetotrophic methanogenesis: $CH_3COO^- + H^+ \rightarrow CH_4 + CO_2$

(Equation 4-2)

Hydrogenotrophic methanogenesis: $4H_2 + CO_2 \rightarrow CH_4 + 2H_2O$

(Equation 4-3)

Overall: $4C_2H_5COO^- + 2H_2O + 4H^+ \rightarrow 7CH_4 + 5CO_2$

(Equation 4-4)

Although the relative abundance of methanogens in the inocula are different (higher in the anaerobic sludge, lower in others), after enrichment, the relative abundance of archaea was approximately 50% in all digesters. However, the composition of archaeal populations is distinct (Figure 4-1-(a)). The methanogen population included both hydrogenotrophic and acetoclastic methanogens, as expected given that propionate is converted into both acetate and hydrogen before being converted to methane (Equations 4.1-4.4). While *Methanosaeta* was the dominant acetoclastic methanogen for most enrichments, *Methanosarcina* was more abundant in C. The population composition of hydrogenotrophic methanogens was distinct in all five enrichments. S was inoculated with the secondary treatment sludge from a wastewater treatment plant and it mainly consisted of *Methanosaeta* (36.2%), *Methanofollis* (26.1%), and *Methanobacterium* (23.2%). L and W were from lab scale anaerobic bioreactors fed with dairy manure and sucrose respectively. Nevertheless, L was predominated by *Methanoculleus* (69.4%) while W was dominated by *Methanospirillum* (48.0%) followed with *Methanobacterium* (28.8%). Both D and C were inoculated with manure, from dairy cow and cattle respectively. However, the methanogen community differed considerably between C and D. D is dominated by *Methanosaeta* (49.4%), followed by *Methanoculleus* (39.6%) while C was consisted of *Methanobacterium* (53.1%), *Methanoculleus* (23.4%) and *Methanosarcina* (18.8%). It is interesting that the sludge used to inoculate L was from lab scale anaerobic bioreactor fed with dairy manure (inoculum of D). *Methanoculleus* was shown as the most abundant hydrogenotrophic methanogens in both L and D, indicating that inoculum might play a comparatively important role in shaping the microbial community.

The bacterial populations were also different in the five enrichments started with different inocula. However, all enrichments shared the same population, i.e. *Syntrophobacter*, as the

dominant constituent (Figure 4-1-(b)). It should be noted that *Syntrophobacter* has been identified as a syntrophic partner of methanogens during syntrophic propionate oxidation in other studies (Boone and Bryant 1980, Chen et al. 2005b, De Bok et al. 2003, Houwen et al. 1990). Despite the diversity of hydrogenotrophic methanogens observed in the enrichments, *Syntrophobacter* seems to be a specific syntrophic partner common with hydrogenotrophic methanogen partners. The other important bacteria included *Mesotoga* (19.4%, 22.2%, and 18.7% in S, C, and W respectively), *Cryptanaerobacter* (11.8% in D), *Aminobacterium* (10.7% in L), *Thermovirga* (9.3%, 9.7%, and 8.4% in W, S, and D respectively), *Lentimicrobiaceae* (11.1% in C), and *Spirochaetaceae* (8.3% in C). The functions of those bacteria are not fully understood but there are several possible explanations. First, they might fermenters of intermediates produced in the enrichment cultures. Second, they might be scavengers of the dead cells in the enrichments. Third, they might be populations present in the inoculum (De Vrieze et al. 2017, Werner et al. 2011). The most interesting possibility of all is that they could be the so-called dark matter that is required to form an intricate syntrophic supported food web (Nobu et al. 2015).

3.2 Shift of microbial community between transfers of the propionate enrichment

Apart from population sources, time is also an important factor to consider for multiple studies pointed out the microbial succession happens even during stable operation along with time (Connaughton et al. 2006, Haruta et al. 2004, Wu et al. 2016).

Comparison of the microbial community were compared after 3 and 5 transfers in Figure 4-2. While the microbial community contains around 9% of acetoclastic *Methanosaeta* in both transfers, the compositions of hydrogenotrophic methanogens varied (Figure 4-2). At the end of third transfer, there are an average of 18% *Methanobacterium* and 30% *Methanospirillum* in the propionate enrichment cultures. However, by the end of fifth transfer, the predominance of the two methanogens swapped, with an average of 43% and 7% of *Methanobacterium* and *Methanospirillum* respectively. Despite of the swap of methanogens, their syntrophic partner, Syntrophobacter, did not alter, signifying its specificity during anaerobic propionate degradation.

The community structure for bacteria between the two transfers is also more similar compared to archaeal populations. The only major switch is between W5 (increased by 6.2%) and Mesotoga (decreased by 3.0%) while all other bacterial population changes were under 3% (Figure 4-3).

As for methanogens, *Methanobacterium*, *Methanoculleus*, *Methanofollis*, *Methanospirillum*, and *Methanolinea* all appeared in some propionate enrichment cultures with different inoculum as hydrogen scavengers supporting the specific *Syntrophobacter* to degrade propionate syntrophically (Figures 4-1 and 4-2). Those methanogens have also been reported in several studies to work with *Syntrophobacter* in syntrophic propionate oxidation (Botsch and Conrad 2011, Dong et al. 1994, Gallert and Winter 2008, Li et al. 2017). Biomass communities sampled after the 3rd and 5th transfers from the same enrichment cultures indicated variation in relative importance of Methanobacterium and *Methanospirillum*, while *Syntrophobacter* remained unchanged. The phylogenetic distances are small among the hydrogenotrophic methanogens (Figure 4-4), and they all convert H_2 and CO_2 to methane to maintain low H_2 partial pressure as required for the oxidation of propionate by *Syntrophobacter*. The underlying conditions favoring one partner of *Syntrophobacter* over the other still needs investigation.

3.3 Impact of different propionate concentration on the microbial assembly of the enrichments

The previous sections clearly demonstrate that *Syntrophobacter* within *Proteobacteria* were associated with hydrogenotrophic methanogens in propionate enrichments regardless of inoculum, which is consistent with other studies (De Bok et al. 2003, Leng et al. 2018, Li et al. 2012, Sedano-Núñez et al. 2018). However, it remains unknown how the concentration of propionate could influence the kinetics and microbial community structures in propionate conversion. Therefore, propionate enrichments of different substrate concentration were tested. For the higher concentration enrichments, the biomass was transferred to a new bottle after the culture stops producing biogas. For the lower concentration ones, the same portion of feedstock was added again after the end of methane production and repeated 10 times before being transferred to the next bottle.

This group of comparison experiment was also inoculated with the same sludge from previous lab scale anaerobic bioreactor fed with sucrose to eliminate the difference caused by source population. The microbial community in the higher concentration (150 mM, P-150) propionate enrichments was shown to be less diverse than the lower concentration (15 mM, P-15) ones (Figure 4-5), which can be explained by propionate inhibition of many microbial populations. The slightly higher diversity in the P-15-3 (biomass after utilization of propionate for 10 times in the 3rd transfer) than it in the P-15-5 (5th transfer) may be caused by the decrease of redundant populations. The difference in microbial community structure between the two transfers of the lower concentration propionate enrichments was already discussed in the previous section. This section will focus on the distinction in the archaeal and bacterial community between propionate enrichments of higher concentration and lower concentration. More than 40% of the microbial populations belong to archaea for all the enrichments although the compositions are different (Figure 4-6). P-15-3 and P-15-5 contained both hydrogenotrophic methanogens (*Methanobacterium* and *Methanospirillum*) and acetoclastic ones (*Methanosaeta* and *Methanosarcina*) while P-150 cultures were dominated by *Methanoculleus* (more than 91% of methanogen population), followed by *Methanobacterium* (around 8%), and only 0.67% of the methanogens were acetoclastic *Methanosaeta.*

The concentration of fatty acids (acetate and propionate) as well as chemical oxygen demand (COD) were measured at the start and end points of methane generations to identify potential pathways of propionate conversion. More than 97% of the propionate was consumed in the lower concentration propionate enrichments, based on both COD and VFA concentration results (Table 4-1) while only 66% of the carbon was converted to methane and carbon dioxide in the higher propionate concentration enrichments. It is noticeable that there is little propionate left in the cultures whereas the acetate concentration was high. This result explains the dominant hydrogenotrophic methanogens and rare acetoclastic ones since acetate accumulated in the cultures, suggesting that the higher propionate concentration is inhibitive to acetoclastic methanogens. The unconsumed propionate may be the result of acetate accumulation. The dominance of *Methanoculleus* in the high concentration propionate enrichments also implies that

Methanoculleus is more tolerant of high levels of propionate and acetate than other hydrogenotrophic methanogens. Similar results were observed in a previous study (Lins et al. 2014) where the authors revealed that with the increase in acetate concentration, there was a clear decrease in populations of *Methanobacterium* while those of *Methanoculleus* were rarely affected by any treatment. It is also reported repeatedly that *Methanoculleus* tend to survive under more extreme conditions such as high ammonia concentration (Angenent et al. 2002, Barret et al. 2013, Barret et al. 2012), high COD concentration (Acharya et al. 2011, Botello Su árez et al. 2018), high temperature (Fontana et al. 2016, Lavania et al. 2014), etc.

In digesters fed with different concentrations of propionate, bacterial community compositions were more similar than the archaeal ones. Not surprisingly, s *Syntrophobacter* was the most prominent bacterial genus across all enrichments, indicative of the important role it played in the syntrophic propionate oxidation. Yet, there are still some differences. While *Mesotoga*, *Thermovirga*, and *W5* were also abundant in either P-15-3 or P-15-5 apart from *Syntrophobacter*, more *Cryptanaerobacter* were observed in P-150 along with *Mesotoga* and *W5*, with only little *Thermovirga*. This observation suggests that bacteria have different ability of adaptation to divergent propionate concentrations; i.e., *Cryptanaerobacter* are likely more propionate and/or acetate tolerant while *Thermovirga* maybe more sensitive to higher fatty acids concentration.

As propionate accumulation often leads to inhibition of methanogenesis and causes interruption of methane production during anaerobic digestion, timely utilization of propionate is critical to maintain stable digestion performance. The adaptation of microbial community to high-propionate conditions demonstrated in this section also provides a feasible bioaugmentation strategy that could be used for the recovery of anaerobic digesters upset by propionate accumulation, as *Syntrophobacter* and *Methanoculleus* are capable of converting propionate at high concentrations.

3.4 Verification of two pathways in the propionate enrichment

In previous sections of this chapter *Syntrophobacter* species were observed to oxidize propionate along with hydrogen scavenging methanogens species, which happens via the methyl-malonyl-

coenzyme A (CoA) pathway (Houwen et al. 1991, Plugge et al. 1993, Plugge et al. 2012, Sedano-Núñez et al. 2018). There are other studies using synthetic wastewater with propionate or propionic acid as the carbon source that also reported *Smithella* as one of the important syntrophic acetogens in bacterial communities. *Smithella* dismutate propionate to acetate and butyrate via a six-carbon intermediate; other intermediates and enzymes related to this pathway have not been identified (Ban et al. 2015, de Bok et al. 2001, Li et al. 2018b, Li et al. 2017). It seems that the *Smithella* pathway does not exist in our propionate enrichment since there are no *Smithella* species observed in the biomass of the enrichment cultures. However, this conclusion may be biased by the PCR and sequencing process.

To verify whether *Smithella* pathway exists in our enrichment cultures, a cross-feeding experiment was conducted by transferring the propionate enrichment into replicate bottles, and after utilizing propionate five times, switching the substrate to acetate (P-A) and butyrate (P-B) of similar concentration (as carbon) while keeping propionate (P) as control. For more comparisons, we also developed mature acetate (A) and butyrate (B) enrichments and cross-fed them with propionate (A-P) and butyrate (A-B) and acetate (B-A) and propionate (B-P), respectively. All the enrichment cultures in this section were seeded with the same inoculum, which was from the lab scale anaerobic bioreactor fed with sucrose. If the switched substrate is one of the intermediates of the anaerobic degradation of the original substrate, the enrichment would be expected to produce methane immediately. Similarly, if no biogas is produced from the enrichment culture after switching the substrate, the substitution is unlikely to be an intermediate product of the original substrate. It is well known that acetate can be directly degraded to methane by acetoclastic methanogen *Methanosaeta* and *Methanosarcina* without energy barrier and no propionate and butyrate will be generated during the process (Chen et al. 2017, Conklin et al. 2006, Ma et al. 2006). The acetate enrichment stopped producing methane when the substrate acetate was swapped with either propionate or butyrate, as expected (Table 4-2). As a four-carbon acid, butyrate can be degraded into acids composed of lower carbon, so it is also expected that when butyrate enrichments were cross-fed with acetate and propionate, methane was

generated spontaneously, proving acetate and propionate the intermediates of syntrophic butyrate degradation.

When acetate and butyrate were cross-fed into propionate enrichment, however, the cultures fed with the two substitutions responded differently. When acetate was added into the propionate enrichment, it was utilized quickly, and biogas was produced. On the other hand, when butyrate was used as the substrate instead of propionate, the enrichment produced no methane in more than half a year (the gas production was checked on weekly basis). This phenomenon suggested that while acetate is an obvious intermediate of syntrophic propionate oxidation, butyrate is not; thus, the *Smithella* pathway does not exist in our enrichment cultures. Lack of the *Smithella* pathway may be caused by the high propionate concentration as suggested in several other studies (Li et al. 2015, McMahon et al. 2004, Wang et al. 2019). McMahon et al reported declined *Smithella sp.* with unchanged *Syntrophobacter sp.* during the overloading anaerobic process when the propionate concentration increased (McMahon et al. 2004). Wang et al also demonstrated that *Syntrophobacter* had greater tolerance than *Smithella* under acid inhibition conditions by setting up mesophilic chemostat fed with propionate as the sole carbon source (Wang et al. 2019).

The biomass from the cross-feeding enrichments, as well as the controls, were sequenced. The diversity of the cross-feeding microbial communities is lower than the control ones (Figure 4-7a), which is reasonable because the cross-feeding substrate is an intermediate of the original substrate. The communities of the cross-feeding cultures clearly shifted from the control cultures (Figure 4-7b). As expected, for acetate cross-feeding cultures, the acetoclastic *Methanosaeta* increased while the hydrogenotrophic methanogens decreased (Figure 4-8). The other major population changes included the decrease in the syntrophic partner of the hydrogenotrophic methanogens, *Syntrophobacter* and *Syntrophomonas* for the propionate and butyrate enrichments, respectively (Figure 4-9). There were also some changes in the bacterial populations, such as the increase of *Mesotoga* and *Thermovirga* in both acetate cross-feeding cultures with the concomitant decrease of *W5*, possibly due to different tolerances and adaptation of the bacteria to the fatty acids.

Butyrate enrichments were also cross-fed with propionate for comparison. *Syntrophobacter* within *Proteobacteria* represented more than 35% of the bacterial community in propionate enrichment (Figure 4-8), whereas the butyrate enrichment was dominated by more than 30% *Syntrophomonas* within *Firmicutes*. *Syntrophomonas* are likely involved in syntrophic butyrate degradation and hydrogen formation (Crable et al., 2016). It is also reasonable to see more hydrogenotrophic methanogens in propionate than butyrate and more acetoclastic *Methanosaeta* in butyrate than propionate as propionate produces more H_2/CO_2 and butyrate produces more acetate with syntrophic bacteria, indicative of different proportions of pathways the bacterial and archaeal community built up. The community structure of butyrate enrichments was compared with both propionate enrichment (Figure 4-10-a) and the butyrate cultures cross-fed with propionate (Figure 4-10-b). The results of the two comparisons had a lot in common. For example, compared to butyrate enrichments, both propionate enrichment and the propionate cross-feeding cultures had more hydrogenotrophic *Methanobacterium* and less acetoclastic *Methanosaeta*. Another obvious swap was the syntrophic butyrate degrader *Syntrophomonas* to the syntrophic propionate oxidizer *Syntrophobacter*. There are also some decreases in *Thermovirga*, *Mesotoga*, and *W5*, which have been hypothesized by Nobu et al as dark matter required to form an intricate syntrophic supported food web (Nobu et al. 2015), indicating the more specificity and robustness of *Syntrophobacter* to propionate than *Syntrophomonas* to butyrate. Although only an average of 0.2% *Syntrophobacter* were observed in the butyrate enrichment, once the butyrate substrate was substituted to propionate, the abundance of *Syntrophobacter* dramatically increased to an average of 12.5%, along with the decrease of *Syntrophomonas*. The quick shift of microbial community of the propionate cross-feeding butyrate enrichments towards the community of the propionate enrichment demonstrated the sensitivity of *Syntrophobacter* to propionate, marking it a useful bioaugmentation seed of propionate accumulating digestion.

4. Conclusion

Propionate is an indispensable intermediate in anaerobic digestion, yet it is often to be regarded as a rate-limiting step during the process (Mathai et al. 2015). A better understanding of syntrophic propionate oxidation is essential to enhance reactor performance and to ensure system stability. This study developed several groups of methanogenic propionate-utilizing enrichment cultures to determine the syntrophic propionate oxidation consortia. The results provided evidence to support *Syntrophobacter* as the specific syntrophic acetogenic bacteria while its associated methanogen partners might not be as specific. *Methanoculleus* was found to be dominant under more extreme conditions than other hydrogenotrophic methanogen populations. It indicates that introduction of enriched *Syntrophobacter* and *Methanoculleus* could be a potential bioaugmentation strategy to improve the stability of anaerobic methanogenic conversion processes.

References

CLC Genomics Workbench 9.5.3.

Acharya, B.K., Pathak, H., Mohana, S., Shouche, Y., Singh, V. and Madamwar, D. (2011) Kinetic modelling and microbial community assessment of anaerobic biphasic fixed film bioreactor treating distillery spent wash. *Water Research* 45(14), 4248-4259.

Angenent, L.T., Sung, S. and Raskin, L. (2002) Methanogenic population dynamics during startup of a full-scale anaerobic sequencing batch reactor treating swine waste. *Water Research* 36(18), 4648-4654.

Ban, Q., Zhang, L. and Li, J. (2015) Shift of Propionate-Oxidizing Bacteria with HRT Decrease in an UASB Reactor Containing Propionate as a Sole Carbon Source. *Applied Biochemistry and Biotechnology* 175(1), 274-286.

Barret, M., Gagnon, N., Kalmokoff, M.L., Topp, E., Verastegui, Y., Brooks, S.P.J., Matias, F., Neufeld, J.D. and Talbot, G. (2013) Identification of *Methanoculleus spp.* as Active Methanogens during Anoxic Incubations of Swine Manure Storage Tank Samples. *Applied and Environmental Microbiology* 79(2), 424-433.

Barret, M., Gagnon, N., Morissette, B., Topp, E., Kalmokoff, M., Brooks, S.P., Matias, F., Masse, D.I., Masse, L. and Talbot, G. (2012) *Methanoculleus spp*. as a biomarker of methanogenic activity in swine manure storage tanks. *FEMS Microbiology Ecology* 80(2), 427-440.

Boone, D.R. and Bryant, M.P. (1980) Propionate-degrading bacterium, *Syntrophobacter wolinii sp. nov. gen. nov.,* from methanogenic ecosystems. *Applied and Environmental Microbiology* 40(3), 626.

Botello Suárez, W.A., Da Silva Vantini, J., Duda, R.M., Giachetto, P.F., Cintra, L.C., Tiraboschi Ferro, M.I. and de Oliveira, R.A. (2018) Predominance of syntrophic bacteria, *Methanosaeta* and *Methanoculleus* in a two-stage up-flow anaerobic sludge blanket reactor treating coffee processing wastewater at high organic loading rate. *Bioresource Technology* 268, 158-168.

Botsch, K.C. and Conrad, R. (2011) Fractionation of stable carbon isotopes during anaerobic production and degradation of propionate in defined microbial cultures. *Organic Geochemistry* 42(3), 289-295.

Chen, S., Cheng, H., Liu, J., Hazen, T.C., Huang, V. and He, Q. (2017) Unexpected competitiveness of *Methanosaeta* populations at elevated acetate concentrations in

methanogenic treatment of animal wastewater. *Applied Microbiology and Biotechnology* 101(4), 1729-1738.

Chen, S., Liu, X. and Dong, X. (2005) *Syntrophobacter sulfatireducens sp. nov.*, a novel syntrophic, propionate-oxidizing bacterium isolated from UASB reactors. *International Journal of Systematic and Evolutionary Microbiology* 55(Pt 3), 1319-1324.

Chojnacka, A., Szczesny, P., Blaszczyk, M.K., Zielenkiewicz, U., Detman, A., Salamon, A. and Sikora, A. (2015) Noteworthy facts about a methane-producing microbial community processing acidic effluent from sugar beet molasses fermentation. *PLoS One* 10(5), e0128008.

Chouari, R., Le Paslier, D., Daegelen, P., Ginestet, P., Weissenbach, J. and Sghir, A. (2005) Novel predominant archaeal and bacterial groups revealed by molecular analysis of an anaerobic sludge digester. *Environmental Microbiology* 7(8), 1104-1115.

Conklin, A., Stensel, H.D. and Ferguson, J. (2006) Growth kinetics and competition between *Methanosarcina* and *Methanosaeta* in mesophilic anaerobic digestion. *Water Environment Research* 78(5), 486-496.

Connaughton, S., Collins, G. and O'Flaherty, V. (2006) Development of microbial community structure and actvity in a high-rate anaerobic bioreactor at 18 ℃. *Water Research* 40(5), 1009-1017.

De Bok, F.A.M., Hagedoorn, P.L., Silva, P.J., Hagen, W.R., Schiltz, E., Fritsche, K. and Stams, A.J.M. (2003) Two W‐containing formate dehydrogenases (CO_2‐reductases) involved in syntrophic propionate oxidation by *Syntrophobacter fumaroxidans*. *European Journal of Biochemistry* 270(11), 2476-2485.

de Bok, F.A.M., Stams, A.J.M., Dijkema, C. and Boone, D.R. (2001) Pathway of propionate oxidation by a syntrophic culture of *Methanospirillum hungatei*. *Applied and Environmental Microbiology* 67(4), 1800-1804.

De Vrieze, J., Christiaens, M.E.R., Walraedt, D., Devooght, A., Ijaz, U.Z. and Boon, N. (2017) Microbial community redundancy in anaerobic digestion drives process recovery after salinity exposure. *Water Research* 111, 109-117.

Demirer, G.N. and Speece, R.E. (1998) Anaerobic biotransformation of four 3-carbon compounds (acrolein, acrylic acid, allyl alcohol and n-propanol) in UASB reactors. *Water Research* 32(3), 747-759.

Dhamodharan, K., Kumar, V. and Kalamdhad, A.S. (2015) Effect of different livestock dungs as inoculum on food waste anaerobic digestion and its kinetics. *Bioresource Technology* 180, 237-241.

Dolfing, J. (2013) Syntrophic propionate oxidation via butyrate: a novel window of opportunity under methanogenic conditions. *Applied and Environmental Microbiology* 79(14), 4515-4516.

Dong, X., Plugge, C.M. and Stams, A.J.M. (1994) Anaerobic degradation of propionate by a mesophilic acetogenic bacterium in coculture and triculture with different methanogens. *Applied and Environmental Microbiology* 60(8), 2834-2838.

Fontana, A., Patrone, V., Puglisi, E., Morelli, L., Bassi, D., Garuti, M., Rossi, L. and Cappa, F. (2016) Effects of geographic area, feedstock, temperature, and operating time on microbial communities of six full-scale biogas plants. *Bioresource Technology* 218, 980-990.

Gallert, C. and Winter, J. (2008) Propionic acid accumulation and degradation during restart of a full-scale anaerobic biowaste digester. *Bioresource Technology* 99(1), 170-178.

Goswami, R., Chattopadhyay, P., Shome, A., Banerjee, S.N., Chakraborty, A.K., Mathew, A.K. and Chaudhury, S. (2016) An overview of physico-chemical mechanisms of biogas production by microbial communities: a step towards sustainable waste management. *3 Biotech* 6(1), 72-72.

Gu, Y., Chen, X., Liu, Z., Zhou, X. and Zhang, Y. (2014) Effect of inoculum sources on the anaerobic digestion of rice straw. *Bioresource Technology* 158, 149-155.

Haruta, S., Kondo, M., Nakamura, K., Chanchitpricha, C., Aiba, H., Ishii, M. and Igarashi, Y. (2004) Succession of a microbial community during stable operation of a semi-continuous garbage-decomposing system. *Journal of Bioscience and Bioengineering* 98(1), 20-27.

Hidalgo, D. and Mart ń-Marroqu ń, J.M. (2014) Effects of inoculum source and co-digestion strategies on anaerobic digestion of residues generated in the treatment of waste vegetable oils. *Journal of Environmental Management* 142, 17-22.

Houwen, F.P., Dijkema, C., Stams, A.J.M. and Zehnder, A.J.B. (1991) Propionate metabolism in anaerobic bacteria; determination of carboxylation reactions with ^{13}C-NMR spectroscopy. *Biochimica et Biophysica Acta (BBA) - Bioenergetics* 1056(2), 126-132.

Houwen, F.P., Plokker, J., Stams, A.J.M. and Zehnder, A.J.B. (1990) Enzymatic evidence for involvement of the methylmalonyl-CoA pathway in propionate oxidation by *Syntrophobacter wolinii*. *Archives of Microbiology* 155, 52-55.

Lavania, M., Cheema, S., Sarma, P.M., Ganapathi, R. and Lal, B. (2014) Methanogenic potential of a thermophilic consortium enriched from coal mine. *International Biodeterioration & Biodegradation* 93, 177-185.

Leng, L., Yang, P., Singh, S., Zhuang, H., Xu, L., Chen, W.H., Dolfing, J., Li, D., Zhang, Y., Zeng, H., Chu, W. and Lee, P.H. (2018) A review on the bioenergetics of anaerobic microbial metabolism close to the thermodynamic limits and its implications for digestion applications. *Bioresource Technology* 247, 1095-1106.

Li, C., Moertelmaier, C., Winter, J. and Gallert, C. (2015) Microbial community shifts during biogas production from biowaste and/or propionate. *Bioengineering (Basel, Switzerland)* 2(1), 35-53.

Li, J., Ban, Q., Zhang, L. and Jha, A. (2012) Syntrophic propionate degradation in anaerobic digestion: A review. *International Journal of Agriculture and Biology* 14(5).

Li, Y., Sun, Y., Li, L. and Yuan, Z. (2018a) Acclimation of acid-tolerant methanogenic propionate-utilizing culture and microbial community dissecting. *Bioresource Technology* 250, 117-123.

Li, Y., Sun, Y., Li, L. and Yuan, Z. (2018b) Acclimation of acid-tolerant methanogenic propionate-utilizing culture and microbial community dissecting. *Bioresource Technology* 250, 117-123.

Li, Y., Sun, Y., Yang, G., Hu, K., Lv, P. and Li, L. (2017) Vertical distribution of microbial community and metabolic pathway in a methanogenic propionate degradation bioreactor. *Bioresource Technology* 245, 1022-1029.

Lins, P., Reitschuler, C. and Illmer, P. (2014) *Methanosarcina spp*., the key to relieve the start-up of a thermophilic anaerobic digestion suffering from high acetic acid loads. *Bioresource Technology* 152, 347-354.

Liu, Y., Balkwill, D.L., Aldrich, H.C., Drake, G.R. and Boone, D.R. (1999) Characterization of the anaerobic propionate-degrading syntrophs *Smithella propionica gen. nov., sp. nov*. and *Syntrophobacter wolinii*. *International Journal of Systematic and Evolutionary Microbiology* 49 Pt 2, 545-556.

Ma, K., Liu, X. and Dong, X. (2006) *Methanosaeta harundinacea sp. nov.*, a novel acetate-scavenging methanogen isolated from a UASB reactor. *International Journal of Systematic and Evolutionary Microbiology* 56(Pt 1), 127-131.

Mathai, P.P., Zitomer, D.H. and Maki, J.S. (2015) Quantitative detection of syntrophic fatty acid-degrading bacterial communities in methanogenic environments. *Microbiology* 161(6), 1189-1197.

McCarty, P.L. and Smith, D.P. (1986) Anaerobic wastewater treatment. *Environmental Science & Technology* 20(12), 1200-1206.

McMahon, K.D., Zheng, D., Stams, A.J., Mackie, R.I. and Raskin, L. (2004) Microbial population dynamics during start-up and overload conditions of anaerobic digesters treating municipal solid waste and sewage sludge. *Biotechnology and Bioengineering* 87(7), 823-834.

Muller, N., Worm, P., Schink, B., Stams, A.J. and Plugge, C.M. (2010) Syntrophic butyrate and propionate oxidation processes: from genomes to reaction mechanisms. *Environmental Microbiology Reports* 2(4), 489-499.

Nobu, M.K., Narihiro, T., Rinke, C., Kamagata, Y., Tringe, S.G., Woyke, T. and Liu, W.-T. (2015) Microbial dark matter ecogenomics reveals complex synergistic networks in a methanogenic bioreactor. *The ISME journal* 9(8), 1710-1722.

Plugge, C.M., Dijkema, C. and Stams, A.J.M. (1993) Acetyl-CoA cleavage pathway in a syntrophic propionate oxidizing bacterium growing on fumarate in the absence of methanogens. *FEMS Microbiology Letters* 110(1), 71-76.

Plugge, C.M., Henstra, A.M., Worm, P., Swarts, D.C., Paulitsch-Fuchs, A.H., Scholten, J.C.M., Lykidis, A., Lapidus, A.L., Goltsman, E., Kim, E., McDonald, E., Rohlin, L., Crable, B.R., Gunsalus, R.P., Stams, A.J.M. and McInerney, M.J. (2012) Complete genome sequence of *Syntrophobacter fumaroxidans* strain (MPOBT). *Standards in Genomic Sciences* 7(1), 91-106.

Qiao, S., Tian, T., Qi, B. and Zhou, J. (2015) Methanogenesis from wastewater stimulated by addition of elemental manganese. *Scientific Reports* 5, 12732.

Rice, E.W., Baird, R.B., Eaton, A.D. and Clesceri, L.S. (2012) Standard methods for the examination of water and wastewater, 22nd Edition, American Public Health Association, American Water Works Association, Water Environment Federation.

Saidu, M., Yuzir, A., Salim, M.R., Salmiati, Azman, S. and Abdullah, N. (2013) Influence of palm oil mill effluent as inoculum on anaerobic digestion of cattle manure for biogas production. *Bioresource Technology* 141, 174-176.

Sedano-Núñez, V.T., Boeren, S., Stams, A.J.M. and Plugge, C.M. (2018) Comparative proteome analysis of propionate degradation by Syntrophobacter fumaroxidans in pure culture and in coculture with methanogens. *Environmental Microbiology* 20(5), 1842-1856.

Wang, H.-Z., Yan, Y.-C., Gou, M., Yi, Y., Xia, Z.-Y., Nobu, M.K., Narihiro, T. and Tang, Y.-Q. (2019) Response of propionate-degrading methanogenic microbial communities to inhibitory conditions. *Applied Biochemistry and Biotechnology*.

Werner, J.J., Knights, D., Garcia, M.L., Scalfone, N.B., Smith, S., Yarasheski, K., Cummings, T.A., Beers, A.R., Knight, R. and Angenent, L.T. (2011) Bacterial community structures are unique and resilient in full-scale bioenergy systems. *Proceedings of the National Academy of Sciences* 108(10), 4158.

Wu, L., Yang, Y., Chen, S., Zhao, M., Zhu, Z., Yang, S., Qu, Y., Ma, Q., He, Z., Zhou, J. and He, Q. (2016) Long-term successional dynamics of microbial association networks in anaerobic digestion processes. *Water Research* 104, 1-10.

Yilmaz, P., Parfrey, L.W., Yarza, P., Gerken, J., Pruesse, E., Quast, C., Schweer, T., Peplies, J., Ludwig, W. and Glöckner, F.O. (2014) The SILVA and "All-species Living Tree Project (LTP)" taxonomic frameworks. *Nucleic acids research* 42(D1), D643-D648.

Zhang, L. and Jahng, D. (2010) Enhanced anaerobic digestion of piggery wastewater by ammonia stripping: Effects of alkali types. *Journal of Hazardous Materials* 182, 536-543.

Zhu, Z., Hsueh, M.K. and He, Q. (2011) Enhancing biomethanation of municipal waste sludge with grease trap waste as a co-substrate. *Renewable Energy* 36(6), 1802-1807.

Appendix: Tables and Figures

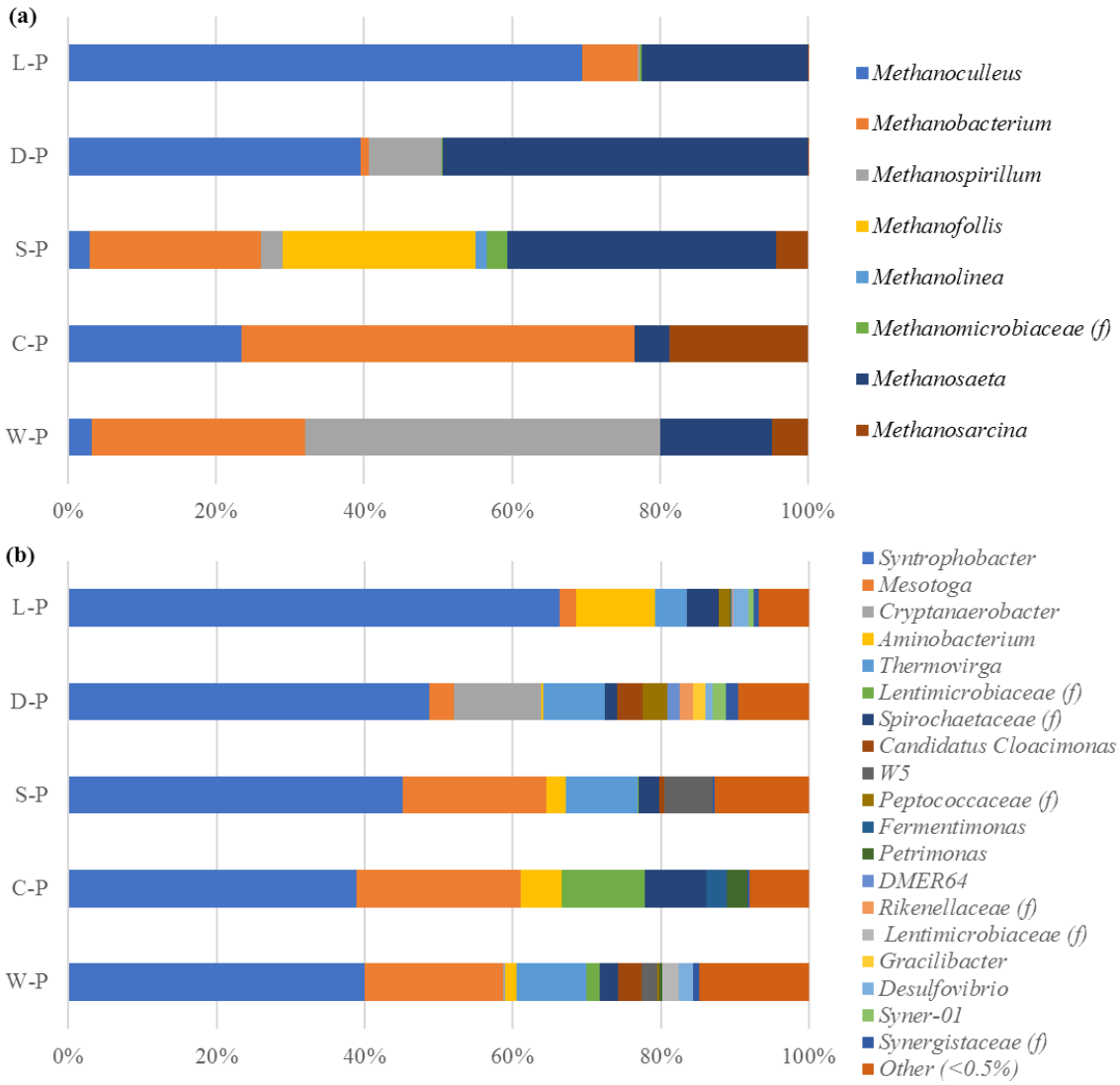

Figure 4-1. Archaeal (a) and Bacterial (b) community composition after five transfers on genera level showing the impact of different inocula on the microbial community structures of the propionate enrichments. Inoculum: L-sludge from lab scale anaerobic digestion fed with dairy manure; D-dairy manure; S-sludge from secondary treatment from Knoxville Utility Board; C-cattle manure; W-sludge from lab scale anaerobic bioreactor fed with sucrose.

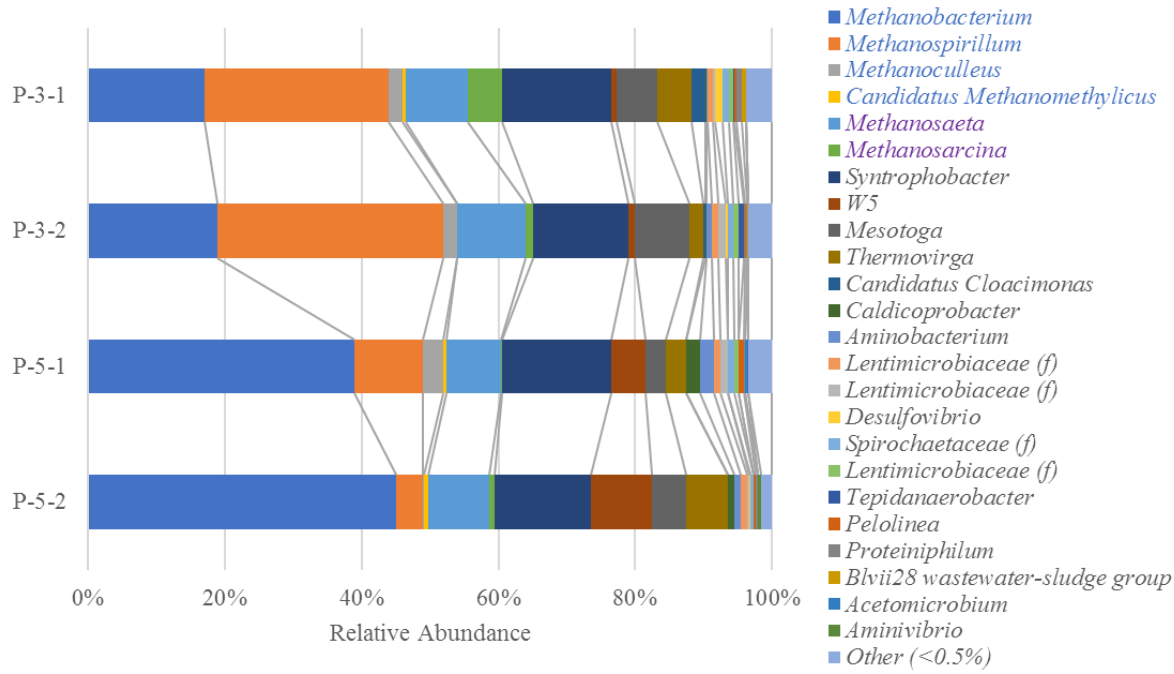

Figure 4-2. Microbial community shift between the 3rd and 5th transfers of propionate enrichment. In P-X-Y, P represents propionate; X represents the transfer; and Y represents the replicates. The taxonomy is listed on its affiliated genera or the most confident classification achievable with the level shown in "()". "f"-family. Labels in blue: hydrogenotrophic methanogens; purple: acetoclastic methanogens; black: bacteria.

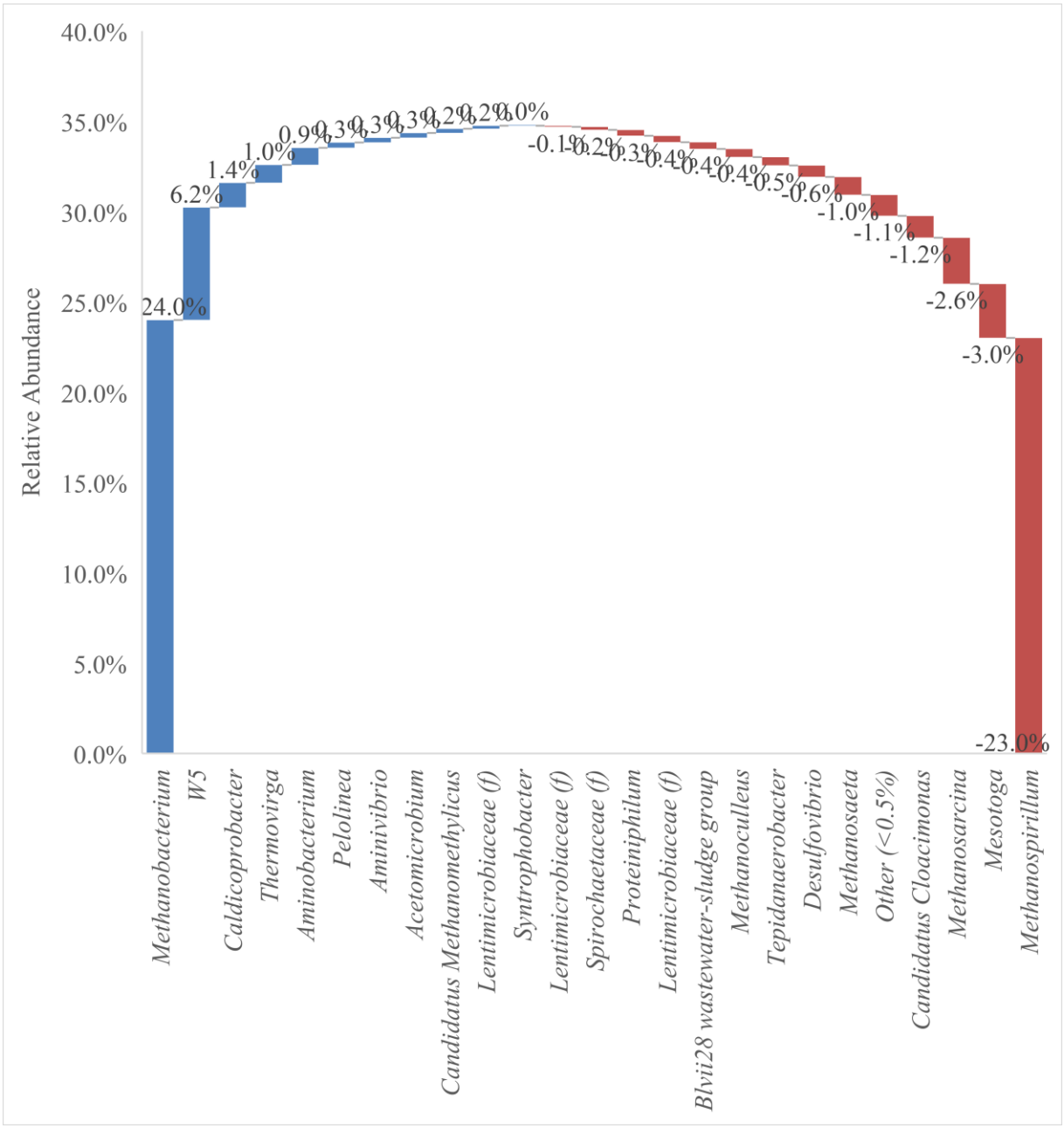

Figure 4-3. Difference in relative abundance of major archaeal and bacterial genus populations (average relative abundance > 0.5%) from the 3rd transfer to the 5th transfer. The populations are represented on their affiliated genera or the most confident classification achievable with the level shown in "()" . "f"-family. Blue: increase; Orange: decrease.

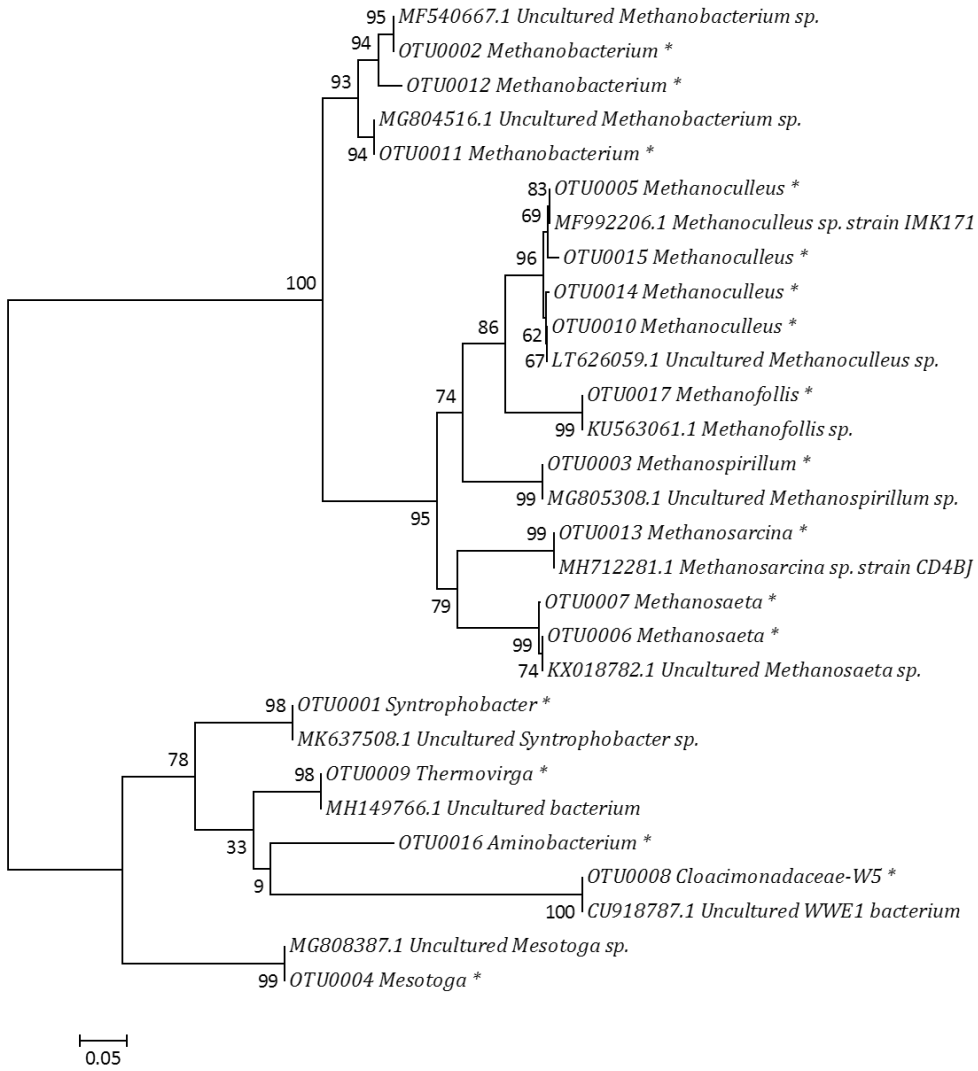

Figure 4-4. The OTU (*) sequences classified in this research were obtained by CLC genomic workbench. The reference 16S rRNA gene sequences were searched using the BLAST program at the National Center for Biotechnology Information (NCBI). All the sequences were aligned with homologous sequences using Clustal Omega. The tree was reconstructed by MEGA 7 software using the neighbor-joining method. The optimal tree with the sum of branch length = 2.16922708 is shown. The percentage of replicate trees in which the associated taxa clustered together in the bootstrap test (1000 replicates) are shown next to the branches. The tree is drawn to scale, with branch lengths in the same units as those of the evolutionary distances used to infer the phylogenetic tree. The evolutionary distances were computed using the Maximum Composite Likelihood method and are in the units of the number of base substitutions per site.

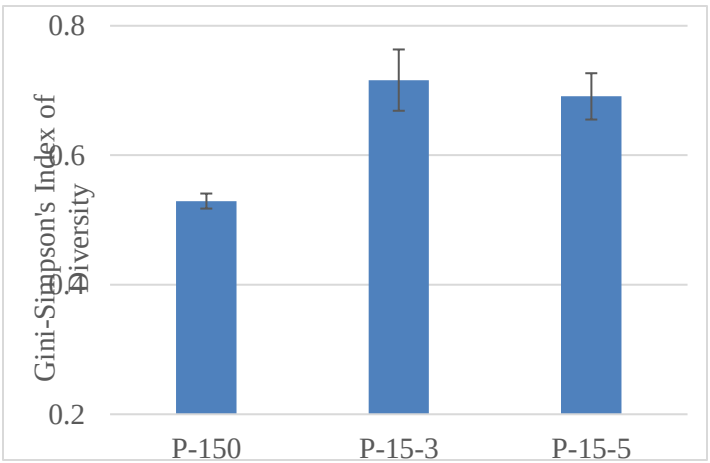

Figure 4-5. Gini-Simpson's index of diversity based on OTUs classified from the amplicon sequencing results of the propionate enrichment inoculated with sludge from lab scale anaerobic bioreactor. All the enrichment cultures have replicate. In P-X-Y: P represents propionate; X represent the concentration in mM; and Y represents the transfer.

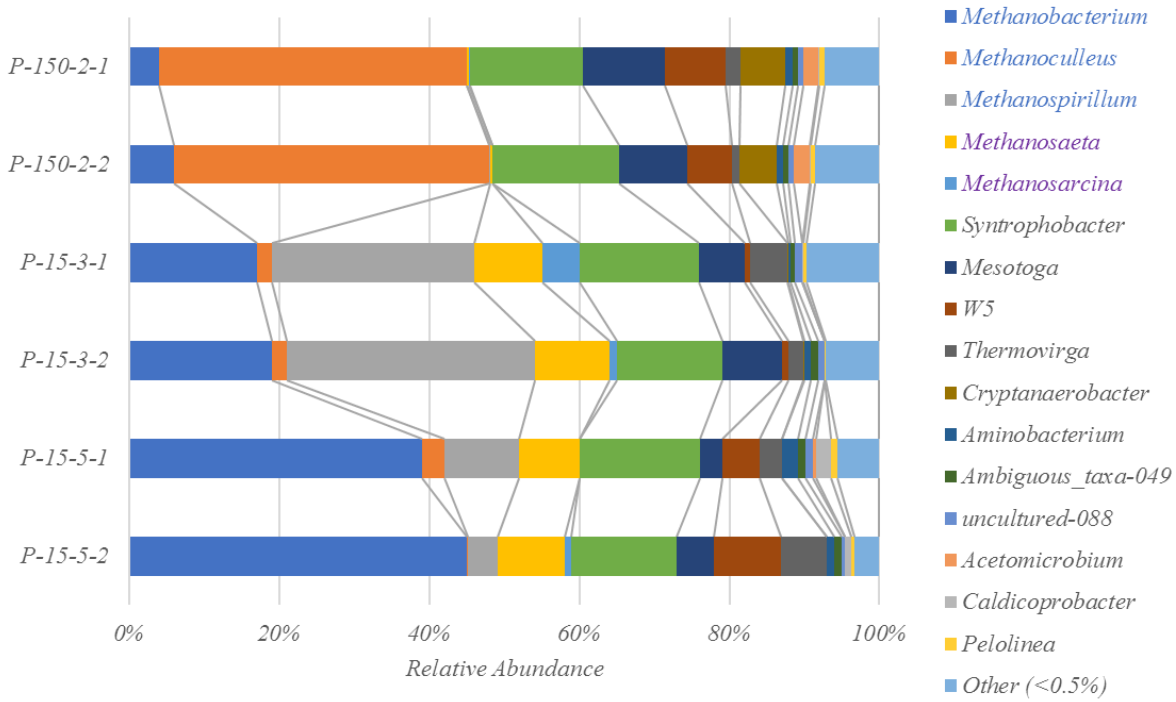

/

Figure 4-6. Difference in microbial community compositions of propionate enrichment of different concentrations on genus level. In P-X-Y-Z, P represents propionate; X represents concentration in mM; Y represents the transfer; and Z represents the replicates. Labels in blue: hydrogenotrophic methanogens; purple: acetoclastic methanogens; black: bacteria.

Table 4-1. Average measured acetate and propionate concentrations in the propionate enrichments of different concentrations on genus level. In P-X-Y, P represents propionate; X represents concentration in mM; and Y represents the transfer.

	Acetate (mMol/L)	Propionate (mMol/L)	COD (mg/L)
P-150 start	0	148.0	16852.7
P-150 end	64.96	12.6	5568.6
Removal rate	N/A	91.5%	66.4%
P-15-3 start	0	15.0	1680.0
P-15-3 end	0.28	0.26	47.0
Removal rate	N/A	98.3%	97.2%
P-15-5 start	0	15.0	1680.0
P-15-5 end	0.24	0.32	51.2
Removal rate	N/A	97.9%	97.0%

Table 4-2. Methane production condition after the cross-feeding (switch of substrate)

Cross-feeding	Methane Production?
Acetate → Propionate (A-P)	No
Acetate → Butyrate (A-B)	No
Propionate → Acetate (P-A)	Yes
Propionate → Butyrate (P-B)	No
Butyrate → Acetate (B-A)	Yes
Butyrate → Propionate (B-P)	Yes

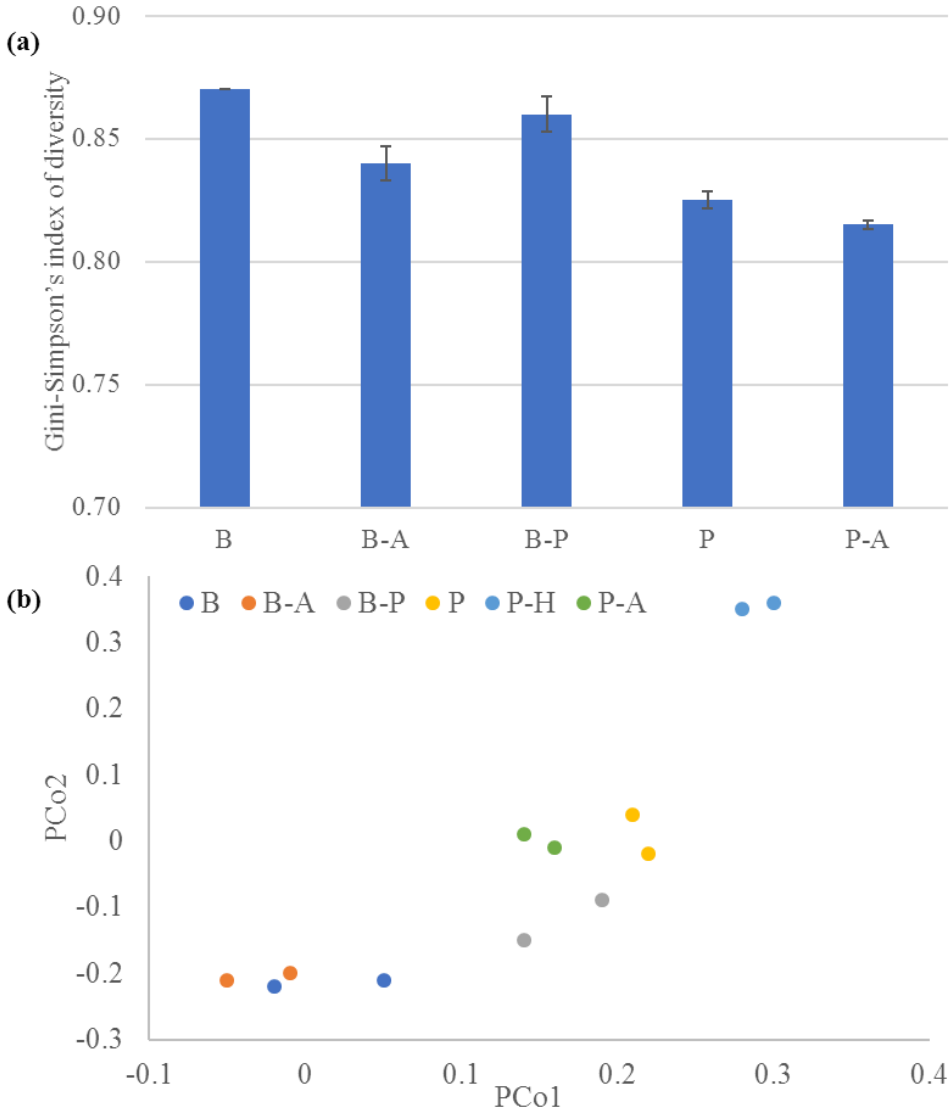

Figure 4-7. (a) Gini-Simpson's index of diversity and (b) Principal coordinate analysis (PCoA) of the microbial communities based on OTUs classified from the amplicon sequencing results of the enrichment and the cross-feeding cultures. B: butyrate enrichment; B-A: butyrate enrichment cross-feeding with acetate; B-P: butyrate enrichment cross-feeding with propionate; P: propionate enrichment; P-H: high concentration propionate enrichment; P-A: propionate enrichment cross-feeding with acetate.

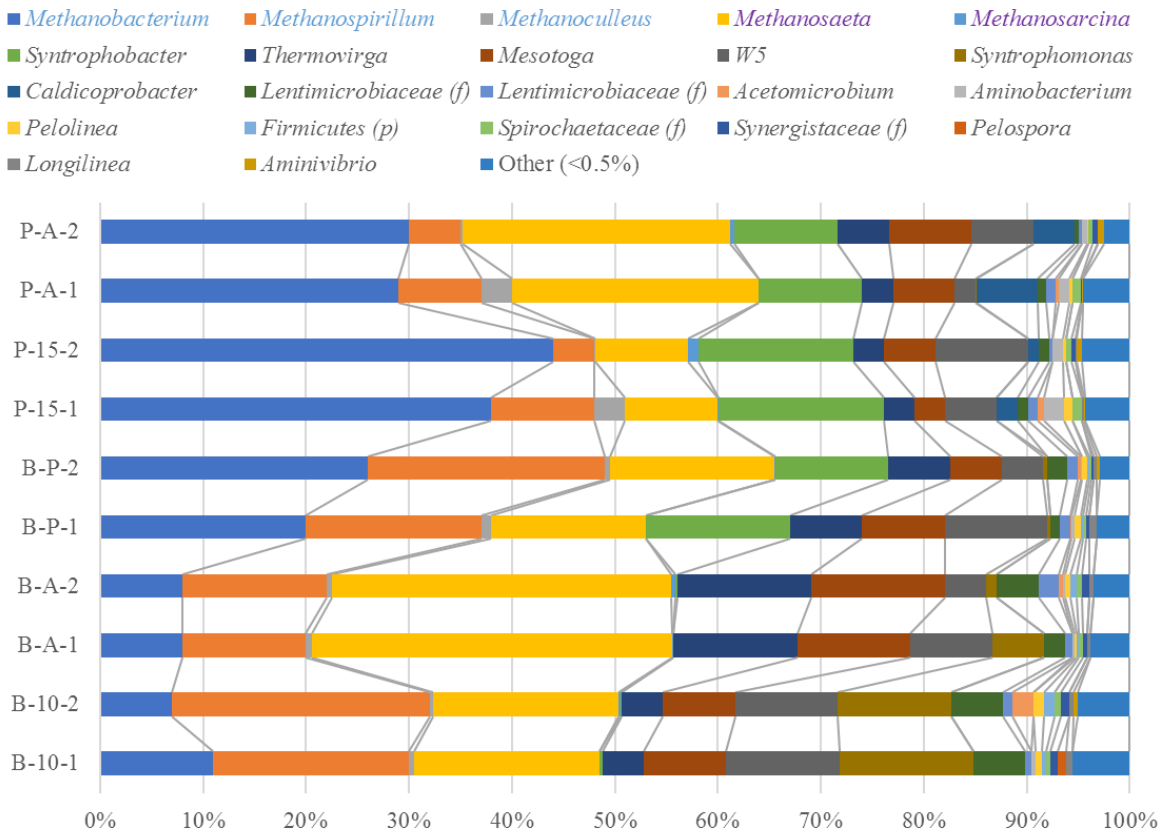

Figure 4-8. Difference in microbial community compositions of cross-feeding cultures and the control ones based on genus level or the most confident classification achievable with the level shown in "()" . "f"-family; "p"-phylum. B-10: 10 mM butyrate enrichment; B-A: butyrate enrichment cross-feeding with acetate; B-P: butyrate enrichment cross-feeding with propionate; P-15: 15 mM propionate enrichment; P-A: propionate enrichment cross-feeding with acetate. "1" and "2" stands for replicates. Labels in blue: hydrogenotrophic methanogens; purple: acetoclastic methanogens; black: bacteria.

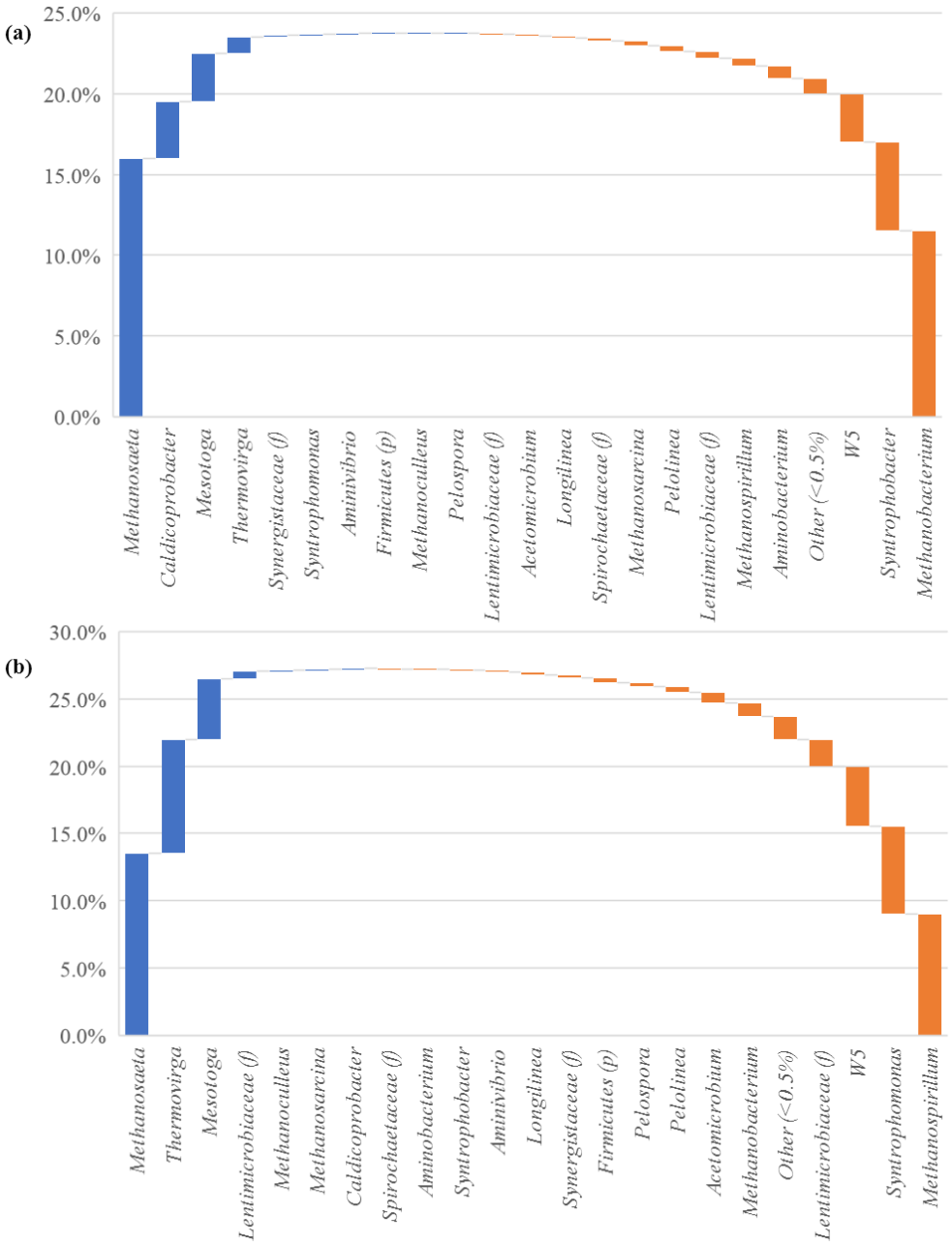

Figure 4-9. Difference in relative abundance of major archaeal and bacterial populations (average relative abundance > 0.5%) in comparison of (a) propionate enrichment and propionate cross-feeding with acetate; and (b) butyrate enrichment and butyrate cross-feeding with acetate. The populations are represented on their affiliated genera or the most confident classification achievable with the level shown in "()" . "f"-family; "p"-phylum. Blue: increase; Orange: decrease.

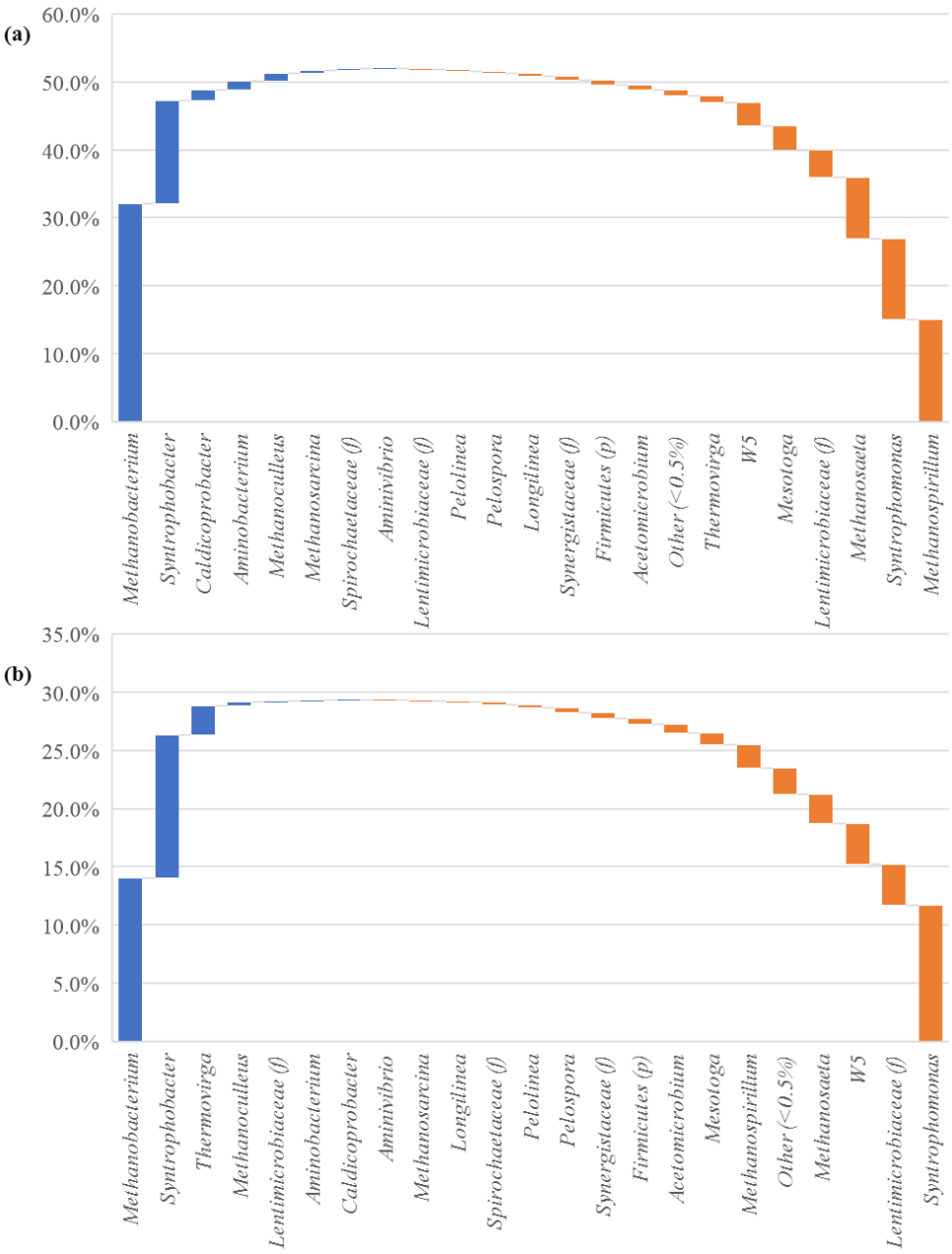

Figure 4-10. Difference in relative abundance of major archaeal and bacterial populations (average relative abundance > 0.5%) in comparison of (a) butyrate enrichment and propionate enrichment; and (b) butyrate enrichment and butyrate cross-feeding with propionate. The populations are represented on their affiliated genera or the most confident classification achievable with the level shown in "()" . "f"-family; "p"-phylum. Blue: increase; Orange: decrease.

CHAPTER V - CONCLUSION

This research uses anaerobic digestion as a model system to better understand the microbial community assembly mechanism, the microbial interactions, and the impact of source populations on the development of microbial community structures. In Chapter 1, basic concepts of the microbial food web in the anaerobic digestion process and the two known community assembly mechanisms were introduced. In Chapter 2, 13 replicate laboratory-scale semi-continuous anaerobic reactors were inoculated with the same culture and maintained under the identical operational and environmental conditions for over a year. Sterile feed stock with mono substrate was used to eliminate the immigration of other external microbial populations. The results revealed that despite the change in community composition between time points, overall community structure was remarkably consistent among the 13 replicates, indicating that non-random mechanisms such as selective pressure shapes the changing trajectory of the community structure over long periods of time. Overall community function, as suggested by metagenomics functional analysis, was maintained even as the community structure changes through swapping of OTUs playing similar metabolic and ecological roles. Chapter 3 aimed to gain a deeper understanding of the methanogenesis associated with acetate, propionate, and butyrate as they are the most common intermediates after acidogenesis and acetogenesis processes and act as precursors of methanogenesis. Enrichments were set up and kinetics of the anaerobic degradation of the fatty acids was determined by the accumulative methane yields. Acetate demonstrated the highest specific growth rate among the selected fatty acid with similar carbon concentration based on mg/L COD while propionate the lowest. The long adaptation time of propionate degradation was indicative of its higher inhibition potential. Microbial community structures were analyzed by 16S rRNA sequencing and PICRUSt gene prediction to understand the role of methanogens and other bacterial populations in the methanogenesis phase. Based on the results, a food web was proposed for anaerobic degradation of the short chain fatty acids, including both acetoclastic and hydrogenotrophic methanogens, syntrophic bacteria, and other redundant bacteria populations. Chapters 4 developed several groups of propionate enrichment cultures to identify the syntrophic propionate oxidizers and to investigate the effect of diverse sources of inoculum, different sampling points, and altered substrate concentrations on the microbial

community structures of propionate enrichment. The results provided various evidences to demonstrate *Syntrophobacter* as the specific obligate syntrophic proton-reducing acetogenic bacteria while its associated methanogen partners are not definitive although *Methanoculleus* tend to be dominant under more extreme conditions, which indicates that the introduction of enriched *Syntrophobacter* and *Methanoculleus* may be more effective bioaugmentation facing accumulation of propionate to obtain a desired process function.

APPENDIX

Supplementary information for chapter 2

We seek to quantify the variability in microbial populations that arises from the stochastic nature of birth-death, and reactor sampling processes among various taxa in the microbial community, also called ecological drift (Velland, 2010). We begin with the following assumptions:

- Each day a fraction of the total cells equal to 1/SRT are removed from the reactor during sampling.
- Each reactor is completely mixed, and cells are sampled without bias through a binomial process
- Average cell death rates are 0.015 day^{-1} for methanogens and 0.1 day^{-1} for other taxa in the reactors (Pavlostathis and Gossett, 1985)
- There is no selective pressure (neutral model assumption)
- Between sampling periods, the biomass population grows at an average rate sufficient to replace the cells removed by sampling and lost by death
- Speciation does not occur
- No microorganisms from the external environment are added to the reactor during sampling or feeding
- The reactors are operated for a period of 110 days

Let n_i be the number of cells of taxon j in the reactor, with a total of J different taxons. Then the total number of cells in the reactor (N) is equal to:

$$N = \sum_{j=1}^{J} n_j$$

Let x_j be the relative abundance of cells of taxon j in the reactor:

$$x_j = \frac{n_j}{N}$$

Simulation by exact stochastic simulation

The processes of cell death and growth can be mapped onto a system of chemical reactions that is amenable to exact stochastic simulation by Gillespie's algorithm (Gillespie, 1976). The system consists of a 2*J reaction channels that may occur in the system at any given time that affect the population n_j of each taxon according to:

$$n_j \xrightarrow[k_{i,j}]{} n_j + \nu_i \ \{i=1,2;\ j=1,2\ldots J\}$$

When i =1, $\nu_1 = 1$, and the reaction represents a growth process in which the number of cells of taxa j increases by 1 through binary fission of a single cell. Similarly, when i =2, $\nu_2 = -1$ and the reaction represents a death reaction in which the population of taxa j decreases by one cell. The rates of the birth and death reactions are given by $k_{i,j}$. In Gillespie's direct method, the time τ required for the next reaction of any type to occur in the system is calculated from:

$$\tau = \frac{1}{a}\ln\left(\frac{1}{r_1}\right)$$

$$a = \sum_{j=1}^{J}\left(k_{1,j}n_j + k_{2,j}n_j\right)$$

where r_1 is a uniform random number on the interval of 0 to 1. Next, a second uniform random number is used to randomly select which reaction occurred. The probability of each reaction channel firing is: $k_{i,j}n_j$ /a.

The final step in the algorithm is to update n_j according to which reaction fired and to update the time to $t = t+\tau$.

Note that the reaction time and reaction probabilities are affect by the populations n_j, and must be updated after each reaction occurs.

Sampling events can be simulated in similar manner. In this case, N/SRT successive sampling reactions will each occur instantaneously ($\tau = 0$):

$$n_j \rightarrow n_j - 1$$

Each of the N/SRT reactions are chosen randomly according to probability $n_{j,s}/N$, where $n_{j,s}$ is the number of cells of taxa j at the beginning of the sampling period.

Each day begins with a sampling event, followed by a 24-hour period in which cell death and growth occurs until the sampling event the following day. The process is continued for 110 days

allowing the stochastic population trajectory of each taxa j to be simulated. In order to obtain a representative sampling of possible population trajectories, the entire 110-day simulation could be repeated multiple times. However, since each day requires on the order of $2N(\frac{1}{SRT} + \overline{k_2})$ reactions to be simulated, the simulation becomes computationally infeasible for large N and an approximate method is needed.

Tau-leaping approximation of Gillespie's algorithm

The tau-leaping approximation (Gillespie, 2001) of Gillespie's algorithm takes advantage of the fact that under certain conditions, the reaction propensities $k_{i,j}n_j$ remain relatively constant over the sequence of many reaction events. In the tau-leaping algorithm, τ is defined to be a time interval large enough for many reactions to occur, but not so large as to allow the propensity of any reaction to change significantly. Gillespie (2001) provides an algorithm for finding the most computationally efficient value of τ, but as will be seen, the particulars of our system allow us to use a convenient fixed value of τ. In this case, the stochastic trajectory of each n_j resulting from birth-death processes is given by:

$$n_{j,t+\tau} = n_j + \wp(\tau \cdot k_{1,j} \cdot n_{j,t}) - \wp(\tau \cdot k_{2,j} \cdot n_{j,t})$$

where $\wp$ is a Poisson random variable. Daily reactor sampling events can be simulated using a binomial process:

$$n_j = n_{j,s} - \mathcal{B}(n_{j,s}, \frac{1}{SRT})$$

Where $\mathcal{B}(n_{j,s}, \frac{1}{SRT})$ is a Binomially distributed random variable of $n_{j,s}$ trials with probability 1/SRT.

Quantifying ecological drift

In our system, cell density was measured to be 2.6×10^{12} cells per ml, giving a total of 2.6×10^{14} cells in the 100 ml system. The SRT is 33 days. For illustrative purposes, we assumed the following relative abundances in the system:

x_j (methanogens)	x_j (other organisms)
0.00001	0.00001
0.0001	0.0001
0.001	0.001
0.01	0.01
0.1	0.1
0.2	0.2
	0.3778

The results of the 110 day experiment were simulated 1000 times using the tau-leaping method with τ = 1 hour = 1/24 day. Average cell death rates $k_{2,j}$ were set to 0.015 day^{-1} for methanogens and 0.1 day^{-1} for other taxa (Pavlostathis and Gossett, 1985). For the purposes of estimating ecological drift, a neutral theory assumption was made that on average cell growth would replace cells lost through sampling or regrowth. Under these assumptions the $k_{1,j}$ is given by:

$$k_{1,j} = k_{2.j} + \left(\frac{SRT}{SRT - 1}\right)^{1/m} - 1$$

where m is the number of periods of duration τ that occur between sampling events. The results of the simulation are shown in Figure S3. Even for taxa with the smallest relative abundance, ecological drift can account for less than 0.01% change in population over the course of the 110-day experiment. These results demonstrate convincingly that ecological drift does not significantly contribute to the observed time-dependent changes in relative abundances in the reactors in this system or other typical wastewater treatment systems characterized by high populations of microorganisms.

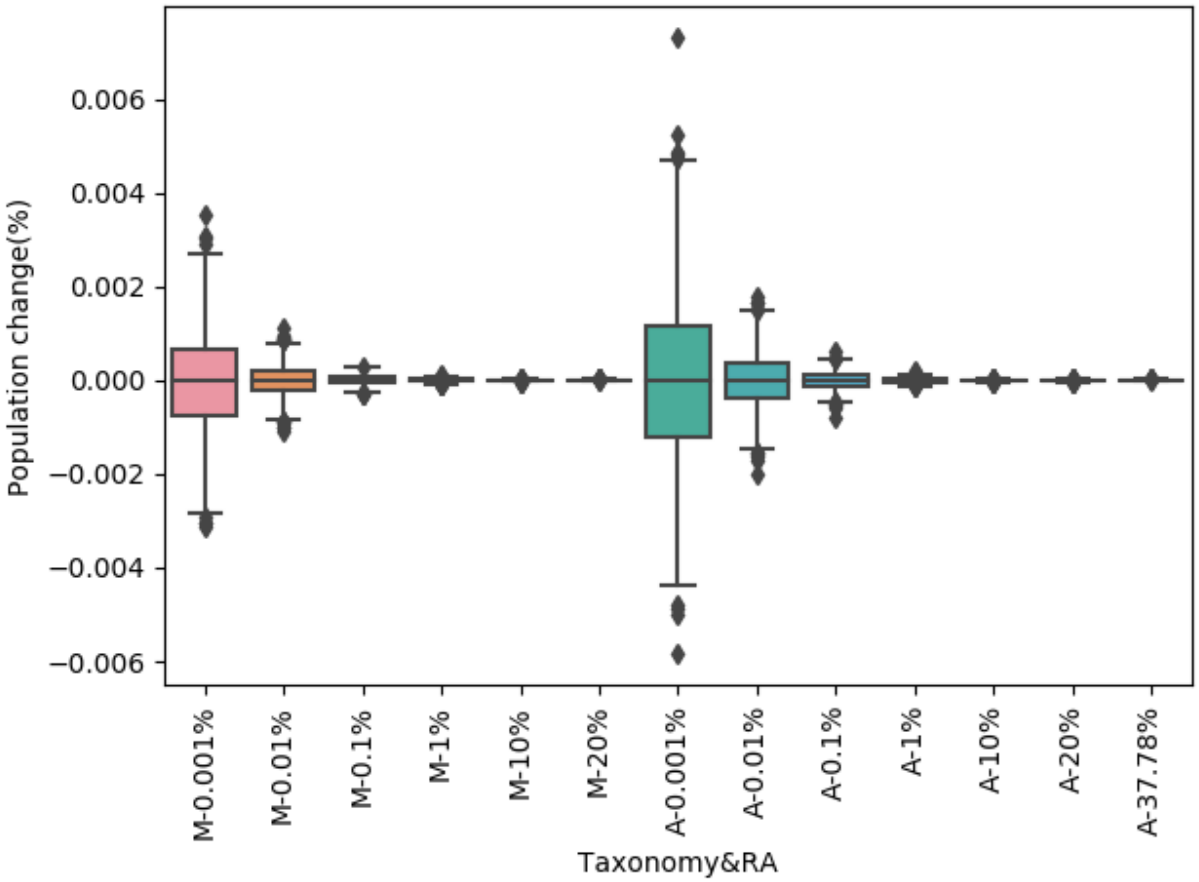

Figure S-1. Average simulated population change (in %) after 110 days. Simulations were repeated 1000 times. Box edges represent 75% and 25% tails, inside bar median, error bars maximum and minimum, and dots outliers.

References

Gillespie, D.T. (1976) A general method for numerically simulating the stochastic time evolution of coupled chemical reactions. *Journal of Computational Physics* 22(4), 403-434.

Gillespie, D.T. (2001) Approximate accelerated stochastic simulation of chemically reacting systems. *The Journal of Chemical Physics* 115(4), 1716-1733.

Pavlostathis, S.G. and Gossett, J.M. (1986) A kinetic model for anaerobic digestion of biological sludge. *Biotechnology and Bioengineering* 28(10), 1519-1530.

Vellend, M. (2010) Conceptual synthesis in community ecology. *The Quarterly Review of Biology* 85(2), 183-206.

VITA

Liu Cao grew up in Shanghai, China and graduated in Shanghai High School in 2008. She obtained her Bachelor of Science in Environmental Engineering from East China University of Science and Technology in 2012. She received her Master of Science in Civil and Environmental Engineering from University of Missouri-Columbia where she conducted research on eliminating drinking water disinfection by-products under the supervision of Dr. Enos C. Inniss in 2014. She is pursuing the Ph.D. in the department of Civil and Environmental Engineering with Dr. Chris D. Cox and Dr. Qiang He at University of Tennessee, Knoxville and expects to finish the dissertation in July 2019.